Journal
of
The Franklin Institute
Devoted to Science and the Mechanic Arts

Vol. 246 AUGUST, 1948 No. 2

STABILIZATION OF CARRIER-FREQUENCY SERVOMECHANISMS. II. DESIGN FORMULAE FOR PROPORTIONAL-DERIVATIVE NETWORKS.*

BY

ANDREW SOBCZYK, Ph.D.[1]

ABSTRACT.

In an alternating current servomechanism, the error is proportional to the modulation envelope of a modulated-carrier error signal. It is shown in part I that for stability and fidelity of the servo, it is highly desirable that the effect of the controller includes a proportional-derivative action on the modulation envelope. This action may be obtained with various forms of RC networks, including the parallel "T," bridge "T," and Wien Bridge forms.

This part contains detailed design procedures and tables of values for the various types of proportional-derivative networks. Several forms of parallel "T" networks arise from the fact that there are five independent time constants in the network, while in order to realize the desired transfer characteristic it is necessary to impose only four conditions. It is indicated how the remaining degree of freedom may be used to obtain the most suitable input and output impedances for the source and load impedances with which the parallel "T" is to be used. The derivations for the parallel "T" formulae are given in an Appendix.

Tolerance requirements on the components of parallel "T" and bridge "T" networks are derived. If ± 1 per cent components are used at 60 cycles, the resonant frequency will lie between 56.4 and 63.6 cycles, and the notch width (rejection bandwidth) will be within ± 0.99 cps. of the correct value. In order to guarantee that the phase shift at 60 cycles is within $\pm 10°$, the percentage deviation of each part must be less than $(9.0/T_d\omega_0)$, where ω_0 is the carrier angular frequency, T_d the derivative time constant.

1. INTRODUCTION.

In a servo controller characteristic, including the servo motor and load, time lags inevitably are present. The stability of the servo-

* This paper is a continuation of part I, published in the JOURNAL OF THE FRANKLIN INSTITUTE, Vol. 246, July, 1948, p. 21. Part III will follow in the September issue.

[1] Formerly with Radiation Laboratory, Massachusetts Institute of Technology, Cambridge, Mass.; now at Watson Laboratories, Cambridge Field Station, Cambridge, Mass.

(Note—The Franklin Institute is not responsible for the statements and opinions advanced by contributors in the JOURNAL.)

mechanism is greatly improved by adding to the voltage proportional to the error, which is amplified and applied to the control winding of the servo motor, a component proportional to the derivative of the error. The latter component compensates for the presence of the time lags; effectively it endows the controller with a quality of being able to anticipate and appropriately correct the errors.

In an alternating current servo, the error is the modulation envelope of a modulated-carrier error voltage. Differentiation of the modulation envelope has previously [2] been accomplished approximately by a "resonant" form of parallel "T" network, that is a network in which there is complete rejection, and a discontinuity [3] in phase shift, a jump from $-90°$ to $+90°$, at the carrier frequency, the magnitude of the response

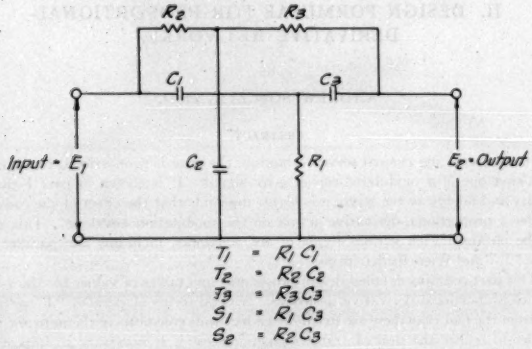

FIG. 1.

at other frequencies being approximately proportional to the deviation from the carrier frequency. (A more complete description is given in following sections.) The component with modulation proportional to the error is then obtained by a divider or transformer arrangement and combined with the differentiated component to give the desired proportional-derivative stabilizing effect.

In the following sections formulae are presented for a number of forms of parallel "T" networks which to the writer's knowledge have not been previously discussed. These networks give both the proportional and differentiated components directly in the envelope of the modulated output.

Sections 13 through 15 are devoted to derivation of the tolerance requirements on the components of parallel "T" and bridge "T" net-

[2] It is discussed, for example, in an unpublished memorandum by G. T. Coate.

[3] The discontinuity arises from the fact that the magnitude is taken to be non-negative at all frequencies. Change of sign of the amplitude response is equivalent to 180° phase shift.

works. Formulae are obtained for the variations (1) of parallel "T" resonant frequency ω_0, (2) of derivative time constant T_d (or, equivalently, of notch width $1/\pi T_d$), (3) of phase shift at carrier frequency, (4) of input and output impedance, in terms of the variations of the individual components of the networks from their correct values. From these formulae are derived percentage tolerances for the components. Gain-phase margin diagrams are given to show the effect of varying T_d, and of incorrect resonant frequency ω_0. (The effect of incorrect carrier phase has been discussed in part I.)

2. PARALLEL "T" NETWORKS.

The parallel "T" network is shown in Fig. 1. Let time constants be defined as follows:

$$T_1 = R_1C_1, \quad T_2 = R_2C_2, \quad T_3 = R_3C_3, \quad S_1 = R_1C_3, \quad S_2 = R_2C_3.$$

Except for the impedance level, which always may be changed by simple scale transformation of the R's and C's, the parallel "T" is determined by the five constants T_1, T_2, T_3, S_1, S_2. For if these constants are known, and if any one of the components, say for example, C_3, is arbitrarily specified, then the other components are determined:

$$R_1 = S_1/C_3, \quad R_2 = S_2/C_3, \quad R_3 = T_3/C_3, \quad C_1 = T_1/R_1, \quad C_2 = T_2/R_2.$$

3. TRANSFER CHARACTERISTIC; INPUT AND OUTPUT IMPEDANCES.

The transfer characteristic of the parallel "T" is

$$\frac{E_2}{E_1} = \frac{T_1T_2T_3p^3 + T_1(S_2 + T_3)p^2 + (T_1 + S_1)p + 1}{T_1T_2T_3p^3 + [T_1(S_2 + T_3) + T_2(T_1 + S_1 + T_3)]p^2 + (T_1 + S_1 + T_2 + S_2 + T_3)p + 1}. \tag{1}$$

The appropriate form which this is made to assume in order to obtain the approximate proportional-derivative characteristic at carrier frequency ω_0 is

$$\frac{E_2}{E_1} = \frac{(Up + 1)\left(\frac{1}{\omega_0^2}p^2 + \frac{2}{n\omega_0}p + 1\right)}{(Up + 1)\left(\frac{1}{\omega_0^2}p^2 + \frac{2}{m\omega_0}p + 1\right)} = \frac{m}{n}\frac{\left[1 + jT_d\frac{\omega + \omega_0}{2\omega}(\omega - \omega_0)\right]}{\left[1 + jl\frac{\omega + \omega_0}{2\omega}(\omega - \omega_0)\right]}, \tag{2}$$

where in the second expression $j\omega$ has been substituted for p, and $T_d = n/\omega_0$ is the derivative time constant, $l = m/\omega_0$ is the time lag. The second expression is obtained by multiplying numerator and denominator of the first by $n\omega_0/2p$, and then factoring n/m out of the

denominator. The choice of the time indeterminate U, the coefficient of p in the linear factor which cancels in the numerator and denominator, does not affect the transfer characteristic. (But it does affect the input and output impedances, as will be seen.) If $E_1 = E(t) \sin \omega_0 t$, the approximation $(\omega + \omega_0)/2\omega \cong 1$ is valid when the modulation $E(t)$ does not have high frequency components of large amplitude.

To realize the above transfer characteristic, the determining constants of the parallel "T" must have the following values:

$$T_1 = \frac{A^2 + B_1U + U^2}{B_2 - B_1} = \frac{g(nu^2 + 2u + n)}{2\omega_0(1 - g)},$$

$$T_2 = \frac{U^2(B_2 - B_1)}{A^2 + B_1U + U^2} = \frac{2(1 - g)u^2}{g\omega_0(nu^2 + 2u + n)},$$

$$T_3 = \frac{A^2}{U} = \frac{1}{u\omega_0}, \tag{3}$$

$$S_1 = B_1 + U - T_1 = \frac{1}{\omega_0} \frac{-gn^2u^2 + 2n(1 - 2g)u + 4(1 - g) - n^2g}{2n(1 - g)},$$

$$S_2 = B_2 - B_1 - \frac{A^2}{U} - T_2 = \frac{[4(1 - g) - gn^2]u^2 + 2(1 - 2g)nu - gn^2}{gnu\omega_0(nu^2 + 2u + n)},$$

where $A^2 = 1/\omega_0^2$, $B_1 = 2/n\omega_0 = 2/T_d\omega_0^2$, $B_2 = 2/m\omega_0 = 2/l\omega_0^2$, $u = U\omega_0$, and the gain $g = m/n$.

The condition for non-negative S_1 is that u be in the interval with end-points $\frac{1}{m} - \frac{2}{n} \pm \frac{1}{m}\sqrt{1 - m^2}$. The condition for non-negative S_2 is that u be in the interval with end-points $\frac{-n^2 + 2mn \pm n^2\sqrt{1 - m^2}}{4n - 4m - mn^2}$. Therefore for realizability, $m < 1$ and u must lie in the common portion of the two intervals. The possible values of u are indicated in Fig. 2. The left and right hand curves, which lie mainly between $u = 0.8$ and $u = 1.2$, are approached asymptotically by, respectively, the right and left boundaries of the regions for u, as m approaches 1.

For the general parallel "T," the input impedance, with the output open-circuited, is

$$Z_i = \frac{T_1T_2T_3p^3 + [T_1(S_2 + T_3) + T_3(T_1 + S_1 + T_3)]p^2 + (T_1 + S_1 + T_2 + S_2 + T_3)p + 1}{(C_1T_2T_3 + C_2T_1T_3 + C_3T_1T_2)p^3 + [C_1(T_3 + T_2 + S_3) + C_2(T_3 + T_1 + S_1)]p^2 + (C_1 + C_2 + C_3)p}. \tag{4}$$

The impedance looking back into the output, with the input short-circuited, is:

$$Z_o = \frac{R_3T_2(S_1 + T_1)p^2 + [R_3(S_1 + T_1 + T_2) + R_2(S_1 + T_1)]p + R_2 + R_3}{T_1T_2T_3p^3 + [T_1(S_2 + T_3) + T_2(T_1 + S_1 + T_3)]p^2 + (T_1 + S_1 + T_2 + S_2 + T_3)p + 1}. \quad (5)$$

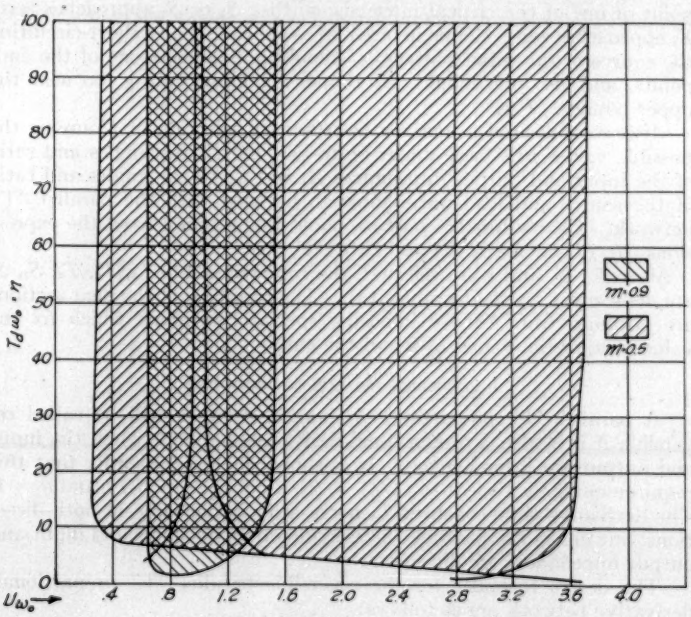

FIG. 2. Possible values of $U\omega_0$. Gain $= \frac{m}{n}$ (m cannot be $\geqq 1$).

The impedances Z_i and Z_o may be expressed in terms of U and one of the parallel "T" constants, say, for example, C_3:

$$Z_i(C_3, U) = \frac{1}{C_3} \frac{(Up + 1)\left(\frac{1}{\omega_0^2}p^2 + B_2p + 1\right)}{\left[\left(\frac{1}{S_1} + \frac{1}{S_2}\right)\frac{1}{\omega_0^2} + U\right]Up^3 + (B_2 - B_1)\left(\frac{T_1}{S_1} + \frac{U}{S_2}\right)p^2 + \left(\frac{T_1}{S_1} + \frac{T_2}{S_2} + 1\right)p}, \quad (6)$$

$$Z_o(C_3, U) = \frac{T_2(B_1 + U)p^2 + [(B_1 + U)(1 + S_2U\omega_0^2) + T_2]p + (1 + S_2U\omega_0^2)}{C_3U\omega_0^2(Up + 1)\left(\frac{1}{\omega_0^2}p^2 + B_2p + 1\right)}, \quad (7)$$

where T_1, T_2, S_1, S_2 are given in terms of U by formulae (3) above. From the expression for Z_i, it is evident that as U approaches an end-point of one of the critical intervals, so that S_1 or S_2 approaches zero, Z_i approaches zero. Thus in order to avoid practically short-circuiting the source of the input voltage, U should not be near one of the end-points, and also one should not choose a voltage gain g too near the upper bound $1/T_d\omega_0$.

If it were desired to make a discriminate selection of U among the possible values, the basis might be to best match the angles and ratio of the input and output impedances Z_i and Z_o to the angles and ratio of the source and load impedances to be used with the parallel "T" network. Charts for this purpose could be prepared from the expressions (6), (7) for $Z_i(C_3, U)$ and $Z_o(C_3, U)$.

After T_d, U, and g are selected, the time constants T_1, T_2, T_3, S_1, S_2 are determined by the formulae (3). The formulae in the next sections are obtained from (3) by imposing special conditions which fix the value of u, or the values of u and the gain g.

4. REVERSIBLE PARALLEL "T" NETWORKS.

A parallel "T" proportional-derivative network will be called reversible if it is also a proportional-derivative network when the input and output are interchanged. It is shown in the Appendix that this requirement is equivalent to $C_3/C_1 = R_2/R_3$, or $S_1T_3 = S_2T_1$, and $u = 1$. The derivative time constant T_d necessarily is the same in both directions, but unless the parallel "T" is symmetric, the gains and input and output impedances are different.

The design formulae for the reversible parallel "T" proportional-derivative network are as follows:

$$T_1 = \frac{g}{1-g}\frac{(n+1)}{\omega_0},$$

$$T_2 = \frac{1-g}{g}\frac{1}{\omega_0}\frac{1}{(n+1)},$$

$$T_3 = \frac{1}{\omega_0},$$

$$S_1 = \frac{1}{\omega_0}\left[\frac{(2+n)(1-g) - gn(n+1)}{n(1-g)}\right],$$

$$S_2 = \frac{1}{\omega_0}\left[\frac{2(1-g)(n+1) - n(gn+1)}{gn(n+1)}\right], \quad (8)$$

where $T_d\omega_0 = n$ and g is the gain in the forward direction. The gain g and n may be selected as desired; the gain g' in the reverse direction then may be seen to be

$$g' = \frac{g(n^2 + 2n + 2) - (n + 2)}{g(2n^2 + 3n + 2) - (n^2 + 2n + 2)}. \tag{9}$$

To express g in terms of g', it is necessary merely to interchange g and g'. Figure 3 shows the values and relationship of the forward and reverse

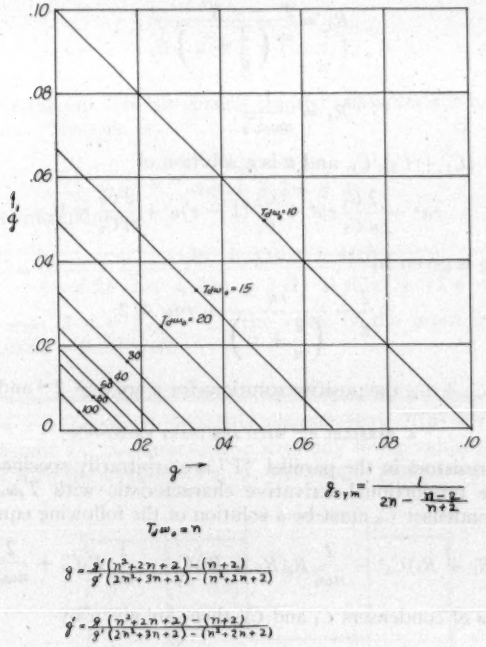

FIG. 3. Forward and reverse gains for reversible parallel "T."

gains g and g', for several values of $T_d\omega_0 = n$.

If the parallel "T" is symmetric, that is $C_3 = C_1$ and $R_2 = R_3$, or $S_1 = T_1$ and $S_2 = T_3$, the gain is

$$g = g' = g_{sym.} = \frac{1}{2n - \dfrac{n - 2}{n + 2}}. \tag{10}$$

5. PARALLEL "T" WITH ARBITRARY CONDENSERS.

Let us assume that the values of the condensers C_1, C_2, C_3 in the parallel "T" are known or specified, and determine the values of R_1, R_2, R_3 to realize any desired $T_d = n/\omega_0$. Eliminating g and u from Eqs. 3, we find

$$R_1 = \frac{1}{\omega_0}\frac{\left(\frac{2}{n}+u\right)}{(C_1+C_3)},$$

$$R_2 = \frac{r}{\omega_0}\frac{u^2}{\left(\frac{2}{n}+u\right)C_2}, \tag{11}$$

$$R_3 = \frac{1}{u\omega_0 C_3},$$

where $r = (C_1 + C_3)/C_1$, and u is a solution of

$$ru^3 - \frac{2}{n}\frac{C_2}{C_3}ru^2 + \frac{C_2}{C_3}(1-r)u + \frac{2}{n}\frac{C_2}{C_3} = 0. \tag{12}$$

The gain g is given by

$$\frac{2}{g} = \frac{rn}{\left(\frac{2}{n}+u\right)} + rnu + 2. \tag{13}$$

For $C_1 = C_2 = C_3$, the positive solutions for u are $u = 2^{-\frac{1}{2}}$ and $u = 2/n$.

6. PARALLEL "T" WITH ARBITRARY RESISTORS.

If the resistors in the parallel "T" are arbitrarily specified, then to realize the proportional-derivative characteristic with $T_d\omega_0 = n$, the value of condenser C_3 must be a solution of the following equation:

$$R_1R_3(R_2+R_3)C_3^3 - \frac{2}{n\omega_0}R_3(R_2+R_3)C_3^2 - \frac{1}{\omega_0^2}R_2C_3 + \frac{2}{n\omega_0^3} = 0.$$

The values of condensers C_1 and C_2, then, are given by

$$C_1 = \frac{1}{R_1R_3C_3\omega_0^2} + \frac{2}{R_1n\omega_0} - C_3$$

and

$$C_1C_2 = \frac{1}{R_1R_2R_3^2C_3^2\omega_0^4}.$$

The gain is given by

$$\frac{2}{gn} = \frac{1}{\omega_0R_1C_1}\left(1 + \frac{2}{n\omega_0R_3C_3} + \frac{1}{\omega_0^2R_3^2C_3^2}\right) + \frac{2}{n}.$$

For the case of equal resistors, $R_1 = R_2 = R_3 = R$, the two positive solutions of the cubic are $RC_3 = 2^{-\frac{1}{2}}\omega_0^{-1}$ and $RC_3 = 2/n\omega_0$. The values of the condensers corresponding to the first solution are:

$$C_3 = \frac{1}{2^{\frac{1}{2}}R\omega_0},$$

$$C_1 = \frac{1}{R\omega_0}\left(2^{-\frac{1}{2}} + \frac{2}{n}\right)$$

$$C_2 = \frac{1}{R\omega_0}\frac{2}{\left(2^{-\frac{1}{2}} + \frac{2}{n}\right)}.$$

The indeterminate U in the general transfer characteristic has the value $U = 2^{\frac{1}{2}}/\omega_0$. The gain is:

$$g = \frac{2^{\frac{1}{2}}n + 4}{3n^2 + 3\cdot 2^{\frac{1}{2}}n + 4}.$$

The input impedance is:

$$Z_i = \frac{(3n^2 + 3\sqrt{2}\,n + 4)jR}{(-5.25\sqrt{2}\,n^2 - 18n - 2\sqrt{2}) + j(2n^2 + \sqrt{2}\,n + 4)}.$$

For the case of $n = T_d\omega_0 = 15$, the value of the input impedance is $Z_i = (0.0882 - 0.3606j)R$.

7. DIVIDER CIRCUITS TO INCREASE AND DECREASE T_d.

Given a proportional derivative characteristic $B(p)$ with derivative time constant T_d', a characteristic with any lower value of T_d may be obtained with the circuit of Fig. 4, assuming a perfect voltage divider,

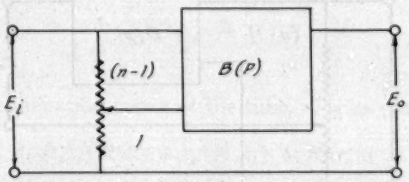

FIG. 4.

that is, neglecting the loading effect of the input impedance of $B(p)$ on the divider. (Actually the frequencies of minimum output and zero phase of $B(p)$ will change; the amount of this shift may be readily calculated; or for fixed divider values $B(p)$ may be designed to give exactly the desired characteristic in combination with the divider.) In par-

ticular, $T_d\omega_0 = n$ may be taken to be ∞ in the formulae of the preceding sections, to obtain a "resonant" parallel "T," and then with suitable divider values any desired T_d may be obtained.

The transfer characteristic of a resonant parallel "T" is:

$$\frac{jl\,\frac{\omega+\omega_0}{2\omega}(\omega-\omega_0)}{1+jl\,\frac{\omega+\omega_0}{2\omega}(\omega-\omega_0)}.$$

If $B(j\omega)$ in Fig. 4 is this transfer characteristic, assuming a perfect divider of ratio $1/n$, the transfer characteristic of Fig. 4 is

$$\frac{E_o}{E_i} = \frac{1}{n}\left[1+\frac{j(n-1)l\,\frac{\omega+\omega_0}{2\omega}(\omega-\omega_0)}{1+jl\,\frac{\omega+\omega_0}{2\omega}(\omega-\omega_0)}\right]$$

$$= \frac{l}{T_d}\left[\frac{1+jT_d\,\frac{\omega+\omega_0}{2\omega}(\omega-\omega_0)}{1+jl\,\frac{\omega+\omega_0}{2\omega}(\omega-\omega_0)}\right],$$

where $T_d = n/\omega_0$, which is the same as (2). Although the gain for the combination of resonant "T" and divider is the same as for the proportional-derivative parallel "T," the former has the disadvantage that the input impedance is lower for equivalent output impedances.

Given a proportional-derivative characteristic $B(p)$, a characteristic with any higher value of T_d may be obtained with the circuit of Fig. 5.

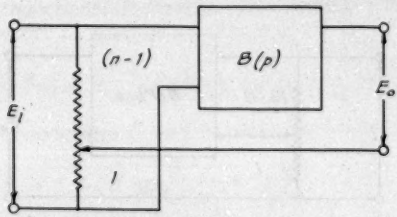

FIG. 5.

In this case there is no loading effect on the divider, so it is unnecessary to make corrective calculations as it is in the case of Fig. 4. If

$$B(p) = \left[1+jT_d'\,\frac{\omega+\omega_0}{2\omega}(\omega-\omega_0)\right]\Big/\left[1+jl\,\frac{\omega+\omega_0}{2\omega}(\omega-\omega_0)\right],$$

then for Fig. 5,

$$\frac{E_o}{E_i} = \frac{n-1}{n}\,\frac{l}{T_d}\,\frac{1 + jT_d\,\dfrac{\omega+\omega_0}{2\omega}\,(\omega-\omega_0)}{1 + jl\,\dfrac{\omega+\omega_0}{2\omega}\,(\omega-\omega_0)},$$

where

$$T_d = (n-1)l/(nl/T_d' - 1), \quad n = (T_d/l - 1)/(T_d/T_d' - 1).$$

This is the same as (2) except that the gain is lower by the factor $(n-1)/n$. If $n < T_d'/l$, T_d is negative, and a servo using the circuit of Fig. 5 then naturally would be less stable than a proportional servo.

A scheme for increasing T_d, in which input and output have a common terminal (which may be grounded), is shown in Fig. 6.

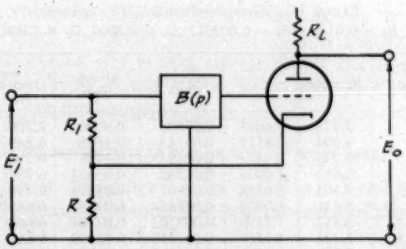

FIG. 6.

If T_d' is the derivative time constant of $B(p)$, it may be shown that the derivative time constant T_d of E_o/E_i is given by

$$T_d = \frac{T_d'}{1 - \dfrac{(\mu+1)a}{\mu(1-b)}} \cong \frac{R+R_1}{R_1}\,T_d',$$

where μ is the amplification factor of the tube, r_p is its plate resistance, and

$$a = R(r_p + R_L)/[R(R_1 + r_p + R_L) + R_1(r_p + R_L)],$$

$$(1-b) = (R+R_1)(r_p + R_L)/[R(R_1 + r_p + R_L) + R_1(r_p + R_L)].$$

8. NUMERICAL VALUES FOR 60-CYCLE PARALLEL "T" 's.

Following is a table of values of R's and C's for various parallel "T" networks of the types described in the preceding sections, for a carrier frequency of 60 cycles. The R's and C's are numbered as in Fig. 1.

The "notch width" of a band-rejection network is defined as the

TABLE I.—*Symmetric Parallel "T" Networks, $f_o = 60$ cps.*
$R_2 = R_3 = 0.002652$, $C_1 = C_3 = 1.000$.

T_{sec}	Notch Interval, cps.	$R_1 \times 10^3$	C_2	Forward Gain	Reverse Gain	Input Impedance, $Z_i \times 10^3$	Output Impedance, $Z_o \times 10^3$
2.5	±24	2.387	1.1111	0.2045	0.2045	$1.667(1-j)$	$1.869(1-j)$
5	±12	1.856	1.4286	0.1045	0.1045	$1.481(1-j)$	$1.465(1-j)$
7.5	±9	1.680	1.5790	0.06934	0.06934	$1.425(1-j)$	$1.418(1-j)$
10	±6	1.591	1.6667	0.05172	0.05172	$1.399(1-j)$	$1.395(1-j)$
15	±4	1.503	1.7647	0.03421	0.03421	$1.373(1-j)$	$1.372(1-j)$
20	±3	1.459	1.8182	0.02552	0.02552	$1.361(1-j)$	$1.360(1-j)$
30	±2	1.414	1.8750	0.01691	0.01691	$1.349(1-j)$	$1.349(1-j)$
40	±1.5	1.392	1.9048	0.01264	0.01264	$1.343(1-j)$	$1.343(1-j)$
50	±1.2	1.379	1.9231	0.01009	0.01009	$1.340(1-j)$	$1.340(1-j)$
60	±1.0	1.370	1.9355	0.008400	0.008400	$1.337(1-j)$	$1.337(1-j)$
∞	(Resonant)	1.326	2.0000			$1.326(1-j)$	$1.326(1-j)$

TABLE II.—*Reversible Parallel "T" Networks.*
$R_2 = 0.01326$, $R_3 = 0.002652$, $C_1 = 0.2000$, $C_3 = 1.000$.

T_{sec}	Notch Interval, cps.	$R_1 \times 10^3$	C_2	Forward Gain	Reverse Gain	Input Impedance, $Z_i \times 10^3$	Output Impedance, $Z_o \times 10^3$
2.5	±24	3.978	0.6667	0.07895	0.3000	$7.200(1-j)$	$1.808(1-j)$
5	±12	3.094	0.8571	0.03743	0.1628	$6.889(1-j)$	$1.574(1-j)$
7.5	±9	2.799	0.9474	0.02423	0.1105	$6.796(1-j)$	$1.487(1-j)$
10	±6	2.652	1.0000	0.01786	0.06417	$6.752(1-j)$	$1.445(1-j)$
15	±4	2.505	1.0588	0.01167	0.05574	$6.710(1-j)$	$1.404(1-j)$
20	±3	2.431	1.0909	0.008654	0.04183	$6.689(1-j)$	$1.384(1-j)$
30	±2	2.357	1.1250	0.005702	0.02787	$6.669(1-j)$	$1.364(1-j)$
40	±1.5	2.321	1.1429	0.004250	0.02090	$6.660(1-j)$	$1.354(1-j)$
50	±1.2	2.298	1.1539	0.003387	0.01671	$6.654(1-j)$	$1.349(1-j)$
60	±1.0	2.284	1.1613	0.002815	0.01392	$6.650(1-j)$	$1.345(1-j)$
∞	(Resonant)	2.210	1.2000			$6.631(1-j)$	$1.326(1-j)$

TABLE III.—*Parallel "T" Networks With Equal Condensers, $u = 1/\sqrt{2}$.*
$R_3 = 0.003751$, $C_1 = C_2 = C_3 = 1.000$.

T_{sec}	Notch Interval, cps.	$R_1 \times 10^3$	$R_2 \times 10^3$	Forward Gain	Reverse Gain	Input Impedance, $Z_i \times 10^3$	Output Impedance, $Z_o \times 10^3$	Reverse Phase Shift at ω_0
2.5	±24	1.998	1.760	0.2259	0.17419	$1.324-1.545j$	$1.798-1.768j$	−5.00°
5	±12	1.468	2.395	0.1105	0.09455	$1.303-1.573j$	$1.565-1.768j$	−1.84°
7.5	±9	1.291	2.723	0.07690	0.06467	$1.303-1.620j$	$1.469-1.768j$	−0.95°
10	±6	1.203	2.934	0.05237	0.04807	$1.289-1.640j$	$1.418-1.768j$	−0.57°
15	±4	1.114	3.155	0.03395	0.03200	$1.280-1.675j$	$1.364-1.768j$	−0.27°
20	±3	1.070	3.286	0.02505	0.02394	$1.274-1.695j$	$1.337-1.768j$	−0.16°
30	±2	1.026	3.427	0.01640	0.01590	$1.267-1.717j$	$1.306-1.768j$	−0.06°
40	±1.5	1.004	3.503	0.01218	0.01202	$1.264-1.729j$	$1.293-1.768j$	−0.04°
50	±1.2	0.9907	3.550	0.009682	0.009500	$1.261-1.737j$	$1.285-1.768j$	−0.02°
60	±1.0	0.9818	3.582	0.008034	0.007910	$1.260-1.742j$	$1.279-1.768j$	−0.01°
∞	(Resonant)	0.9378	3.751			$1.250-1.768j$	$1.250-1.768j$	

length of the frequency interval between the points at which the output is $\sqrt{2}$ times the minimum output. A proportional-derivative network may be characterized as well by the notch width, as by the derivative time constant T_d. The notch widths in the following table are for the ideal proportional-derivative characteristic $[1 + jT_d(\omega - \omega_0)]$; they are only slightly different from the actual ones for the parallel "T" networks. Evidently for the ideal characteristic at 60 cycles, the end points of the notch interval are at distances $\pm \frac{1}{2\pi T_d} = \pm \frac{60}{n}$ cps. from 60 cps., where $T_d\omega_0 = n$.

The R's and C's in Tables I, II, and III are in corresponding units, as for example megohms and microfarads. As mentioned previously, a parallel "T" with any desired different impedance level may be obtained from the values in the table by multiplying R's by any constant and dividing C's by the same constant. For a carrier frequency f different from 60 cycles, if $f = 60a$, divide either the R's or C's by a, divide T_d by a, multiply notch width by a; and Z_i/R_3 and Z_o/R_3 at carrier frequency are unchanged.

9. DESIGN FORMULAE FOR BRIDGE "T" NETWORKS.

The two forms of the bridge "T" proportional-derivative networks, Fig. 7(a) and (b), may be obtained as special cases of the parallel "T"

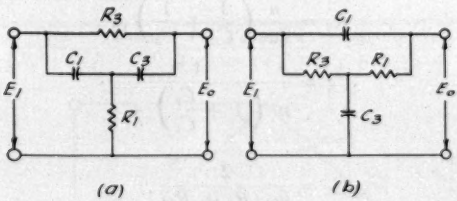

FIG. 7.

in Fig. 1, (a) by taking $R_2 = 0$, and (b) by taking $C_1 = \infty$. In (b), R_2 of Fig. 1 is changed to R_3, R_3 is changed to R_1, C_2 to C_1, C_3 to C_2, for convenience, so that similar formulae will apply to both (a) and (b).

The transfer characteristic is

$$\frac{E_o}{E_1} = \frac{T_1T_3p^2 + (T_1 + S_1)p + 1}{T_1T_3p^2 + (T_1 + S_1 + T_3)p + 1},$$

where $T_1 = R_1C_1$, $T_3 = R_3C_3$; and $S_1 = R_1C_3$ in case (a), $S_1 = R_3C_1$ in case (b).

To realize the proportional derivative characteristic (2), with derivative time constant T_d and lag l, or gain $g = l/T_d$, the time constants

T_1, T_3, S_1 are given by the following formulae:

$$T_3 = \frac{2}{\omega_0^2}\left(\frac{1}{l} - \frac{1}{T_d}\right) = \frac{2}{\omega_0^2 T_d}\left(\frac{1}{g} - 1\right),$$

$$T_1 = \frac{1}{2\left(\frac{1}{l} - \frac{1}{T_d}\right)} = \frac{T_d}{2\left(\frac{1}{g} - 1\right)},$$

$$S_1 = \left[\frac{2}{T_d\omega_0^2} - \frac{1}{2\left(\frac{1}{l} - \frac{1}{T_d}\right)}\right] = \frac{2}{T_d\omega_0^2} - \frac{T_d}{2\left(\frac{1}{g} - 1\right)}.$$

For positive S_1, $g < 4/(4 + n^2)$, where $n = T_d\omega_0$. For the parallel "T," the upper bound of gain is $1/n$. Thus for n greater than 2, the gains attainable with the bridge "T" are considerably smaller than those which can be obtained with the parallel "T." (Also, since the time lag l is smaller, the relative amplification at frequency $3\omega_0$, the predominant frequency of synchro "hash," is greater for the bridge "T.")

The following formulae in terms of arbitrary C_1, C_3 for case (a), and in terms of arbitrary R_1, R_3 for case (b), may be more convenient. For case (a),

$$R_1 = \frac{2}{n\omega_0(C_1 + C_3)},$$

$$R_3 = \frac{n}{2\omega_0}\left(\frac{1}{C_1} + \frac{1}{C_3}\right),$$

$$g = \frac{4}{n^2\left(1 + \frac{C_3}{C_1}\right) + 4}.$$

For case (b),

$$C_1 = \frac{2}{n\omega_0(R_1 + R_3)},$$

$$C_3 = \frac{n}{2\omega_0}\left(\frac{1}{R_1} + \frac{1}{R_3}\right),$$

$$g = \frac{4}{n^2\left(1 + \frac{R_3}{R_1}\right) + 4}.$$

The formulae for (b) are obtained from those for (a) by interchanging R_1 with C_1, and R_3 with C_3.

From the above formulae, it is clear that any bridge "T" is reversible, with the same T_d but different gains in the forward and reverse directions, unless it is symmetric, that is $C_1 = C_3$ in case (a) $R_1 = R_3$ in case (b).

10. INPUT AND OUTPUT IMPEDANCES.

For bridge "T" (*a*), the input impedance (with the output open-circuited) is

$$Z_i = R_1 + \frac{(T_3p + 1)}{C_1T_3p^2 + (C_1 + C_3)p}.$$

The output impedance (with the input short-circuited) is

$$Z_o = \frac{R_3[(S_1 + T_1)p + 1]}{T_1T_3p^2 + (T_1 + S_1 + T_3)p + 1},$$

where $S_1 = R_1C_3$.

For bridge "T" (*b*), the input impedance (with the output open-circuited) is

$$Z_i = \frac{1}{C_1p} + \frac{R_3(T_1p + 1)}{(T_1 + S_1)p + 1},$$

where $S_1 = R_3C_1$. The output impedance (with the input short-circuited) is

$$Z_o = \frac{R_1T_3p + (R_1 + R_3)}{T_1T_3p^2 + (S_1 + T_1 + T_3)p + 1}.$$

11. FORMULAE FOR WIEN BRIDGE.

The Wien Bridge proportional-derivative circuit is shown in Fig. 8. The transfer characteristic is:

$$\frac{E_o}{E_i} = \frac{R_2}{(R_1 + R_2)} \frac{T_3T_4p^2 + [T_3 + T_4 - (R_1/R_2)S_4]p + 1}{T_3T_4p^2 + (T_3 + T_4 + S_4)p + 1},$$

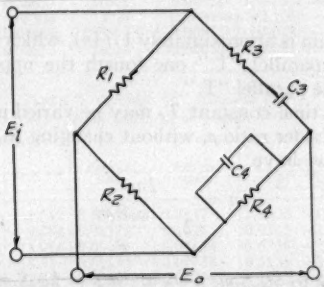

FIG. 8.

where $T_3 = R_3C_3$, $T_4 = R_4C_4$, $S_4 = R_4C_3$. The independent variables of the transfer characteristic may be taken to be T_3, T_4, S_4, and the divider ratio $\rho = R_2/(R_1 + R_2)$. Solving for T_3, T_4, S_4 in terms of

$T_d\omega_0 = n$, $l\omega_0 = m$, and ρ, we obtain:

$$T_3 = \frac{1}{\omega_0}\left[\frac{\rho}{n} + \frac{(1-\rho)}{m}\right] \pm \frac{1}{\omega_0}\left[\left(\frac{\rho}{n} + \frac{(1-\rho)}{m}\right)^2 - 1\right]^{\frac{1}{2}},$$

$$T_4 = \frac{1}{\omega_0}\left[\frac{\rho}{n} + \frac{(1-\rho)}{m}\right] \mp \frac{1}{\omega_0}\left[\left(\frac{\rho}{n} + \frac{(1-\rho)}{m}\right)^2 - 1\right]^{\frac{1}{2}},$$

$$S_4 = \frac{2\rho}{\omega_0}\left(\frac{1}{m} - \frac{1}{n}\right).$$

For a given m and ρ, the condition for realizability is $n \leqq \rho m/(m + \rho - 1)$. From the form of the transfer characteristic, the gain is $\rho m/n$. For maximum gain, $\rho = m = n - [n(n-1)]^{\frac{1}{2}} > n - [(n-0.5)^2]^{\frac{1}{2}} = 0.5$, the radical vanishes, and $T_3 = T_4 = 1/\omega_0$, $S_4 = 2(n-1)^{\frac{1}{2}}/\omega_0 n^{\frac{1}{2}}$. The maximum gain is $2\rho - 1$. For the usual values of $T_d\omega_0 = n$, the maximum obtainable gain is approximately $1/(4n)$, which is one half the gain of the symmetric parallel "T," one fourth the upper bound of gains obtainable with the parallel "T."

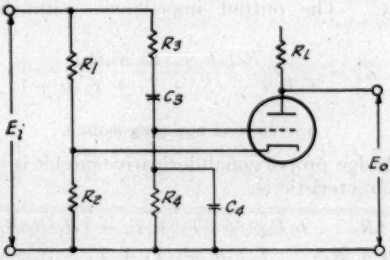

FIG. 9.

The derivative time constant T_d may be varied in the Wien Bridge by changing the divider ratio ρ, without changing R_3, C_3, R_4, C_4. Solving for $T_d\omega_0 = n$, we have

$$n = \frac{2m}{2 - \dfrac{\omega_0 S_4 m}{\rho}}.$$

Thus as ρ decreases to $\frac{1}{2}\omega_0 S_4 m$, $n \to \infty$; if $\rho = \frac{1}{2}\omega_0 S_4 m$, the Wien Bridge is "resonant"; and as ρ increases to 1, by the realizability condition, n decreases to a value not greater than 1. For any R_3, C_3, R_4, C_4 such that $T_3 T_4 \omega_0^2 = 1$, any desired T_d may be obtained by taking ρ to be sufficiently small. Since $2/m\omega_0 = T_3 + T_4 + S_4$, the maximum time lag $l = m/\omega_0$ (but not maximum gain) will be obtained if $T_3 = T_4 = 1/\omega_0$

and R_4 and C_3 are as small as possible. For $T_3 = T_4 = 1/\omega_0$, the realizability condition is $n \leqq 2\rho/[(S_4\omega_0 + 2)\rho - S_4\omega_0]$.

A vacuum tube circuit similar to Fig. 6 may be used with the Wien Bridge in order to have a common input and output terminal (which may be grounded). See Fig. 9. It may be shown that the transfer characteristic is:

$$\frac{E_o}{E_i} = \frac{-R_L R_2(\mu - 1)\left[(T_3p + 1)(T_4p + 1) - \dfrac{(R_2 + R_1\mu)S_4p}{R_2(\mu - 1)}\right]}{[R_2(R_1 + r_p + R_L) + R_1(r_p + R_L)][(T_3p + 1)(T_4p + 1) + S_4p]}.$$

If the amplification factor μ is very large compared to $R_2/R_1 = \rho/(1-\rho)$, then except for the gain factor, this transfer characteristic is the same as the transfer characteristic for Fig. 8.

12. NUMERICAL VALUES FOR BRIDGE "T" NETWORKS.

The remarks on Tables I, II, and III for parallel "T" networks apply also to Tables IV, V, and VI for 60-cycle Bridge "T" networks.

TABLE IV.—*Symmetrical Bridge "T" Networks (a)*:[4]
$C_1 = C_2 = 1.000$.

T_{sec}	Notch Interval, cps.	$R_1 \times 10^3$	$R_2 \times 10^3$	Gain	Input Impedance, $Z_i \times 10^3$	Output Impedance, $Z_o \times 10^3$
2.5	±24	1.0610	6.63	0.24242	$1.7079 - 2.135j$	$1.6075 - 2.009j$
5	±12	0.5305	13.26	0.07407	$0.9878 - 2.470j$	$0.9824 - 2.456j$
7.5	±9	0.3536	19.89	0.03433	$0.6838 - 2.564j$	$0.6830 - 2.561j$
10	±6	0.2653	26.53	0.01961	$0.5203 - 2.602j$	$0.5201 - 2.601j$
15	±4	0.1768	39.79	0.008811	$0.3505 - 2.629j$	$0.3506 - 2.629j$
20	±3	0.1326	53.05	0.004975	$0.2639 - 2.639j$	$0.2639 - 2.639j$
30	±2	0.08841	79.58	0.002217	$0.1764 - 2.647j$	$0.1764 - 2.647j$
40	±1.5	0.06631	106.1	0.001248	$0.1325 - 2.649j$	$0.1325 - 2.649j$
50	±1.2	0.05305	132.6	0.0007994	$0.1060 - 2.650j$	$0.1060 - 2.650j$
60	±1.0	0.04420	159.2	0.0005552	$0.08836 - 2.651j$	$0.08836 - 2.651j$
100	±0.6	0.02653	265.3	0.0002000	$0.05304 - 2.652j$	$0.05304 - 2.652j$

TABLE V.—*Bridge "T" Networks (a)*.[4]
$C_1 = 1.000$, $C_2 = 2.500$.

T_{sec}	Notch Interval, cps.	$R_1 \times 10^3$	$R_2 \times 10^3$	Forward Gain	Reverse Gain	Input Impedance, $Z_i \times 10^3$	Output Impedance, $Z_o \times 10^3$
2.5	±24	0.6062	4.642	0.15456	0.3137	$1.5305 - 1.914j$	$0.7175 - 0.8979j$
5	±12	0.3031	9.284	0.04372	0.1026	$0.9565 - 2.391j$	$0.4059 - 1.015j$
7.5	±9	0.2020	13.926	0.01991	0.04834	$0.6737 - 2.527j$	$0.2772 - 1.040j$
10	±6	0.1516	18.57	0.01130	0.02778	$0.5159 - 2.580j$	$0.2098 - 1.049j$
15	±4	0.1010	27.85	0.005054	0.01254	$0.3493 - 2.619j$	$0.1408 - 1.056j$
20	±3	0.07579	37.14	0.002849	0.007092	$0.2634 - 2.634j$	$0.1058 - 1.058j$
30	±2	0.05052	55.70	0.001268	0.003165	$0.1763 - 2.644j$	$0.07064 - 1.0597j$
40	±1.5	0.03789	74.27	0.0007138	0.001783	$0.1324 - 2.648j$	$0.05301 - 1.0603j$
50	±1.2	0.03031	92.84	0.0004569	0.001142	$0.1060 - 2.649j$	$0.04242 - 1.06052j$
60	±1.0	0.02526	111.4	0.0003174	0.0007930	$0.08835 - 2.650j$	$0.03536 - 1.0607j$
100	±0.6	0.01516	185.7	0.0001143	0.0002856	$0.05304 - 2.652j$	$0.02122 - 1.0609j$

[4] To obtain values for Bridge "T" (*b*), in Tables IV and V interchange R_1 with C_1, and R_2 with C_2.

TABLE VI.—*Maximum Gain Wien Bridge Networks.*

$R_3 = 0.002653$, $C_3 = 1.000$.

$Z_1 = (R_1 + R_2)$ in parallel with Z_1'. $Z_2 = R_1R_2/(R_1 + R_2)$ in series with Z_2'.

T_{deg}	Nötch Interval, cps.	$R_2/(R_1 + R_2) = p = m$	$R_4 \times 10^3$	C_4	Gain	$Z_1' \times 10^3$	$Z_2' \times 10^3$
5	±12	0.5279	4.745	0.5590	0.05572	$5.024(1-j)$	$1.252(1-j)$
10	±6	0.5162	5.033	0.5270	0.03234	$5.168(1-j)$	$1.291(1-j)$
15	±4	0.5086	5.125	0.5175	0.01724	$5.214(1-j)$	$1.303(1-j)$
20	±3	0.5064	5.171	0.5130	0.01282	$5.237(1-j)$	$1.309(1-j)$
30	±2	0.5042	5.216	0.5086	0.008476	$5.259(1-j)$	$1.315(1-j)$
40	±1.5	0.5032	5.238	0.5064	0.006330	$5.271(1-j)$	$1.318(1-j)$
50	±1.2	0.5025	5.252	0.5051	0.005050	$5.277(1-j)$	$1.319(1-j)$
60	±1.0	0.5021	5.260	0.5042	0.004220	$5.282(1-j)$	$1.320(1-j)$
100	±0.6	0.5013	5.278	0.5025	0.002512	$5.291(1-j)$	$1.322(1-j)$
∞	(Resonant)	0.5000	5.305	0.5000		$5.305(1-j)$	$1.326(1-j)$

Wien Bridge, $R_3 = 0.002653 = 2R_4$, $C_4 = 2.0 = 2C_3$, $m = 0.8$.

T_{deg}	$R_2/(R_1 + R_2) = p$	Gain
5	0.2381	0.03810
10	0.2174	0.01739
15	0.2113	0.01127
20	0.2083	0.008333
30	0.2055	0.005479
40	0.2041	0.004081
50	0.2033	0.003252
60	0.2027	0.002702
100	0.2016	0.001612
∞	0.2000	

Wien Bridge, $R_4 = 0.005305 = 2R_3$, $C_3 = 1.0 = 2C_4$, $m = 0.5$.

T_{deg}	$R_2/(R_1 + R_2) = p$	Gain
5	0.5556	0.05556
10	0.5263	0.02632
15	0.5172	0.01724
20	0.5128	0.01282
30	0.5085	0.008474
40	0.5063	0.006329
50	0.5051	0.005050
60	0.5042	0.004201
100	0.5025	0.002502
∞	0.5000	

13. VARIATION OF RESONANT FREQUENCY ω_0 OF PARALLEL "T" NETWORK.

For any parallel "T," the numerator of the transfer characteristic is of the form:

$$\left(\frac{u}{\omega_1}p + 1\right)\left(\frac{1}{\omega_1^2}p^2 + \frac{2}{n\omega_1}p + 1\right)$$

for some ω_1, u, and n. By comparison with the transfer characteristic (1) in section 3, it may be seen that the relations between these quantities and the parallel "T" constants are:

$$\frac{u}{\omega_1^3} = T_1T_2T_3 = a,$$

$$\frac{1}{\omega_1^2}\left(1 + \frac{2u}{n}\right) = T_1(S_2 + T_3) = b,$$

$$\frac{1}{\omega_1}\left(\frac{2}{n} + u\right) = (T_1 + S_1) = c.$$

Eliminating u and n, we obtain:

$$a^2x^3 - acx^2 + bx - 1 = 0,$$

where $x = \omega_1^2$. If $\Delta_i = dR_i/R_i$, $\epsilon_i = dC_i/C_i$, we have

$$da = a(\Delta_1 + \Delta_2 + \Delta_3 + \epsilon_1 + \epsilon_2 + \epsilon_3),$$
$$db = b\Delta_1 + T_1S_2\Delta_2 + T_1T_2\Delta_3 + b(\epsilon_1 + \epsilon_3),$$
$$dc = c\Delta_1 + T_1\epsilon_1 + S_1\epsilon_3,$$

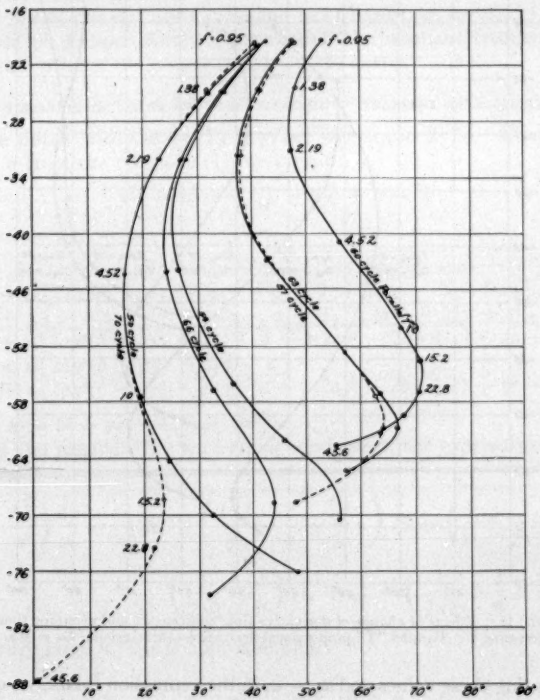

FIG. 10. Effect of incorrect ω_0 on gain-phase diagram for 60-cycle parallel "T" servo. $T_d = 15/2\pi 60$, motor time constant = 0.2 sec. Values of ω_0 from $2\pi 50$ to $2\pi 70$ (ω_0 = parallel "T" frequency).

and

$$\begin{aligned} Qdx = {} & \Delta_1[(cx^2 - 2ax^3)a - bx + acx^2] \\ & + \Delta_2[(cx^2 - 2ax^3)a - xS_2T_1] \\ & + \Delta_3[(cx^2 - 2ax^3)a - xT_1T_3] \\ & + \epsilon_1[(cx^2 - 2ax^3)a - bx + ax^2T_1] \\ & + \epsilon_2[(cx^2 - 2ax^3)a] \\ & + \epsilon_3[(cx^2 - 2ax^3)a - bx + ax^2S_1], \end{aligned}$$

where $Q = (3a^2x^2 - 2acx + b)$.

For the parallel "T" with equal condensers, section 5, we have $T_1 = S_1 = (2/n + u)/2\omega_0$, $T_2 = S_2 = 1/\omega_0(2/n + u)$, $T_3 = 1/u\omega_0$.

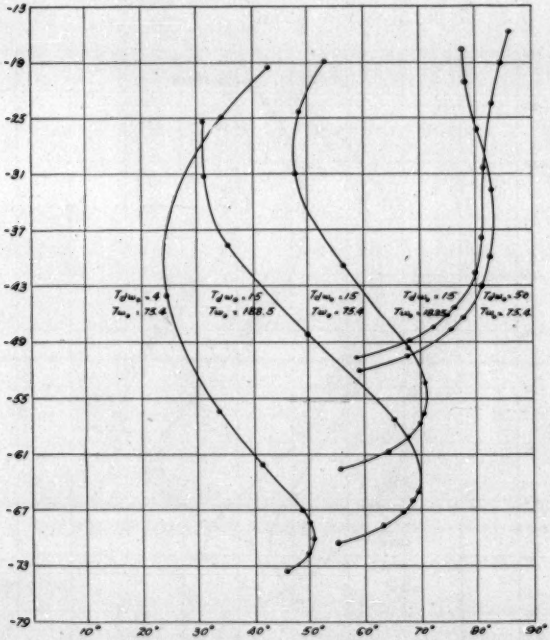

FIG. 11. Effects of change of derivative time constant T_d and of motor time constant T. Parallel "T" proportional-derivative characteristic, $k_{\omega_0} = 0.5$.

Substituting these values and $\omega_1 = \omega_0$ in the expression for dx, we obtain:

$$\left(1 + \frac{2\sqrt{2}}{n}\right)\frac{d\omega_0}{\omega_0} = \left(1 - \frac{\sqrt{2}}{n}\right)(\Delta_1 + \Delta_2) + \Delta_3 + \left(\frac{5}{4} - \frac{1}{\sqrt{2}n}\right)(\epsilon_1 + \epsilon_3) + \left(\frac{1}{2} - \frac{\sqrt{2}}{n}\right)\epsilon_2.$$

For fairly large n, this is approximately:

$$\frac{d\omega_0}{\omega_0} = \Delta_1 + \Delta_2 + \Delta_3 + \frac{5}{4}(\epsilon_1 + \epsilon_3) + \tfrac{1}{2}\epsilon_2.$$

For 5 per cent tolerance on resonant frequency ω_0 of the parallel "T" with equal condensers, taking $\Delta_1 = \Delta_2 = \Delta_3 = \Delta$ and $\epsilon_1 = \epsilon_3 = \epsilon$, $0.05 = 3\Delta + 10\epsilon/4 + \epsilon_2/2$. Therefore, in order to insure that ω_0 will fall in the range 2π 57 to 2π 63 (see curves in Fig. 10), the appropriate tolerances on the parallel "T" components are ± 0.83 per cent for R_1, R_2, R_3, ± 0.67 per cent for C_1, C_3, and ± 1.67 per cent for C_2. Uniform tolerance of ± 1 per cent will insure that the resonant frequency will fall within a band of ± 6 per cent from the correct value.

14. VARIATION OF NOTCH WIDTH OF PARALLEL "T" TRANSFER CHARACTERISTIC.

The notch width is $1/\pi T_d = y/2\pi$, where $y = 2/T_d$. Eliminating ω_1 and u from the relations (1), we obtain:

$$y(b - ay)^2 - c(b - ay) + a = 0.$$

Differentiating, we have:

$$\begin{aligned} R\,dy = {} & \Delta_1[2ay^2(b - ay) - acy - a + b(2ay^2 - 2by + c) + (b - ay)c] \\ & + \Delta_2[2ay^2(b - ay) - acy - a + T_1S_2(2ay^2 - 2by + c)] \\ & + \Delta_3[2ay^2(b - ay) - acy - a + T_1T_3(2ay^2 - 2by + c)] \\ & + \epsilon_1[2ay^2(b - ay) - acy - a + b(2ay^2 - 2by + c) + (b - ay)T_1] \\ & + \epsilon_2[2ay^2(b - ay) - acy - a] \\ & + \epsilon_3[2ay^2(b - ay) - acy - a + b(2ay^2 - 2by + c) + (b - ay)S_1], \end{aligned}$$

where $R = b^2 + ac - 4aby + 3a^2y^2$.

For the parallel "T" with equal condensers, the expression for $R\,dy$ becomes:

$$\begin{aligned} \left(\frac{3}{2} - \frac{\sqrt{2}}{n}\right)\frac{dy}{\omega_0} = {} & \frac{1}{\sqrt{2}}\Delta_1 + \left(\frac{2\sqrt{2}}{n^2} - \frac{2}{n} - \frac{1}{2\sqrt{2}}\right)\Delta_2 - \left(\frac{1}{n} + \frac{1}{2\sqrt{2}}\right)\Delta_3 \\ & + \left(\frac{1}{2\sqrt{2}} - \frac{1}{n}\right)(\epsilon_1 + \epsilon_3) - \left(\frac{1}{2\sqrt{2}} + \frac{2}{n} - \frac{2\sqrt{2}}{n^2}\right)\epsilon_2. \end{aligned}$$

For fairly large n, this is approximately:

$$\frac{3}{2}\frac{dy}{\omega_0} = \frac{1}{\sqrt{2}}\Delta_1 + \frac{1}{2\sqrt{2}}(-\Delta_2 - \Delta_3 + \epsilon_1 - \epsilon_2 + \epsilon_3).$$

Therefore if all components of the parallel "T" are correct within ± 1 per cent, dy/ω_0 will not exceed $7\sqrt{2}/6 = 1.65$ per cent in numerical value. That is, the notch width will be within ± 1.65 per cent of the carrier frequency of its correct value. For 60-cycle carrier frequency and ± 1 per cent tolerances, the variation in notch width cannot exceed $0.0165 \times 60 = 0.99$ cps. (For $T_d\omega_0 = 15$, the notch width then would be (8 ± 0.99) cps.; for $T_d\omega_0 = 30$, (4 ± 0.99) cps.).

Figure 11 shows the effect of variation of T_d (and also the effect of variation of motor time constant T).

15. VARIATION OF PHASE SHIFT AT CARRIER FREQUENCY.

The phase shift at carrier frequency ω_0 is

$$\phi = \text{arc tan}\frac{b\omega_0^2 - 1}{c\omega_0 - a\omega_0^3} - \text{arc tan}\frac{(b + T_2T_3 + T_2c)\omega_0^2 - 1}{(c + T_2 + S_2 + T_3)\omega_0 - a\omega_0^3}.$$

For fairly large n, for small variations of the parts from their correct values, the major part of the variation of ϕ is the variation of the first term; the second term is practically constant and equal to arc tan U. Accordingly for simplicity we calculate only the variation of the first term. Let the first term be denoted by ψ. Then we have:

$$\begin{aligned}A^3d\tan\psi = {} & \Delta_1[\omega_0(c - a\omega_0^2)] + \Delta_2[\omega_0^3(cT_1S_2 - a + aT_1T_3\omega_0^2)] \\ & + \Delta_3[\omega_0^3(cT_1T_3 - a + aT_1S_2\omega_0^2)] + \epsilon_1[\omega_0(bS_1\omega_0^2 - a\omega_0^2 + T_1)] \\ & + \epsilon_2[a\omega_0^3(b\omega_0^2 - 1)] + \epsilon_3[\omega_0(bT_1\omega_0^2 - a\omega_0^2 + S_1)],\end{aligned}$$

where $A = (c\omega_0 - a\omega_0^3)$. For the parallel "T" with equal condensers,

$$d\tan\psi = \frac{n}{2}(\Delta_1 + \Delta_2) + \left(\frac{n}{2} + \frac{1}{\sqrt{2}}\right)\Delta_3 + \left(\frac{5n}{8} + \frac{1}{2\sqrt{2}}\right)(\epsilon_1 + \epsilon_3) + \frac{n}{4}\epsilon_2,$$

and arc tan U = arc tan $2^{-\frac{1}{2}} = 35.26°$. Since tan $45.26° = 1.0094$ and tan $25.26° = 0.4720$, the conditions for phase shift within $\pm 10°$ are $d\tan\psi < +0.3023$ and $-0.2351 < d\tan\psi$. Thus in case $n = T_0\omega_0 = 15$, the appropriate tolerances are $+0.67$ per cent, -0.52 per cent for R_1, R_2; $+0.61$ per cent, -0.48 per cent for R_3; $+0.52$ per cent, -0.40 per cent for C_1, C_3; $+1.34$ per cent, -1.05 per cent, for C_2; or a uniform tolerance of $+0.65$ per cent, -0.51 per cent on all parts.

For the symmetric parallel "T," the corresponding conditions are $-0.0572 < 1.488\Delta_1 + 1.811(\Delta_2 + \Delta_3) + 2.055(\epsilon_1 + \epsilon_3) + \epsilon_2$ for $-10° < \phi$, and $0.66\Delta_1 + 1.397(\Delta_2 + \Delta_3) + 1.227(\epsilon_1 + \epsilon_3) + \epsilon_2 < 0.04$ for $\phi < +10°$, which requires a uniform tolerance of $+0.58$ per cent, -0.56 per cent on all parts. (For n different from 15, the tolerances should be multiplied by approximately $15/n$.)

For the resonant symmetric parallel "T" with perfect divider, the conditions are:

$$-45.7\Delta_1 - 54.16\Delta_2 - 53.3\Delta_3 - 59.3\epsilon_1 - 33.72\epsilon_2 - 60.2\epsilon_3 < 1.72 \quad \text{for} \quad -10° < \phi,$$

$$22.4\Delta_1 + 40.3\Delta_2 + 40.9\Delta_3 + 36.7\epsilon_1 + 30.8\epsilon_2 + 36.1\epsilon_3 < 1.2 \text{ for } \phi < 10°,$$

which requires the same uniform tolerance of $+0.58$ per cent, -0.56 per cent on all parts.

For the symmetric bridge "T," the corresponding conditions are:

$$-0.0235 < \Delta_1 + \epsilon_1 + \Delta_3 + \epsilon_3 < 0.0235 \quad \text{for} \quad -10° < \phi < 10°,$$

which requires a uniform tolerance of ± 0.59 per cent on all parts. (For n different from 15, multiply tolerances by $15/n$.)

For the general bridge "T," if ϕ is the phase shift at carrier frequency,

$$\tan \phi = -(\Delta_1 + \epsilon_1 + \Delta_3 + \epsilon_3) \frac{nr}{2\left(\frac{4}{n^2} + r\right)},$$

where $r = (C_1 + C_3)/C_1$ (R_1, C_1, R_3, C_3 are as in Fig. 7(a), section 9; C_1 is the condenser on the input side).

For the bridge "T" with values as in Fig. 12, $T_d\omega_0 = 11$, and the conditions for phase shift at 60 cycles within $\pm 10°$ are:

$$-0.32 < \Delta_1 + \epsilon_1 + \Delta_3 + \epsilon_3 < 0.32,$$

which requires ± 0.8 per cent tolerance on all parts, or for example ± 1.5 per cent tolerance on C's if the R's are held to within ± 0.1 per

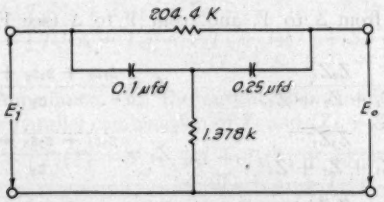

FIG. 12.

cent. The input impedance at 60 cycles in k is $Z_i = 4.24 - 26.16j$. The fractional change of this impedance as a function of the variations of the components is:

$$\frac{\Delta Z_i}{Z_i} = (0.0211 + 0.0895j)\Delta_1 - (0.607 + 0.416j)\Delta_3 - (0.927 + 0.117j)\epsilon_1 - (0.659 + 0.209j)\epsilon_3.$$

This result will be used in a calculation of tolerance on the components of a phase lag network in Part III.

APPENDIX.

Analysis of the Parallel "T" Network.

In this appendix the method will be indicated by means of which the formulae of sections 3 through 6 were derived. In the last section, formulae are obtained to realize a proportional-derivative characteristic with phase shift of the carrier.

1. Transfer Characteristic and Input and Output Impedances.

It is convenient to transform each "T" (or "Y") of the parallel "T" to its equivalent "π" (or "Δ") of impedances. The formulae for

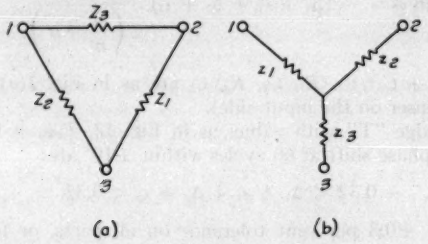

FIG. 13.

transformation from Δ to Y, and from Y to Δ (see Fig. 13), are as follows:

$$z_1 = \frac{Z_2Z_3}{Z_1+Z_2+Z_3}, \qquad Z_1 = \frac{z_1z_2+z_1z_3+z_2z_3}{z_2},$$

$$z_2 = \frac{Z_3Z_1}{Z_1+Z_2+Z_3}, \qquad Z_2 = \frac{z_1z_2+z_1z_3+z_2z_3}{z_3},$$

$$z_3 = \frac{Z_1Z_2}{Z_1+Z_2+Z_3}, \qquad Z_3 = \frac{z_1z_2+z_1z_3+z_2z_3}{z_1}.$$

These formulae are well known. If unfamiliar to the reader, they may be established easily by a simple application of Kirchoff's laws.

In the parallel "T" as in Fig. 1, let $z_1' = R_1$, $z_2' = R_2$, $z_3' = 1/C_2p$; $z_1'' = 1/C_1p$, $z_2'' = 1/C_3p$, $z_3'' = R_1$. Then after the transformation of

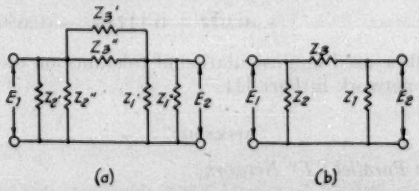

FIG. 14. Networks equivalent to the parallel "T" network.

each "T" to its equivalent "π," the parallel "T" network becomes the network shown in Fig. 14(*a*). For $k = 1, 2, 3$, let Z_k be the impedance

of the parallel combination of Z_k' and Z_k''. Then it may be seen that

$$Z_2 = \frac{(T_2p + a)[(S_1 + T_1)p + 1]}{(T_2p + a)C_1p + [(S_1 + T_1)p + 1]C_2p},$$

$$Z_3 = \frac{R_3(T_2p + a)[(S_1 + T_1)p + 1]}{T_3T_1(T_2p + a)p^2 + [(S_1 + T_1)p + 1]},$$

$$Z_1 = \frac{(R_3C_2p + b)[(S_1 + T_1)p + 1]}{(R_3C_2p + b)C_3p + [(S_1 + T_1)p + 1]C_2p},$$

where the time constants are as previously defined, and $a = 1 + R_2/R_3$, $b = 1 + R_3/R_2$.

The impedance looking back into the output, with the input short-circuited (formula 5, section 3), is the parallel combination of Z_3 and Z_1:

$$Z_o = \frac{R_3(T_2p + a)[(S_1 + T_1)p + 1]}{T_3p(T_1p + 1)(T_2p + a) + (T_2p + 1)[(S_1 + T_1)p + 1]}$$

$$= \frac{R_3\{T_2(S_1 + T_1)p^2 + [a(S_1 + T_1) + T_2]p + a\}}{T_1T_2T_3p^3 + [T_1(S_2 + T_3) + T_3T_2 + T_2(T_1 + S_1)]p^2 + (T_1 + S_1 + T_2 + S_2 + T_3)p + 1}.$$

The input impedance with the output open-circuited (formula 4, section 3) is the parallel combination of Z_2 and $(Z_3 + Z_1)$:

$$Z_i = \frac{T_1T_2T_3p^3 + [T_2(T_1 + S_1 + T_3) + T_1(T_3 + S_2)]p^2 + (T_1 + S_1 + T_2 + S_2 + T_3)p + 1}{(C_1T_2T_3 + C_2T_1T_3 + C_3T_1T_2)p^3 + [C_1(T_3 + T_2 + S_2) + C_2(T_3 + T_1 + S_1)]p^2 + (C_1 + C_2 + C_3)p}.$$

The input impedance with any load similarly may be calculated as the parallel combination of Z_2 and $(Z_3 + \bar{Z}_1)$ where $\bar{Z}_1$ is the parallel combination of Z_1 and the load.

The transfer characteristic (formula 1, section 3) is:

$$\frac{E_2}{E_1} = \frac{Z_1}{Z_3 + Z_1}$$

$$= \frac{T_1T_2T_3p^3 + T_1(S_2 + T_3)p^2 + (T_1 + S_1)p + 1}{T_1T_2T_3p^3 + [T_1(S_2 + T_3) + T_3T_2 + T_2(T_1 + S_1)]p^2 + (T_1 + S_1 + T_2 + S_2 + T_3)p + 1}. \quad (1)$$

2. Determination of Constants to Realize the Proportional-Derivative Characteristic.

The transfer characteristic may be written in factored form as follows:

$$\frac{E_2}{E_1} = \frac{(U_1p + 1)(A_1^2p^2 + B_1p + 1)}{(U_2p + 1)(A_2^2p^2 + B_2p + 1)}, \quad (2)$$

where $U_1A_1^2 = U_2A_2^2 = T_1T_2T_3$. To obtain a proportional-derivative network at frequency ω_0, we take $U_1 = U_2 = U$, $A_1 = A_2 = A = 1/\omega_0$. Then, if we let $B_1 = 2/T_d\omega_0^2$, $B_2 = 2/l\omega_0^2$, divide numerator and denominator of (2) by B_1p/l, and replace p by $j\omega$, we obtain the characteristic:

$$\frac{E_2}{E_1} = \frac{l}{T_d}\frac{1 + jT_d\dfrac{\omega + \omega_0}{2\omega}(\omega - \omega_0)}{1 + jl\dfrac{\omega + \omega_0}{2\omega}(\omega - \omega_0)} = g\frac{1 + jT_d\dfrac{\omega + \omega_0}{2\omega}(\omega - \omega_0)}{1 + jgT_d\dfrac{\omega + \omega_0}{2\omega}(\omega - \omega_0)}. \tag{3}$$

To solve for the constants in the parallel "T" network which will give a transfer characteristic of the form (3), we compare (2) with (1). We thus obtain:

$$T_1T_2T_3 = A^2U, \tag{a}$$

$$T_1(S_2 + T_3) = A^2 + B_1U, \tag{b}$$

$$T_1 + S_1 = B_1 + U, \tag{c}$$

$$T_2(T_3 + T_1 + S_1) = (B_2 - B_1)U, \tag{d}$$

$$T_2 + S_2 + T_3 = B_2 - B_1. \tag{e}$$

Substituting from (a), (b), (c) into (d) and (e), we obtain $T_1T_2 = U^2$. Then from (a), $T_3 = A^2/U$. Substituting the value of T_3 in (c) and (b), we are able to solve for T_2 and S_2. Then $T_1 = U^2/T_2$, and we solve (c) for S_1. Collecting results, we obtain the group of formulae (3) of section 3.

3. Proportional-Derivative Characteristic with Phase Shift of Carrier.

If $T_d\omega_0 = n$ is quite small (in the vicinity of 2 or 3), the upper bound arc tan $2/n$ will permit a useful amount of intrinsic phase shift. To obtain the proportional-derivative effect on the modulation, with phase shift of the carrier, the parallel "T" transfer characteristic should have the form:

$$\frac{E_2}{E_1} = \frac{Up + 1}{\alpha^{-2}Up + 1}\frac{(A^2p^2 + B_1p + 1)}{(A^2\alpha^2p^2 + B_2p + 1)}$$

$$= \left(\frac{l}{T_d}\right)\frac{Uj\omega + 1}{\alpha^{-2}Uj\omega + 1}\frac{1 + jT_d\dfrac{\omega + \omega_0}{2\omega}(\omega - \omega_0)}{1 + jl\dfrac{\alpha\omega + \omega_0}{2\omega}(\alpha\omega - \omega_0)}$$

where $\alpha \neq 1$, where as before $A = 1/\omega_0$, $B_1 = 2/T_d\omega_0^2$, $B_2 = 2/l\omega_0^2$.

Comparing the above transfer characteristic with the parallel "T" characteristic (1), we have:

$$\begin{aligned} T_1T_2T_3 &= A^2U, \\ T_1(S_2 + T_3) &= A^2 + B_1U, \\ T_1 + S_1 &= B_1 + U, \\ T_2(T_3 + T_1 + S_1) &= (\alpha^{-2}B_2 - B_1)U + A^2(\alpha^2 - 1), \\ T_2 + S_2 + T_3 &= (\alpha^{-2} - 1)U + (B_2 - B_1). \end{aligned}$$

Solving for T_1, T_2, T_3, S_1, S_2, we obtain the following formulae for determination of the constants in the parallel "T" network to give the phase-shifting proportional-derivative characteristic:

$$T_1 = \frac{B_1(A^2 + B_1U + U^2)}{[(B_2 - B_1)B_1 - A^2(\alpha^2 - 1)] + (B_2 - B_1)(1 - \alpha^{-2})U + (\alpha^{-2} - 1)U^2},$$

$$T_2 = \frac{A^4(\alpha^2 - 1) + A^2[B_2(\alpha^{-2} - 1) + B_1(\alpha^2 - 1)]U + [B_1(\alpha^{-2}B_2 - B_1) - A^2(\alpha^{-2} - 1)]U^2}{B_1(A^2 + B_1U + U^2)},$$

$$T_3 = \frac{A^2U\{[(B_2 - B_1)B_1 - A^2(\alpha^2 - 1)] + (B_2 - B_1)(1 - \alpha^{-2})U + (\alpha^{-2} - 1)U^2\}}{A^4(\alpha^2 - 1) + A^2[B_2(\alpha^{-2} - 1) + B_1(\alpha^2 - 1)]U + [B_1(\alpha^{-2}B_2 - B_1) - A^2(\alpha^{-2} - 1)]U^2},$$

$$S_1 = B_1 + U - T_1,$$

$$S_2 = (\alpha^{-2} - 1)U + (B_2 - B_1) - T_2 - T_3.$$

When the input and output of the parallel "T" are reversed, that is when $R_2 \rightleftarrows R_3$ and $C_1 \rightleftarrows C_3$, it may be seen that the coefficients in the numerator of the transfer characteristic are unchanged. Thus when a phase-shifting proportional-derivative parallel "T" is reversed, it is still a phase-shifting proportional-derivative parallel "T" with the same T_d, but in general with a different gain and phase-shift.

Blind Guidance by Ultrasonics (Frank H. Slaymaker and Willard F. Meeker, *Electronics*, May, 1948).—An effort to develop artificial devices for the military blind has led to the invention of a portable radar-like device employing pulsed frequency modulation. This device gives a single audio frequency tone corresponding to any given obstacle distance, and simultaneous echoes from different distances are identified by combinations of individual tones. The complete experimental equipment weighs 5½ lb. and operates at 65 kc. detecting obstacles up to 30 ft. Tests are being planned to determine the best method of using such devices—whether by headphones, tone conduction receiver, or controlled electrical shock.

Increased Uses of Turbojet by Augmentation.—The useful range of the turbojet can be expanded by augmenting the thrust in a number of different ways so that it fulfills more military requirements.

These plans for augmentation serve as a means of gaining more thrust for little additional weight and complication, without resorting to extra large engines or additional engines for most airplane applications.

Methods of augmentation include the reheat cycle or "tailpipe burning," engine overspeed, "bleed-burn" cycle, water injection in the combustion chambers, and water or ammonia or carbon dioxide injection in the compressor inlet.

The most practical augmentation process is the reheat cycle. In this method, additional fuel is burned in the hot air after it has expanded through the turbine, yielding a much higher temperature than could be withstood by the stressed turbine blades. Final expansion then takes place at the discharge end of the exhaust pipes, where the gas is ejected at a much higher velocity than without reheat, increasing the thrust accordingly.

Results show that at 600 mph., and with "tailpipe burning," the net thrust is almost equal to the output of two turbojet engines operating in the normal manner. However, full advantage of the reheat cycle cannot be realized unless adequate space is provided for the tailpipe burner, since a burner of adequate size is essential to obtain stable and efficient combustion over a wide range of fuel flows at all altitudes.

Augmentation is necessary because jet-propelled airplanes require longer take-off runs than a propeller-driven plane. Operation out of small emergency landing fields or airports located at high altitudes or in equatorial regions, and the frequent needs for a plane carrying a heavy pay load require an augmented thrust for a successful take-off.

In addition, poor climbing rates and lack of a high degree of maneuverability result when thrust falls off in the light air found in higher altitudes. The effect would be greater still, were it not for the increase in jet velocity. This shortcoming is overcome by augmenting the thrust at this altitude through the use of the reheat cycle.

Additional thrust is obtained at the expense of high specific liquid consumptions, but with only a slight increase in the weight of the whole propulsion unit. Until more progress is made in the field of high temperature metallurgy and more effective means are found to protect parts that are exposed to high temperatures, thrust augmentation will be used.

R. H. O.

THE MECHANISM OF LIGHTNING DISCHARGE.

BY

LEONARD B. LOEB,[1] Ph.D.

The first great step in liberating mankind from the thralls of superstitious fear at the awesome and dazzling phenomenon of the lightning stroke was made by Benjamin Franklin in his famous kite experiment when he drew some of the lightning from the clouds and stored it in a Leyden jar just as one did static electricity. Much further advance into an understanding of the very intricate mechanisms at work required two important developments: first, an understanding of the mechanism of the ordinary sparks at atmospheric pressure proceeding from impulsively applied potentials; and second, an analysis of lightning by means of visual and electrical recording devices acting over time scales measured in microseconds. The first of the missing data was supplied beginning effectively in 1939–40, when Loeb and Meek in America (1)[2] and quite independently, Raether in Jena, Germany (2) on different approaches, developed the streamer mechanism for spark breakdown. The second of the missing data was supplied effectively beginning in 1934 when Schonland, Collens and their associates applied the technique of the Boys moving camera lens of high speed to a study of South African thunderstorms (3). Both advances were the culmination of years of effort by many workers leading up to the ultimate clarification. Among these, one must number the pioneering studies of Townsend on spark breakdown (4), the important time lag studies beginning in 1923 and the following years, the studies of photoelectric ionization of gases beginning with those of A. M. Cravath (6), and corona studies at the University of California (7). Likewise one must consider the pioneering studies of Walter (8) with moving camera, of C. V. Boys (8) and others who preceded Schonland, and the many engineering and other investigations of lightning strokes using electrical and magnetic pickups (9,42) whose value improved with the improvement of detecting, recording and oscillographic techniques.

Assume for simplicity the uniform field between parallel condenser plates in air at atmospheric pressure. The gap length is δ, the field $X = \frac{V}{\delta}$ with V the applied potential. The upper plate is the anode. In sparking phenomena the characteristic variable for the ionization phenomena is the ratio X/p of field strength X in volts per centimeter to pressure p in millimeters of Hg. For a gap with $\delta = 1$ cm., the

[1] Professor of Physics, University of California, Berkeley, Calif.

[2] The boldface numbers in parentheses refer to the references appended to this paper.

sparking potential $V_s = 31.6$ kv. and $X_s/p = 41.6$ at atmospheric pressure. Assume one initiating electron to start from the cathode. As it crosses the gap of length δ, it creates an avalanche of $e^{\alpha\delta}$ new electrons and positive ions by cumulative ionization by collision in the gas (4). Here α is the first Townsend (4) coefficient representing the average number of ionizing acts of an electron per centimeter path along X. With $\delta = 1$ under the conditions cited for air, $\alpha\delta = 17$, and $e^{\alpha\delta} = 2.4 \times 10^7$ ions. Fifty per cent of these are produced within 0.041 cm. of the anode. A cloud track picture of such avalanches by Raether (2) is shown as Fig. 1 for three different impulsive time intervals below sparking thus yielding velocities of avalanche advance. The radius ρ of the avalanche can be estimated by the electron diffusion in the avalanche in the 5×10^{-8} sec. of crossing the gap (10). It is of the order of 0.013

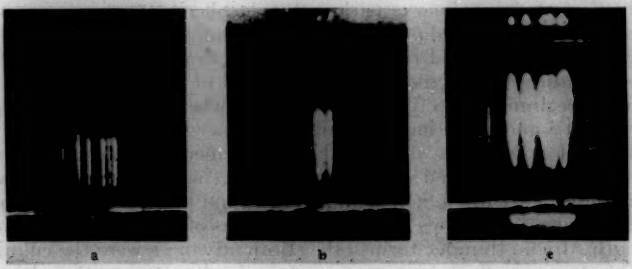

FIG. 1. Showing Raether's cloud track photographs of electron avalanches using pulsed fields of different duration below breakdown. From the time interval which increases progressively from a through c, the velocity of advance of avalanche tips can be determined.

cm. The electrons in this avalanche with velocities about 100 times that of the positive ions enter the anode and leave behind a positive ion space charge whose density creates a field X^1 at a distance ρ from the center of about 0.013 cm. of 6000 v. per centimeter. If the potential had been 5 per cent higher the value of X^1 would have been 140,000 v. per centimeter, for α is very field sensitive. In the avalanche head accompanying the ionization there were produced some $fe^{\alpha\delta}$ high energy photons (light quanta), capable of ionizing the gas molecules present (11). The value of f is not as yet known, though estimates are possible (40,41). These photons are mostly emitted over an interval of 10^{-7} sec. In the vector sensitive field $X^1 + X$ extending out a distance Δx^1 beyond ρ as shown in Fig. 2 the value of α is very much increased (12,13). If now with the high absorption coefficient μ for such photons in air (of the order of one half of these are absorbed in 10^{-1} cm. (14,40)) the photoelectrons produced in the sensitive volume can ionize in the distance

Δx^1 to produce the same density of ions existing in the original space charge, the space charge will be extended into the gap by Δx^1 (11). The process will then repeat itself and the positive space charge will advance back across the gap from anode to cathode. As it does so, the electrons created by the advance stream up its length to the anode giving a conducting plasma which acts to distort the field in the gap and still more enhance $X + X^1$. The velocity of advance from anode to cathode of this process is high ($\sim 10^8$ cm. per second), and becomes higher as it approaches the cathode because of increased field distortion (2,7,12,15,16).

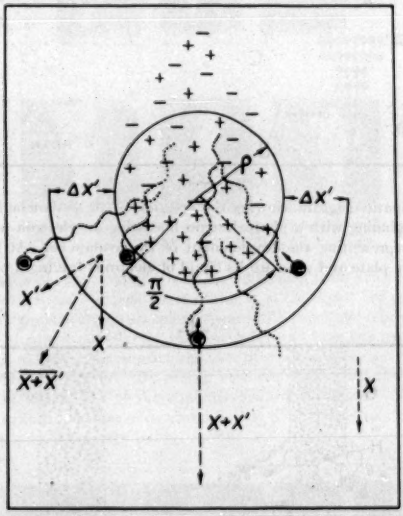

FIG. 2. Schematic diagram showing the positive space charge left behind by an electron avalanche. Its radius is ρ and the sensitive zone ΔX^1. Fields are represented by dashed arrows. Dotted curves indicate photons liberating electrons in different regions about the zone. The zone is of width ΔX^1.

The mechanism is called a *streamer*. It was discovered by Raether in cloud track pictures (2) and was first observed by Loeb and by Kip in positive corona (7). Its properties are now well established. The mechanism of streamer formation is illustrated in the schematic diagrams of Figs. 3 and 4, and cloud track pictures of such streamers by Raether (2) are shown in Figs. 5 and 6. A great deal is known about such streamers today (7,17): they have an ion density of the order of 10^{14} ions per cubic centimeter and 10^{10} ions are produced per centimeter of length; their velocity ranges from 2×10^7 to 2×10^8 cm. per second

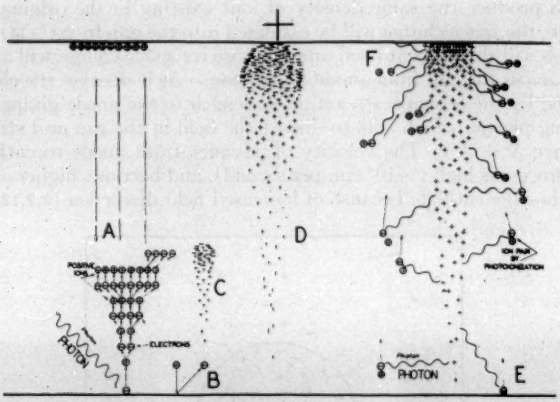

FIG. 3. Schematic diagram showing the creation of an avalanche between two parallel plate electrodes beginning with a photoelectron liberating an electron for the negative plate A, C, D, and F, representing the development of the avalanche. At F the avalanche has reached the positive plate and gives up its cloud of electrons leaving a positive space charge.

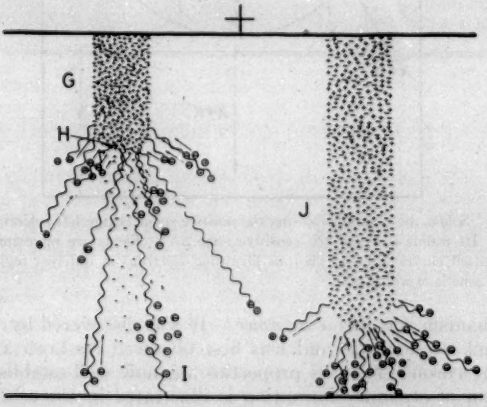

FIG. 4. A schematic diagram, a continuation of Fig. 3, showing the mechanism of positive streamer advance. At G the streamer has advanced part-way across the gap and at J it has nearly bridged the gap. Field distortion at this point is high. Note also that the diameter of the channel is very much exaggerated for clarity in reproduction.

depending on the imposed field and the field distortion produced; they represent a displacement current of the order of 0.1 to 1 amp. in the gap; and their initial rate of development $\frac{di}{dt} \sim 10^8$ amp. per second is capable of shock exciting electrical systems and produces much elec-

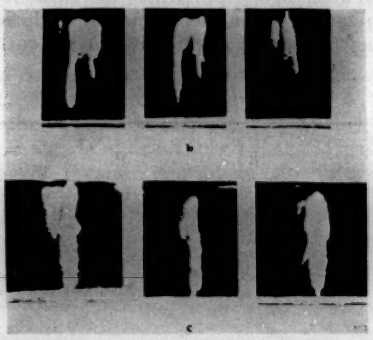

FIG. 5. Raether's photographs of streamers developing from avalanches. The negative electrode is at the bottom and the positive electrode is at the top. The avalanche can be seen in each case proceeding upward with an enlargement at its upper end representing the streamer advance before the streamer could cross the electrodes and give the spark. The time scale here is of the order of 10^{-7} sec., representing the time of crossing of the avalanche and the return of the streamer at higher velocity. By proper choice of timing Raether could calculate the approximate speed of the motion of the streamer toward the anode. Notice branching and on two of the photographs, pictures of avalanches that did not lead to streamers because they started their careers later during the pulse.

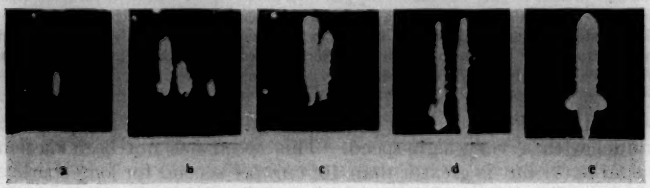

FIG. 6. Further pictures of Raether's showing avalanches producing streamers. These pictures are taken with different times of application after the sparking voltage had been applied. Beginning at the left, one sees avalanches crossing at three consecutively longer time intervals. The last two pictures indicate returning streamers. The one at the extreme right indicates a streamer with two equal branches. Note that the width of these photographs is highly exaggerated because of differences between the time of application of the voltage and the condensation of the cloud.

trical noise. Representing a field distortion the streamers can propagate themselves as long as the total field strength they are moving in is high enough, and the gaseous density is such as to insure photoionization in the gas. It has been estimated from corona studies that the minimum field under standard conditions in air is of the order of 4400 v. per centimeter (18).

When the streamer head approaches the cathode the intense local photoelectric ionization of the metal and the high field existing cause the release of such a flood of electrons from the cathode that a steep

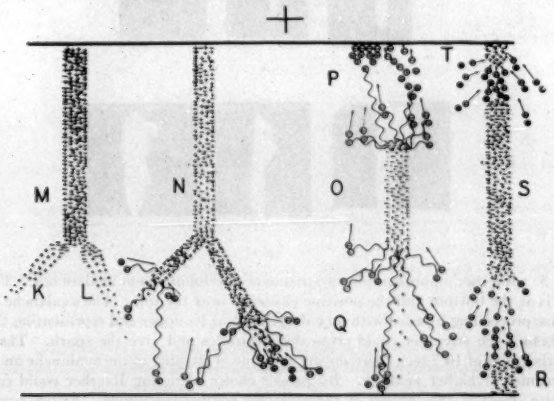

FIG. 7. Schematic diagram indicating the process of branching in streamer advance M and N, and the development of midgap streamers in over-volted gaps. Note that at O the avalanche proceeded part-way across the gap before starting a streamer toward the negative electrode. S is a later stage in which the streamer has advanced well across the gap causing serious distortion and producing an intense avalanche R at the negative electrode and an anode streamer T at the positive electrode. Such breakdown had been observed by Dunnington and White well before the streamer theory had been developed.

potential gradient suddenly develops and sweeps up the pre-ionized channel with a very high speed. This speed has not been measured on sparks (2) but is greater than 10^9 cm. per second for long sparks according to Meek and Allibone (19). In lightning it ranges from 10^9 to 10^{10} cm. per second (3). Similar speeds have been observed for such ionizing potential waves by Snoddy, Dieterich, and Beams at lower pressures (20). The velocity of such ionizing potential waves in plasma according to the latter authors, depends on the electron or ion density in the channel plasma and on the steepness of the potential gradient of the front of the wave. The intense ionization produced by the poten-

tial wave ionizing from possibly 1 to 30 per cent of the molecules in the channel leads to the brilliant return stroke. This intense adiabatic energy input is responsible for the light, heat, and noise of the spark. Following the return stroke, channel temperatures of the order of 10,000 to 18,000° are reached (21). The heated channel expands at the rate of about 10^6 cm. per second until the expansion cools the channel (22).

The quantitative condition for streamer advance has recently been indicated as roughly of the form $\epsilon f e^{\alpha\delta} = 1$ (11). Here ϵ is the chance that a photoelectron is created in the volume between ρ and Δx^1 (Fig. 2) such that it can create an avalanche sufficient to extend the streamer tip. ϵ is complex and depends on the imposed field X, the space charge tip field X^1 and thus on the size of Δx^1 as well as on μ the absorption coefficient for photoionization in the gas. Through ρ and μ the quantity ϵ is critically pressure dependent (23). For long gaps or divergent fields, or for slight over-voltages, $\frac{V - V_s}{V_s}$, the length of an

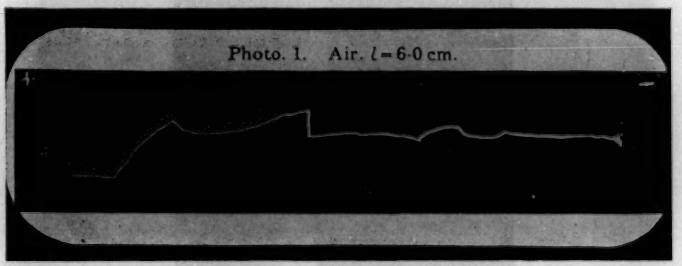

FIG. 8. A beautiful photograph of a spark by Terada and Nakaya, showing the crooked nature of a spark for a long spark with a weak guiding field.

avalanche x to produce a streamer can be less than the gap length δ. This leads to what are known as midgap and anode breakdown streamers first observed by Dunnington and later by White and by Allibone and Meek (24). The geometrical position of the single photoelectron, or the creation of two simultaneously appearing well located photoelectrons, in Δx^1 can lead either to crooked paths (usually in weak fields X) or to forked paths branching in the direction of progress, occurring chiefly in strong and in strongly divergent fields (25). The schematic diagrams illustrating the origin of midgap streamers and branches paths is shown in Fig. 7 as appearing in overvolted uniform fields. Figure 8 shows a crooked spark photographed by Terada and Nakaya (26). In Fig. 9 is shown a branched lightning stroke advancing from cloud to

ground, and Fig. 10 shows a branched streamer taken within 1.25 $\times 10^{-8}$ sec. in a highly divergent field produced by an overvolted point as photographed by Gorrill with a cloud chamber (15). Figure 11 is a photograph of a midgap breakdown observed by White in CO_2 in

FIG. 9. A detail of one of Schonland's fixed camera photographs of a lightning stroke showing a branching in the direction of progress and some decrease in intensity through narrowing of the channel and less halation, as the return stroke moves upward. All luminosity here is caused by the return stroke.

intervals of the order of 10^{-9} sec. with Kerr cell shutter, cathode at left (24).

When one turns from the discussion of the simple uniform field spark to long sparks in air and to lightning, conditions are somewhat altered. In such events the fields under consideration are often localized and very high with steep local gradients near points or clouds. Again

most of the fields are impulsive;[3] that is they are suddenly created by surge generators in sparks or by the turbulent and violently convective gas mass motions about charged drops in thunder showers (27,28,29,42). All data on lightning discharge indicate the sudden and probably localized appearance of high field gradients very shortly before discharge. There are the rare cases where apparently high fields of longer duration appear causing St. Elmo's fire or corona from tall pointed conductors on the ground. Actually where such manifestations occur the cloud-to-ground field on the average is not high, ~2700 v. per centimeter, but

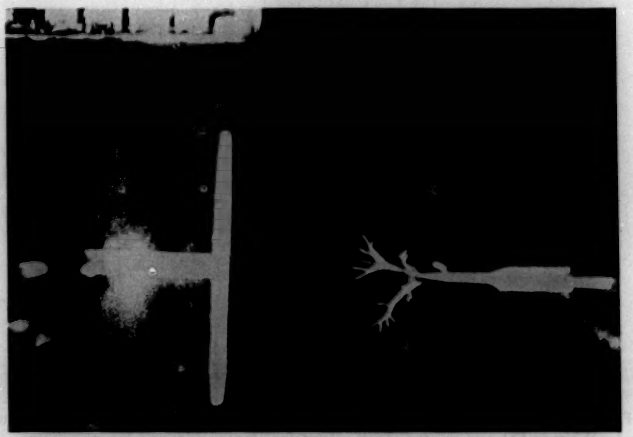

FIG. 10. Cloud photograph of a positive corona streamer from a positive point to negative plane taken by Gorrill with impulse voltage applied for 1.25×10^{-8} sec. Note that the streamer did not travel very far. Longer duration of the impulse field causes the branches to progress further across to the plate. Note the heavy branching in the direction of propagation.

long conductors projecting into the field distort the field and focus on themselves the high local gradient leading to St. Elmo's fire or even to invited lightning strokes. These are *not* the rule in the common lightning strokes observed and in which we are interested. Sounding balloon and airplane measurements indicate that there are in storms usually gradients less than 300 v. per centimeter or else sudden fields leading to discharge (27,28). There is some divergence of opinion as to fields measured near the ground or on airplanes in flight just before

[3] It is not profitable to discuss breakdown under constant or alternating high fields for long sparks or lightning. In long sparks the mechanism is complicated by building up of corona and space charge accumulation. Lightning rarely gives high fields of long duration. Most strokes appear to be of the impulsive type.

strokes, but they fix these on the average as lying between 2700 and 4000 v. per centimeter near the point struck. Probe measurements before breakdown of a corona gap by positive point streamers indicate minimum fields of about 4400 v. per centimeter to be required. It is on the basis of mean gradients of such values that the potentials leading to lightning discharge are estimated to be of the order of 10^8 to 10^9 v. depending on length of stroke. It is, therefore, to be anticipated that in all such sparks, despite field distortion by streamer formation and highly localized fields of high order at electrodes or in portions of the

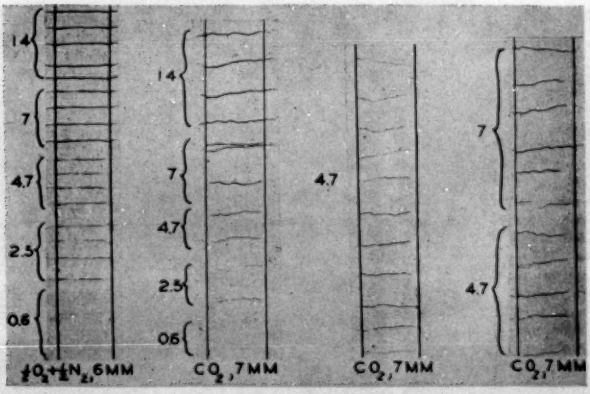

FIG. 11. Actual photographs of midgap streamer breakdown using Kerr cell shutter taken by White in CO_2 and an oxygen and nitrogen mixture at relatively lower pressures. The time scale is indicated by the figures on the left. Notice particularly the shortest time scale photographs in CO_2 at atmospheric pressure where the midgap streamer is just beginning to show. Longer intervals show the sparks crossing the gap. The negative electrode is to the left, the positive is to the right. The extension of the spark behind the electrodes is a reflection on the electrode surfaces. The exact time scales with Kerr cell shutter cannot be fixed. While drawings of visual observations show midgap streamers more clearly at the shorter time intervals, it is believed that actual photographs of these are more suitable for demonstration.

cloud that initiate discharge, there must be minimum field gradients of the order of 2700 v. per centimeter over the whole gap to be traversed before sparks occur. One must, therefore, consider briefly what occurs when sparks start from suddenly positively or negatively charged points or localized high field regions with adequate gradients of lower order between. Studies of long sparks by Allibone and Meek (27) and corona studies at atmospheric pressure indicate that for a *positive metal point* fields must exist very near the metal point surface giving X of about 70,000 v. per centimeter in air to insure deionization of existing negative

O_2 ions to start the discharge (7). As we saw, uniform fields of 1 cm. length require 30,000 v. per centimeter. The high fields initiating lightning could well be less. In more extended regions of uniform fields

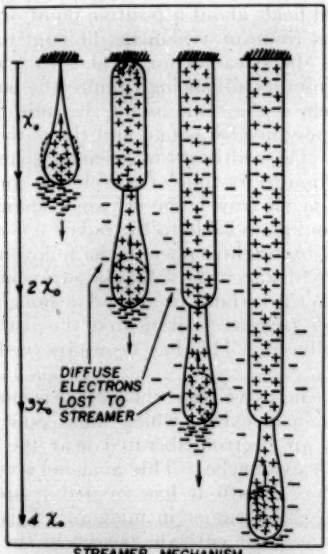

FIG. 12. Schematic diagram illustrating a streamer mechanism for a negative point. The electron avalanche at the extreme right has developed to a distance x_o, where it starts to send a streamer back to the cathode. As this streamer advances, the electron cloud is able to advance $2x_o$ and start a new streamer by which time the first streamer has reached the cathode. Successive steps are indicated by the diagrams to the right extending the streamer mechanism a distance of $4x_o$ into the gap. It is probable that the successive steps x_o after the first should be shorter because of the number of electrons participating, and it is indicated that both the streamer advance upward and the electron avalanche advance downward could produce crookedness and branching not indicated in the figure. The tendency will be for them to move straight forward owing to the number of electrons available for avalanche advance. Note also that with the electrons moving ahead, a certain number of them are lost to the channel by diffusion. These require a small current down the streamer channel in order to maintain the avalanche advance. It is this current which plays an important role in the increase of field gradients causing stepping.

of the order of 10,000 v. per centimeter in air, water drops will be drawn out in fine points to yield positive streamers, thus initiating spark discharge as Macky and earlier studies by Zeleny have shown (30). In

any case, when adequate localized sudden fields of appropriate size occur, a discharge streamer mechanism starts. In detail this process will differ both as regards initiating field and mechanism depending on whether the local charge is positive or negative.

When such local fields about a positive point or cloud region occur, the streamer begins from an avalanche directed towards the cloud or positive point, and the streamer forges ahead outward across the gap pouring electrons from its advancing tip into the positive cloud or electrode. The problem is the same as for the uniform field except that streamer advance may not be as fast and the path in a weak field will be more tortuous. The width of the streamer channel will increase by diffusion in proportion to its time of travel. In long sparks and lightning with 1 to 10 m. of travel, the streamer channel width could be 0.5 to 1 cm. It would be visible to the naked eye close by in the dark were it not masked by brighter phenomena following. It could not be photographed at any distance (7). Breakdown would then follow when it crossed the gap to the cathode or ground although it could be met by a negative streamer process as it neared the cathode with the high field distortion produced. This has been observed in occasional long sparks (19,31).

In the case of the negative point the picture is more complicated (32). When an adequate field exists, which must now be higher than for the positive point, an electron liberated near the cathode or from it proceeds to form an avalanche. This avalanche will proceed out into the gap a distance x_o, until it has created a space charge density sufficient to produce a streamer in midgap. This streamer will now move *backward* towards the cathode as seen in the sequence shown in the schematic diagram of Fig. 12. As the streamer advances the electrons feeding into it allow the electrons ahead of the positive space charge again to move forward another x_o, or perhaps a shorter distance, at the end of which a new streamer proceeds back to join the first streamer which by that time has reached the cathode. There is thus a streamer channel $2x_o$ long from cathode out into the gap with the electrons moving further beyond $2x_o$ to make a streamer $3x_o$ long and so on. Depending on the nature of the imposed field, the successive steps x_o can either be shorter or longer depending on how the field distortion is proceeding. When this process approaches the anode sufficiently closely seriously to distort the field, it may be met by a *positive anode streamer* at which point a potential wave will sweep up the channel from anode to cathode reionizing the plasma and giving a spark. The composite of streamer advance towards the negative point and electron avalanche towards the positive ground can have crookedness in a weak guiding field come both through the streamer advance and the vagaries of the advancing avalanches. However, with the number of these avalanches the forward advance should tend towards straighter paths

than with streamers alone. What evidence we have from long sparks makes this appear to be true as seen in the photograph of the long spark by Allibone and Meek (19,31), where the negative charge is at the top

FIG. 13. A very illuminating photograph of a long spark in air from a negative point (top) to a grounded plane (bottom) with high resistance in series with the point. The moving film camera is moving from left to right as can be seen by the continuation of streaks. Note that the negative point streamer mechanism progresses along relatively straight lines, and that it continues about one fourth of the way from the negative points across the gap. Note the step-like procedures in its development which Allibone and Meek however, do not call proper stepping. In sparks of a meter length stepping should not occur naturally and the effect shown is produced by the use of a high resistance which lowers the potential of the point after a partial discharge. Note also that the negative point streamer is met by an upward branching positive streamer from the positive plate beginning at the extreme left which advances three fourths of the way across the gap meeting the negative streamer at that point. The return stroke can be seen for the positive point immediately to the right of the upward moving positive streamer and at the right of the downward moving negative streamer which completes the junction. Notice the intense illumination over the section of the channel where the two streamers meet resulting in much halation. Notice a subsequent positive streamer occurring at a later time to the right at the bottom of the picture.

of the Fig. 13. It is clear that for such cathode streamer processes the fields must be higher than for positive streamer processes. Experiments with long sparks bear this out in that the *average* potential gradient from positive point to negative plane is 4400 v. per centimeter while with negative point to plane it is of the order of 9000 v. per centimeter (32). This circumstance is very important for long sparks and especially for lightning since over 90 per cent of the observed cloud-to-ground strokes

FIG. 14. A revolving lens Boys camera photograph taken by Schonland and Collens indicating the intricate nature of the pictures. It is to be noted that two lenses were used. The sequence of events is indicated by a, b, c, d, e, and f. a, b, c, and d, are given by successive strokes down the same channel. The motion of the lens in the lower half of the picture is such that the time progresses from right to left as indicated by the bright streaks. Note the length of the bright streaks coming from points of particularly intense ionization.

in all but mountain thunderstorms (42) are from negative clouds. The fact that a positive point starts a breakdown streamer at lower fields can influence the statistics and interpretation of lightning discharges if care is not taken to remember this fact.

The first step in a real understanding of the lightning discharge mechanism came when following C. V. Boys, B. F. J. Schonland and H. Collens and their associates adapted a camera with a rapidly revolv-

ing lens to the study (3). This technique made it possible to study the lightning stroke on a time scale of microseconds. The revolving lens photographs are not easy to interpret as can be seen from the example shown in Fig. 14. However, the results were startling. Later Allibone and Meek (19,31) studied long impulsive sparks with a camera with rapidly moving film with, however, less temporal resolving power. Considering that most discharges observed are from negative cloud to ground, the sequence of events delineated by Schonland are as follows (3):

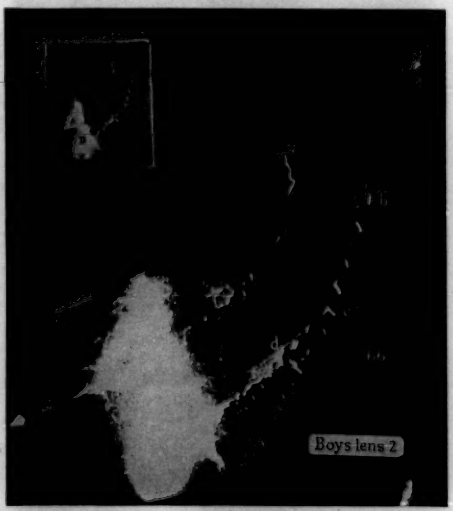

FIG. 15. This is a particularly beautiful photograph of the stepped leader stroke by Schonland and Collens, the large photograph being a detailed picture of the smaller one shown in the insert. The time extends from right to left. Note the separate steps of the leader and also the stepping in the progress of the main branches somewhat above.

1. An invisible process called a *pilot streamer* suddenly starts from a cloud towards the ground into virgin air at a velocity which is generally around 2×10^7 cm. per second but in unusual cases has been observed up to 10^8 cm. per second. Its presence must be inferred since while it itself cannot be seen, its tip is periodically illuminated by later occurrences, and it must be there to carve the path later made visible. This process forging into virgin air yields the tortuous path and the branching characteristic of lightning.

2. After an average of some 50 microseconds (the time varies from

30 to 90 microseconds and is remarkably regular in any stroke), its tip is illuminated by a *stepped leader stroke*. This proceeds from the cloud to the ground at a speed which varies somewhat in different strokes but is of the order of 10^9 cm. per second. Stepped leaders are beautifully illustrated in Figs. 15 and 16. Note the steps for advancing branches

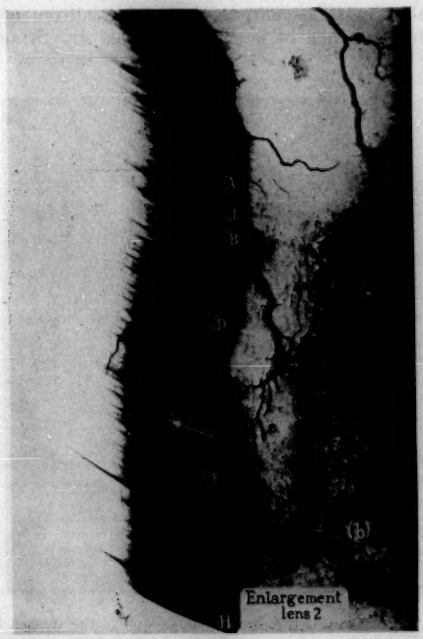

FIG. 16. Another beautiful picture of stepping from the work of Schonland and Collens, time extending from right to left. Note the stepping in the main pilot streamer, ef, and also the stepping of the branch xy. The return stroke is seen at the left and is much blackened by overexposure. The duration of illumination in the return stroke appears to be quite long and is probably caused by successive return strokes up the channel produced by the branching. Overexposure of the main stroke results when the sensitivity of the process is increased to observe the leader.

as well. Whether the pilot streamer has stopped or slowed just before the arrival of the stepped leader is not known. At any rate, after the arrival it surges forward with possibly increased branching at this time. Branching is invariably in the direction of advance as seen in Figs. 9, 14, 15, and 16. The movements of stepped leaders can be picked up by

oscillograph through field disturbances as seen in diagrams of α and β strokes analyzed by Schonland in Figs. 17 and 18. Thus every 5 to 10 m. or 50 microseconds of advance the pilot streamer tip and channel are made visible by a *stepped leader*.

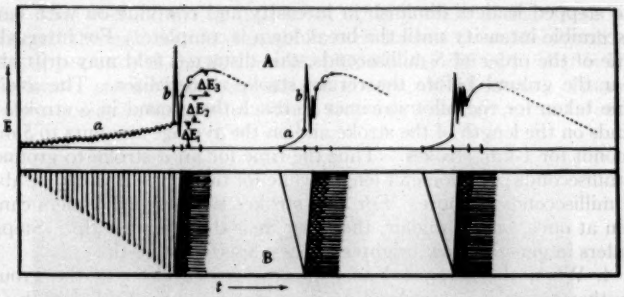

FIG. 17. Diagram from Schonland, Hodges, and Collens, of oscillograms of stepped leader strokes of the α type with schematic indication of the events correlated therewith underneath. Potential in the A part of the figure is upward and t is plotted along the axis of abscissae. Note the oscillations produced by each step and the intense oscillation B caused by the return stroke. The occurrences to the right indicate successive strokes with dart leader with no stepping.

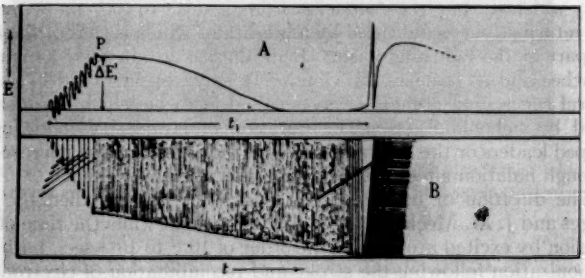

FIG. 18. Drawing of electrical events produced in β type strokes according to Schonland, Hodges, and Collens. The interpretation is similar to that for the α stroke of Fig. 17. Note here the very heavily stepped leaders calling forth intense branching and the slow leader advance of the steps over a period of about 5 milliseconds from the point P to the return stroke at the end of the time interval t_1.

3. Two principal types of strokes are observed. The α type, comprising 65 per cent of observed strokes, is one which advances with relatively even steps all the way to ground as seen in Fig. 17. As it approaches the ground it may be met with a positive streamer from a good

conducting element on the ground and the bright or return stroke appears. In the remaining 35 per cent of the strokes a β process occurs as illustrated in Fig. 18. Here initial stepping is very bright and strong and there is much downward branching. In this event the discharge seems to have spent itself before the streamer reaches ground. Thus the stepped leaders diminish in intensity and continue on with barely discernible intensity until the breakdown is complete. For intervals of time of the order of 5 milliseconds, this distorted field may drift along near the ground before the return stroke materializes. The average time taken for the pilot streamer to reach the ground in α strokes depends on the length of the stroke and on the average amounts to 5 milliseconds for 1-km. strokes. Thus the time for an α stroke to ground is 5 milliseconds per kilometer length while for the β type it would be about 10 milliseconds or more. For long strokes two stepped leaders can be seen at once, one in midair, the other near the streamer tip. Stepped leaders in general grow brighter as they approach the tip.

4. When the stepped leader process comes close to the ground, whether or not it is met by a positive streamer of notable length (**38**), the conducting path of ions is closed and a potential wave of high intensity accompanied by great luminosity passes *up* the channel from ground to cloud. Where the positive streamer meets the pilot above the ground, the junction point is exceptionally bright, as seen in the long spark of Fig. 13 (**31,38**). This "return stroke" travels with a velocity which runs *up* the channel at from 3×10^9 to 10^{10} cm. per second. The return stroke is indicated by a brightness which is that of the blinding part of the lightning flash. It diminishes in intensity as it passes branches and as it nears the cloud. It may appear broad because of several succeeding potential waves called forth largely by branches as noted by Schonland (**3**). The duration of luminosity following the stepped leaders or the return stroke is of the order of some microseconds although halation effects on the plate indicate longer times.

The duration of luminosity in sparks has been studied by J. D. Craggs and J. M. Meek (**21,34**) and indicates that while the time of light emission by excited atoms is of the order of 10^{-7} to 10^{-8} sec., both thermal ionization following the stroke and recombination of electrons and ions cause the longer emissions lasting some 3 microseconds. In argon metastable states carried this time out to 30 microseconds. The much longer duration of emission in certain *spots* in Figs. 13, 14, 15, and 16, cannot be associated with bends in the path in line of sight as at first assumed (**39**). They may be connected with certain peculiar conditions produced with very intense and dense ionization causing a persistence of excitation requiring wave mechanical interpretation (**33,39**).

5. The persistence of *ionization* in the channel beyond the period of luminosity is indicated by *repeated strokes* down the channel. According to Schonland, often associated with a Y-branching at the cloud

end successive strokes will follow down an old channel (3,42). As many as 20 repeated strokes have been observed with an average interval of 0.01 to 0.09 sec. between them. The average number per stroke is 3 (8). This is indicated in the moving camera photograph of Fig. 19 due to Walter (8), and in Fig. 14. Aside from the increased branching at the cloud end indicating that some other portion of the cloud has discharged through the old channel in such strokes these are signalized by the appearance of the *dart leader*. This leader differs in that it is a single leader stroke only stepped down very old channels. Thus it usually proceeds to the ground *without* stepping with an average velocity

FIG. 19. Photograph of successive lightning strokes down the same channel taken with moving camera by Walters. These are to be compared with the photograph obtained on long sparks by Allibone and Meek shown in Fig. 20.

of 2×10^8 cm. per second. Its velocity ranges rather widely from 1×10^8 to 2×10^9 cm. per second depending on the age of the channel it follows and the steepness of the potential waves from the cloud end. It is in general slower than the stepped leader. On reaching the ground it is followed by the bright return stroke up the channel.

One may now interpret the occurrences as follows:

1. With adequate over-all field gradients to ground and local fields in a small section of the cloud ranging from 10 to 60 or more kv. per centimeter created slowly or suddenly by convective air currents, either a disrupted water drop induced discharge or a free electron causes ionization by collision and avalanche and streamer formation. This leads to

a positive streamer advance towards the cloud with further progress of the avalanche on the ground end of the streamer towards the ground in virtue of the field distortion produced. The negative point streamer mechanism already discussed is then initiated and the "pilot streamer" begins its career, drawing a small current of electrons down itself from the cloud to make up for diffusive loss of electrons from the avalanche's head. The streamer channel in 50 microseconds may reach a diameter of 2 to 10 mm. and will have about 10^{14} ions per cubic centimeter. The advance in weak guiding fields will be slow and tortuous and in stronger fields it will be fast and straighter, showing much branching.

After some 50 microseconds of travel the upper end of the streamer channel has undergone some changes. Near the advancing tip the field gradients are high and the advancing electrons have much energy. They cannot attach to O_2 molecules to form ions. However, in the streamer channel the fields are much less and electrons rapidly lose energy so that loss of electrons to form negative ions is considerable. Positive and negative ions then begin to recombine and the conductivity in the older cloud end of the channel begins to decline. Following a statement by Schonland that "the unusual constancy of this phenomenon (time of stepping) cannot be ascribed to any process involved in the cloud but must be led back to some basic physical process," and a later statement that recombination of ions might be involved, J. M. Meek discovered that indeed *recombination* led to just such an expected constancy in the phenomenon (35).

The number of ions n out of an initial number n_0 remaining as a result of recombination after a time t is given by $n = \frac{n_0}{1 + n_0\beta t}$. Here β is the coefficient of recombination of ions which is of the order of 2×10^{-6} in air at 22° and 760-mm. pressure. It is to be noted that n will become inversely proportional to t and roughly independent of n_0 when $n_0\beta t$ becomes much greater than 1. This leads at once to the discovery that in 50 microseconds $n_0\beta t$ exceeds the value 1 if n_0 exceeds 10^{10}. Hence for ion concentrations in excess of 10^{10} ions per cubic centimeter, the decline of ionization becomes largely independent of initial concentration and reaches its value of 10^{10} in about 50 microseconds. Thus, irrespective of initial ion concentration which will be fairly constant in any given channel with minor variations, the ion density will decline to 10^{10} in about 50 microseconds. On this basis Meek evolved a theory (35) for the stepped leader stroke which was later modified by Loeb and Meek (36). This indicates that in any streamer channel, if f represents fraction of the electrons needed in the plasma to act as a current down the streamer channel to make up for diffusive electron loss at the avalanche head and if f_s is the fraction of free electrons left in the channel after a time t by attachment process to O_2 molecules the electrical field

gradient at the cloud end of the streamer channel after 50 microseconds is given by $X = 2 \times 10^7 \left(\frac{f}{f_s}\right)^2$ v. per centimeter. With $f = 0.05$ and $f_s = 0.1$, which are not unreasonable values, X becomes 50250 v. per centimeter. Thus a high field gradient is created at the cloud end by the time the pilot streamer channel has advanced for 50 microseconds. With such a gradient the O_2^- ions in the channel can become deionized and with accompanying intensive electron ionization the potential distortion caused by this gradient sweeps down the channel at a speed that varies with the density of ionization left in the channel plasma. As this density increases down the newer portions of the pilot streamer channel, where there has been less recombination, the stepped leader speeds up and becomes brighter. All variations in the stepping time and velocity can be accounted for by variations in the initial density of ionization and the residual ionization existing at the time of the step. When the stepped leader arrives at the end of the pilot streamer, the latter forges ahead with renewed vigor and much branching and the process repeats.

In the case of β type strokes excessive branching so drains the energy of the cloud available that progressive and vigorous advance and stepping is impeded and the streamer forges ahead only slowly. When either α or β streamer tip advances close enough to the ground a positive streamer will move upward from the ground and at the instant of junction a very intense potential wave sweeps up the pre-ionized channel with very high velocity. This results from the fact that except for the iR drops down the streamer and leader channel the whole potential difference between cloud and ground centers at the junction point. This is clearly seen both in sparks and in lightning where positive streamers from the ground meet the leader well above the ground as in Fig. 13. In most *natural* strokes to ground good conducting points from which a streamer can start are few and far between so that the leader must in most cases advance pretty well towards the ground before the return stroke can materialize. Golde (38) recently estimates 5 m. to open ground and 16 m. to a lightning conductor. If, however, one places a good pointed conductor on top of a high building, the positive field about the good conductor is much increased and positive streamers will advance well up towards the cloud. Thus the strokes will appear to come from the ground as a positive streamer since these start at materially lower field gradients than from a negative cloud. In fact, such a system often *invites* strokes that would otherwise not occur. Hence many more strokes to the Empire State Building were recorded with good grounded conducting points projecting than normally occur. Thus the lightning strokes *usually observed* rarely show streamer processes (38) from ground while long sparks between metal electrodes show streamers passing well toward the center of the gap as seen in Fig. 13.

Allibone and Meek, however, observed that the longer the gap and the lower the resistance in series with the negative point, the more the junction point of positive ground streamer and negative leader approaches the ground (31).

Once junction has been established one observes, as in sparks, the intensely brilliant and noisy return stroke. This as indicated, depend-

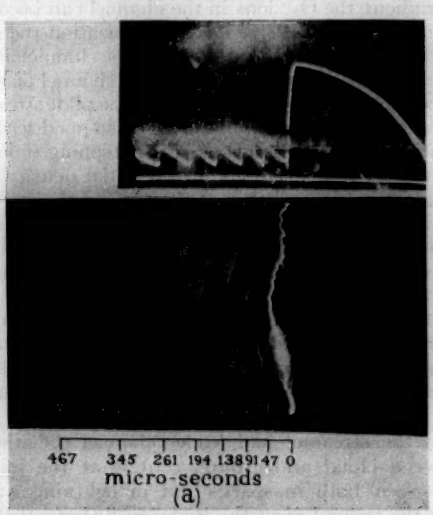

FIG. 20. Lower photograph taken with moving film camera by Allibone and Meek of a meter long spark with aperiodic circuit and high resistance containing capacity giving successive sparks down the pre-established channel. Note that in this case time goes from right to left and that the spark proceeds from the positive point downward. The leader stroke being seen on the right and the return stroke on the left of the first stroke. In this case the positive streamer has been met by a *negative* streamer from the earthed plane. Note the downward branching of the positive streamer and the upward branching of the negative streamer mechanism. Also note the intense brilliance produced at the junction points of the two streamers. Subsequent strokes show less detail of structure. Above is a voltage potential oscillogram indicating the fall of potential with the advent of the return stroke and the subsequent build-up of potential to a lower breakdown value on each successive stroke.

ing on the ion density in the channel and the steepness of the potential gradient, travels up the channel giving what the eye perceives as the lightning stroke. As shown by the Boys and moving film cameras, the stepped leader and streamer when long enough occur earlier in the process, but the time scale is such that the human eye perceives only the return stroke. If there is much branching, the return stroke illumi-

nating them as well as the main channel loses in intensity and presumably in speed as it advances towards the cloud as seen in Fig. 9. The decay in ionization at the upper end of the channel since the last stepped leader makes the luminosity at the cloud end in the return stroke distinctly less (3). Ion densities produced by return strokes in sparks have been estimated by Stark effect broadening as of the order of 10^{19} per cubic centimeter by Dunnington (24) and 3.5×10^{18} per cubic centimeter by Margenau and Watson (37). Careful study by Craggs and

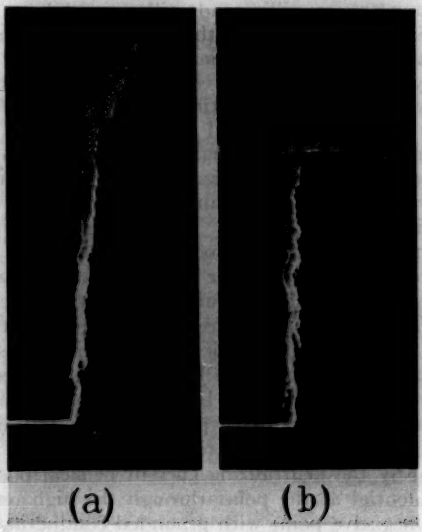

FIG. 21. Showing two sparks from positive points to grounded plane. The time extending from right to left. Note the leader stroke on the right and the return stroke on the left. The reproduction of these negatives is too poor to indicate this clearly. The stepping is produced on a meter long spark by introducing high resistance in connection with the point. It is, therefore, *not natural* stepping.

Meek (21), and by Craggs and Hopwood (34), in sparks in H_2 and A from several different considerations yield of the order of 10^{17} ions per cubic centimeter. In lightning somewhat higher densities could be expected. The exact width of the channel observed in lightning strokes is a matter of controversy. The pilot streamer and stepped leader may be about a centimeter in diameter. With the high energy in the return stroke the radial adiabatic expansion occurs at about 10^5 cm. per second according to Meek from spark studies (22). In the 3 to 20 microseconds

of brilliant luminosity, the channel could broaden by 4 to 5 cm. in both directions. Hence the width observed can range from 2 to 10 cm., which is within the range claimed by estimators. The width of the brightest phase is probably less. The breadth of channels shown by moving lens is partly due to multiple return strokes caused by branching.

Since *ionization* persists for a considerable time beyond the few microseconds of intense luminosity, it is natural to expect that subsequent discharges of a heavily charged cloud portion within the initiating cloud will take place to the recently discharged portion. Thus successive strokes after 10 or so milliseconds will proceed down the old channel possibly showing new branches at the cloud end when not obscured by cloud and rain. These will be initiated by a *dart* leader whose velocity and luminosity will depend on the residual ionization in the old channel. Its progress will generally be continuous as with the *last* step of the leader process and will be followed by a return stroke. Allibone and Meek (19) succeeded in obtaining successive strokes down an old channel with long sparks by putting a capacity across the gap in a non-oscillating circuit with high resistance in series with a negative point as shown in Fig. 20.

Allibone and Meek further reproduced certain of the other phenomena observed in lightning with their long sparks. It was observed that sparks with positive point and grounded plane proceeded more readily than with negative point. The streamer crossed directly as would be expected with velocities of the anticipated magnitude as shown in Fig. 21. The gaps of about a meter in length naturally precluded stepped leaders. *Artificial* stepping could be induced by placing a high resistance in series with the positive point as seen in Fig. 21(*b*). The stepping is, however, caused by a temporary reduction of the positive point potential by the neutralizing current of electrons to it and the recovery of potential at the point through the high resistance. Discharge from a negative point with grounded conducting plane showed the reluctance of the streamer mechanism to proceed smoothly. There was no stepping in the negative process (19,31). Instead there was a series of separate predischarges with final breakdown presumably following along one of the earlier channels as seen in Fig. 13. A tendency to breakdown with midgap streamers was also evident with a negative point indicating the difficulty of the negative streamer mechanism. Positive streamers from the ground always appear in these long sparks since they are favored by the high conductivity of the metal plane.

It is seen in this necessarily rapid survey that since 1935 we have come a long way in the interpretation of one of the most terrifying and conspicuous phenomena observed by mankind from times immemorable. A great deal of further study is needed. It is hoped that by thus bringing together the elements of our accumulated knowledge from

widely different sources enough interest may be stimulated to bring other workers into this field to carry the studies further.

REFERENCES.

(1) L. B. LOEB, "Fundamental Processes of Electrical Discharge in Gases," New York, John Wiley & Sons, Inc., p. 426 (1939); J. M. MEEK, *Phys. Rev.*, Vol. 57, p. 722 (1940); L. B. LOEB AND J. M. MEEK, *J. Applied Phys.*, Vol. 11, pp. 438, 459 (1940); L. B. LOEB AND J. M. MEEK, "Mechanism of the Electric Spark," Stanford Press (1941).

(2) H. RAETHER, *Zeits. f. Phys.*, Vol. 110, p. 611 (1938); Vol. 117, p. 386 (1941); Vol. 117, p. 524 (1941); *Archiv. für Elektrotech.*, Vol. 34, p. 49 (1940).

(3) B. F. J. SCHONLAND AND H. COLLENS, *Proc. Roy. Soc.*, Vol. A143, p. 654 (1934); Vol. A152, p. 595 (1935); Vol. A162, p. 175 (1937); Vol. A164, p. 132 (1938); Vol. A166, p. 356 (1938); D. J. MALAN AND B. F. J. SCHONLAND, *Proc. Roy. Soc.*, Vol. A191, p. 483 (1947).

(4) J. S. TOWNSEND, "Electricity in Gases," Oxford Press (1915).

(5) For the numerous references on this item see L. B. LOEB, "Fundamental Processes," *loc. cit.*, p. 449, References 41 through 50. Also LOEB AND MEEK, "Mechanism of the Electric Spark," *loc. cit.*, p. 32, Reference 19.

(6) A. M. CRAVATH, *Phys. Rev.*, Vol. 47, p. 254(A) (1935); DECHENE, *Jour. de Phys. e Radium*, Vol. 7, p. 533 (1936); E. GREINER, *Zeits f. Phys.*, Vol. 81, p. 543 (1933); H. RAETHER, *Zeits. f. Phys.*, Vol. 110, p. 611 (1938); H. COSTA, *ibid.*, Vol. 113, p. 531 (1939); Vol. 116, p. 508 (1940); W. SCHWIECKER, *ibid.*, Vol. 116, p. 562 (1940).

(7) L. B. LOEB AND A. F. KIP, *J. Applied Phys.*, Vol. 10, p. 142 (1939). Also L. B. LOEB, "Fundamental Processes," *loc. cit.*, p. 514 ff.

(8) B. WALTER, *Jahrb. d. Hamburger. Wiss. Anst.*, Vol. 20 (1903); C. V. BOYS, *Nature*, Vol. 118, p. 749 (1926); Vol. 122, p. 310 (1928).

(9) F. W. PEEK, JR., *Trans. Am. Inst. Electrical Engrs.*, Vol. 48, p. 436 (1939); R. R. PITMAN AND J. J. TOROK, *ibid.*, Vol. 50, p. 568 (1931); E. J. WORKMAN AND R. E. HOLZER, Researches, Albuquerque, N. M., 1938–40. Not yet published; H. NORINDER, JOURNAL FRANKLIN INST., Vol. 225, p. 69 (1936); Vol. 244, pp. 109, 167 (1947); K. B. MCEACHRON, *ibid.*, Vol. 227, p. 149 (1939).

(10) L. B. LOEB AND J. M. MEEK, "Mechanism of the Electric Spark," *loc. cit.*, p. 37.

(11) L. B. LOEB, *Reviews of Modern Physics*, Vol. 20, p. 151 (1948).

(12) H. RAETHER, *Archiv. f. Elektrotech.*, Vol. 34, p. 49 (1940).

(13) L. B. LOEB AND J. M. MEEK, "Mechanism of the Electric Spark," *loc. cit.*, p. 40 ff.

(14) E. G. SCHNEIDER, *J. Optical Soc. Am.*, Vol. 30, p. 128 (1940).

(15) S. GORRILL, Thesis, University of California (1939).

(16) S. ZAVENTZ AND V. HEY, *Jour. Phys. USSR.*, Vol. 11, p. 413 (1946).

(17) Additional data come from as yet unpublished work of Meek and associates at Liverpool.

(18) V. B. WAITHMAN AND W. R. BAKER, *Phys. Rev.*, Vol. 57, p. 252A (1940).

(19) T. E. ALLIBONE AND J. M. MEEK, *Proc. Roy. Soc.*, Vol. A166, p. 97 (1938).

(20) L. B. SNODDY, DIETERICH, and J. W. BEAMS, *Phys. Rev.*, Vol. 50, p. 469 (1936); Vol. 52, p. 739 (1937); F. H. MITCHELL AND L. B. SNODDY, *Phys. Rev.*, Vol. 72, p. 1202 (1947).

(21) J. D. CRAGGS AND J. M. MEEK, *Proc. Roy. Soc.*, Vol. A186, p. 241 (1946).

(22) Paper delivered by J. M. Meek before Phys. Soc. London, April 23, 1947. Not yet published.

(23) C. G. MILLER AND L. B. LOEB, *Phys. Rev.*, Vol. 73, p. 84 (1948).

(24) E. O. LAWRENCE AND F. G. DUNNINGTON, *Phys. Rev.*, Vol. 35, p. 396 (1930); F. G. DUNNINGTON, *ibid.*, Vol. 38, p. 1535 (1931); H. J. WHITE, *ibid.*, Vol. 46, p. 99 (1934); T. E. ALLIBONE AND J. M. MEEK, *Proc. Roy. Soc.*, Vol. A169, p. 246 (1938).

(25) L. B. LOEB AND J. M. MEEK, "Mechanism of the Electric Spark," *loc. cit.*, p. 58 ff.

(26) TERADA AND NAKAYA, *Sci. Papers Inst. Phys. Chem. Research*, Tokyo, Vol. 4, p. 129 (1923); Vol. 8, pp. 1, 63, 103, 197 (1925); Vol. 10, p. 43 (1929).

(27) SIR G. C. SIMPSON AND F. J. SCRASE, *Proc. Roy. Soc.*, Vol. A161, p. 309 (1937). Similar conclusions come from preliminary work of Seville Chapman in 1947.
(28) R. GUNN, *Phys. Rev.*, Vol. 71, p. 181 (1947); also R. GUNN, HALL AND KINZER, *Proc. Inst. Rad. Eng.*, Vol. 34, p. 156 P, April (1946).
(29) Analogous views were also expressed by R. E. HOLZER in a Seminar, University of California, Oct. 28, 1947, on basis of their studies.
(30) W. A. MACKY, *Proc. Roy. Soc.*, Vol. A133, p. 565 (1931); J. ZELENY, *Proc. Camb. Phil. Soc.*, Vol. 71, p. 18 (1914); *Phys. Rev.*, Vol. 16, p. 102 (1920); W. N. ENGLISH, *Phys. Rev.*, Vol. 74, July, 1948.
(31) T. E. ALLIBONE AND J. M. MEEK, *Proc. Roy. Soc.*, Vol. A169, p. 246 (1938).
(32) L. B. LOEB AND J. M. MEEK, "Mechanism of the Electric Spark," *loc. cit.*, p. 71 ff.; also 89 ff.
(33) TH. NEUGEBAUER, *Zeits. f. Phys.*, Vol. 106, p. 474 (1937).
(34) J. D. CRAGGS AND W. HOPWOOD, *Proc. Phys. Soc. London*, Vol. 59, pp. 755, 771 (1947).
(35) J. M. MEEK, *Phys. Rev.*, Vol. 55, p. 972 (1939).
(36) L. B. LOEB AND J. M. MEEK, "Mechanism of the Electric Spark," *loc. cit.*, p. 101 ff.
(37) H. MARGENAU AND W. W. WATSON, *Phys. Rev.*, Vol. 8, p. 22 (1936).
(38) R. H. GOLDE, Letter to the Editor, *Nature*, Vol. 160, p. 395 (1947).
(39) J. D. CRAGGS, W. HOPWOOD, AND J. M. MEEK, *J. Applied Phys.*, Vol. 18, p. 919 (1947).
(40) L. B. LOEB, *Phys. Rev.*, Vol. 73, p. 798 (1948).
(41) L. B. LOEB, *Phys. Rev.*, Vol. 74, Aug., 1948; also L. B. LOEB and R. A. WIJSMANN, *Jour. App. Phys.*, Aug., 1948.
(42) EDMUND A. EVANS, "Study of Mechanism Lightning Discharge," Thesis No. 3781 S78E, Stanford University (1932).

CERTAIN MATTERS CONCERNING SCALING IN THE MAGNETRON WITH SPECIAL REFERENCE TO THE RELATIVE EFFICIENCY OF MAGNETRONS OF DIFFERENT SIZES.*

BY

W. F. G. SWANN,[1] D.Sc.

ABSTRACT.

The paper concerns the comparison of the behavior of two magnetron systems of different sizes, all apparatus from the input terminals of the magnetron to the final radiation antenna being contemplated in the picture. The mathematical comparison of the two systems assumes a specially simple form when the electrical conductivities of the corresponding parts of the systems in the two cases are adjusted to values in the inverse ratio of the scaling in linear dimensions. A scaling of this kind is therefore studied. The conclusions reached are as follows:

For an assigned potential applied to the two models, the power input is the same, the power radiated from the antenna is the same, the power dissipated in Ohm's law heating in all parts is the same, and the power dissipated in back-bombardment or at the anode is the same.

As a corollary to the foregoing, it is inferred that if the corresponding parts of the two models have the same electrical conductivity, then in so far as Ohm's law heating is an important factor at all, it is more important in the small model than in the large one.

INTRODUCTION.

Previous considerations of the problem of scaling have been given by A. M. Clogston [2] and by the writer.[3] The present paper is of more general application and is designed primarily for the discussion of power considerations. It is unlikely that the results here developed are not known, wholly or in part. However, I have found no statement of them, and discussions of the matter with specialists in this field have encouraged me to publish the presentation. The compactness of its nature may make it of interest even to those who are familiar with some or all of its consequences.

PRELIMINARY STATEMENT REGARDING ASSIGNED CONDITIONS.

In order to start the magnetron in operation it is necessary to assign certain magnitudes—a magnetic field, as produced by the magnet, and

---

* A supplementary report on Contract No. OEMsr-358.

[1] Director, Bartol Research Foundation of The Franklin Institute, Swarthmore, Penna.

[2] Voltage and Wave Length Scaling of Magnetrons, Report 52—1/21/43, Radiation Laboratory.

[3] A Theorem on the Correspondence of Conditions in the Steady State Solutions for Magnetrons of Different Sizes. Appendix to Second Report on Contract OEMsr-358, Supplement 1, January 1, 1943.

a "potential difference" between anode and cathode. Regarding the latter assignment, a little more care is necessary in statement. In general, in a problem involving non-statical considerations, there is no such thing as a potential difference between two points in the elementary sense of the phrase.[4] Even if we should have a simple case such as is represented in Fig. 1, there is no sense to speaking of the potential difference between A and B for a case where magnetic flux is changing through $ADBC$, for example. In such a case the line integral from A to B depends upon the path. In the case of the magnetron, there is no sense to speaking, without reservation, of the potential difference between the anode and cathode. The changing magnetic fields resulting from the oscillating currents render meaningless the elementary concept

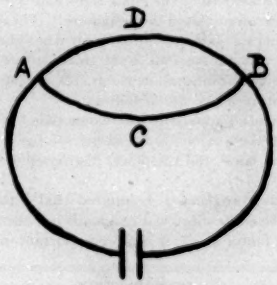

FIG. 1.

of potential difference between different parts of anode and cathode The electric field is everywhere given by

$$\mathbf{E} = -\frac{1}{c}\frac{\partial \mathbf{U}}{\partial t} - \text{grad } \varphi,$$

where φ is the scalar and $\mathbf{U}$ the vector potential, but no less complete a specification of the field has any justification.

In spite of the foregoing remarks, there is sense to speaking of the line integral of $\mathbf{E}$ between two points for a definite path. In the case of the magnetron we shall consider this line integral as the thing specified when the two end points are the input terminals and the path is one which joins these two terminals outside the magnetron, or at any rate in such fashion that the magnetron contributes no changing magnetic flux through the circuit composed of this path and the remainder of the circuit leading to the pulser. In other words, if the magnetron be operated by attachment of its terminals to the poles of a hypothetical

[4] There are, of course, definite values for the vector and scalar potential differences between any two points, these quantities being understood in the sense implied in electrodynamics.

battery of infinitely low resistance, the aforesaid line integral would in this case be equal to the electromotive force of the battery.

Having put this matter upon a firm basis, we shall follow the custom of speaking of the potential difference applied between the magnetron terminals, the term "potential difference" now being understood in the sense of the foregoing line integral.

THE CONTROLLING CONDITIONS FOR OPERATION.

We shall consider the system starting with the input terminals and comprising the magnetron proper, its associated coupling loop, an output antenna and any intermediate tuning apparatus. The operation of this compound device is governed by laws and assigned conditions *a*, *b*, *c*, *d*, as follows:

(*a*) For the present problem, where the permeability is unity in all relevant places.

$$\frac{1}{c}\left(\mathbf{i} + k\frac{\partial \mathbf{E}}{\partial t}\right) = \text{curl}\,\mathbf{H}, \tag{1}$$

$$\rho = \text{div}\,\mathbf{E} \tag{2}$$

$$-\frac{1}{c}\frac{\partial \mathbf{H}}{\partial t} = \text{curl}\,\mathbf{E}, \tag{3}$$

$$0 = \text{div}\,\mathbf{H}, \tag{4}$$

where $\mathbf{i}$ is the current density, and the significance of the other symbols is obvious. These equations apply within the conductors and within all cavities or other spaces in the conductors, also in the free space surrounding the antenna.

(*b*) In the material of the conductors, we shall suppose that the current density is controlled by Ohm's law [5]

$$\mathbf{i} = \sigma\mathbf{E}. \tag{5}$$

(*c*) At a point in the magnetron cavities, the motion of an electron is controlled by

$$\frac{d}{dt}(m\mathbf{u}) = e\left(\mathbf{E} + \frac{[\mathbf{uH}]}{c}\right), \tag{6}$$

where $\mathbf{u}$ is the velocity of an electron and m is its mass. In this con-

[5] If we should use the more complicated equation involving $[\boldsymbol{\omega}\mathbf{H}]/c$, where $\boldsymbol{\omega}$ is the mean velocity of the electrons in the material, that would simply mean including the Hall Effect in our calculations. We shall neglect this refinement, not because it is necessary to do so, but in order not to complicate the main derivation by the inclusion of things of subsidiary interest. However, in an Appendix to this paper, we shall point out that even this Hall Effect conforms to the scaling theorem exactly, and indeed it will appear that the fundamental equations (1) to (4) and (5) may be used in a more general form without affecting the scaling characteristics.

nection, there is no need to limit ourselves to a non-relativistic mass, although the velocities involved are too small to render relativistic considerations important.

(*d*) Any mathematical problem requires, in addition to a specification of the fundamental laws which give the course of events, a specification of the necessary assignments of magnitude which must be made to provide for a unique solution of the problem. A formal procedure would call for a careful analysis of this matter. However, relying upon the generally accepted belief, as substantiated, moreover, by the experimental facts, we shall suppose that the conditions and magnitudes which must be assigned to give a unique solution for the steady state are:

1. The assignment of the magnetic field $\mathbf{H}_m$ of the magnetron magnet.
2. The assignment, in the sense already defined, of the potential difference V between the input terminals of the magnetron.
3. The assignment, for the cathode, of the temperature conditions which will insure operation under conditions of space change limitation, so that the normal component of $\mathbf{E}$ at the cathode is always zero.
4. Assignment of the usual boundary conditions at the junction of two media, viz., equality of the tangential components of $\mathbf{E}$ and $\mathbf{H}$ and equality of the normal components of $D\ (= k\mathbf{E})$ and $B\ (= \mathbf{H}$ in this case, in all relevant places).

Now suppose that quantities in a certain magnetron system are denoted by a subscript unity attached to them, and that we consider another system, which we shall designate by the subscript 2, and in which all linear dimensions are scaled down on the ratio ϵ, where $\epsilon < 1$.

We shall define "corresponding" points and times in the two systems by the relation

$$(x_2, y_2, z_2, t_2) = \epsilon(x_1, y_1, z_1, t_1) \tag{7}$$

in which it will be observed that we are comparing events in system (1) with those at scaled-down times in system (2).

Recognizing that quantities with subscript unity hang together as a solution of (1) to (6), satisfying the boundary conditions, and making $V = V_1$, and $\mathbf{H}_m = \mathbf{H}_{m1}$, we shall consider as candidates for the solution in system (2) the following quantities:

$$\mathbf{E}_2 = \mathbf{E}_1/\epsilon; \qquad \mathbf{H}_2 = \mathbf{H}_1/\epsilon; \tag{8}$$

$$\rho_2 = \rho_1/\epsilon^2; \qquad \mathbf{i}_2 = \mathbf{i}_1/\epsilon^2; \qquad \mathbf{u}_2 = \mathbf{u}_1 \tag{9}$$

so that, of course,

$$\mathbf{H}_{m2} = \mathbf{H}_{m1}/\epsilon.$$

The quantities are to be applied at points x_2, y_2, z_2, and at times t_2 in system (2) related to the corresponding points x_1, y_1, z_1, and times t_1

for system (1) in the manner defined by (7) as already implied. However, we shall regard our system (2) as not only scaled down but as provided with different electrical conductivities as regards its various parts in such fashion that, at corresponding points,[6]

$$\sigma_2 = \sigma_1/\epsilon. \tag{10}$$

However, we shall not scale k. In other words, $k_1 = k_2$.

Now it is immediately obvious that, at corresponding points and times,

$$\frac{\partial \mathbf{E}_2}{\partial t_2} = \frac{1}{\epsilon}\frac{\partial}{\partial t_1}\left(\frac{\mathbf{E}_1}{\epsilon}\right); \qquad \frac{\partial \mathbf{H}_2}{\partial t_2} = \frac{1}{\epsilon}\frac{\partial}{\partial t_1}\left(\frac{\mathbf{H}_1}{\epsilon}\right), \tag{11}$$

$$\left(\frac{\partial \mathbf{E}_2}{\partial x_2}, \frac{\partial \mathbf{E}_2}{\partial y_2}, \frac{\partial \mathbf{E}_2}{\partial z_2}\right) = \frac{1}{\epsilon}\left[\frac{\partial}{\partial x_1}\left(\frac{\mathbf{E}_1}{\epsilon}\right), \frac{\partial}{\partial y_1}\left(\frac{\mathbf{E}_1}{\epsilon}\right), \frac{\partial}{\partial z_1}\left(\frac{\mathbf{E}_1}{\epsilon}\right)\right], \tag{12}$$

$$\left(\frac{\partial \mathbf{H}_2}{\partial x_2}, \frac{\partial \mathbf{H}_2}{\partial y_2}, \frac{\partial \mathbf{H}_2}{\partial z_2}\right) = \frac{1}{\epsilon}\left[\frac{\partial}{\partial x_1}\left(\frac{\mathbf{H}_1}{\epsilon}\right), \frac{\partial}{\partial y_1}\left(\frac{\mathbf{H}_1}{\epsilon}\right), \frac{\partial}{\partial z_1}\left(\frac{\mathbf{H}_1}{\epsilon}\right)\right]. \tag{13}$$

Moreover, if ds is an element of the path of an orbit of an electron in the magnetron cavity, and $\mathbf{u}$ is the electron velocity,

$$\frac{d}{dt}(m\mathbf{u}) = \mathbf{u}\frac{d}{ds}(m\mathbf{u}).$$

Thus since at corresponding points $\mathbf{u}_2 = \mathbf{u}_1$, so that the masses at corresponding points are the same, we have, at corresponding points,

$$\frac{d}{dt_2}(m\mathbf{u}_2) = \frac{1}{\epsilon}\frac{d}{dt_1}(m\mathbf{u}_1). \tag{14}$$

It will now be immediately obvious that if $\mathbf{E}_1$, $\mathbf{H}_1$, ρ_1, $\mathbf{u}_1$, $\mathbf{i}_1$ are solutions of (1) to (6) for system (1) with $\sigma = \sigma_1$, then the corresponding values of these quantities as defined by (8) and (9) are solutions of (1) to (6) at corresponding points and times, provided that at corresponding points σ_2 is given by (10). If they are solutions at all *corresponding* points and times, they are solutions at *all* points and times.

As regards the supplementary conditions, we can regard $\mathbf{H}_{m1}$ as a part of the field of the problem and constituting the whole field at such a point as P for example. We thus see that we must have, as already stated,

$$\mathbf{H}_{m2} = \mathbf{H}_{m1}/\epsilon. \tag{15}$$

Since at corresponding points and times $\mathbf{E}_2 = \mathbf{E}_1/\epsilon$, and since corresponding elements of path in the second and first systems are in the ratio $\epsilon/1$, it is obvious that line integrals of $\mathbf{E}$ between corresponding

[6] The reason for this is simply one of mathematical convenience. There is, of course, *meaning* to a problem in which the conductivities are equal at corresponding points in the two systems. However, in such a problem the solutions are not related by such a simple transformation as is here employed.

points are the same in the two systems. Thus we must have

$$V_2 = V_1. \tag{16}$$

Provided that the temperature conditions are properly chosen in system (2), the space charge limitation will be provided for in that system if it is provided for in the first system. Thus the normal component of **E** at the cathode will be zero in the second system if it is zero in the first.

It will be immediately obvious that the boundary conditions at the surface of two media are satisfied in the second system provided that they are satisfied in the first.

POWER COMPARISONS.

It will be convenient to define n as

$$n \equiv 1/\epsilon.$$

Power Input. The power input is VI. Now $V_1 = V_2$. Again, since at corresponding points $\mathbf{i}_2 = \mathbf{i}_1 n^2$, and since corresponding elements of area ds are related by $ds_2 = ds_1/n^2$, it is obvious that as regards the input current, $I_2 = I_1$. *Hence the input power is the same in the two systems.*

Power Radiated. The power radiated from the antenna is P_{r1}, where

$$P_r = AM^2\nu^4. \tag{17}$$

Here M is the maximum moment of the antenna, ν is the frequency, and A is the same for both systems.

Now considering corresponding elements of volume dv of the antennae in the two systems, we have $dv_2 = dv_1/n^3$. Since $\rho_2 = \rho_1 n^2$ if L is the distance of a point on the antenna from the neutral plane, the distance being measured parallel to the axis of the antenna, $L_2 = L_1/n$.

Now

$$M = \int \rho L dv,$$

where the integration extends all over the antenna. Hence

$$M_2 = \int \rho_2 L_2 dv_2 = \frac{n^2}{nn^3} \int \rho_1 L_1 dv_1 = \frac{M_1}{n^2}.$$

Hence, since $\nu_2 = n\nu_1$, we have, from (17),

$$(P_r)_2 = AM_2^2\nu_2^4 = \frac{AM_1^2}{n^4}\nu_1^4 n^4 = (P_r)_1.$$

Hence the power radiated is the same for the two systems.

Power Absorbed in Ohm's Law Heating. The power absorbed in an element of volume dv is $\mathbf{i}^2 dv/\sigma$. The total power absorbed in Ohm's

law heating is P_o, where

$$P_o = \int \frac{\mathbf{i}^2}{\sigma} dv_1,$$

the integral being extended over all the conductors of the apparatus. Since $\mathbf{i}_2 = n^2\mathbf{i}_1$, and $dv_2 = dv_1/n^3$, and at corresponding places $\sigma_2 = n\sigma_1$

$$(P_o)_2 = \int \frac{\mathbf{i}_1^2 dv_2}{\sigma_2} = \frac{n^4}{n^3 n} \int \frac{\mathbf{i}_1^2 dv_1}{\sigma_1} = (P_o)_1.$$

Hence the power absorbed in Ohm's law heating is the same for the two systems.

Power Absorbed in Back-Bombardment or at the Anode. If dS is an element of the cathode surface, the power P_b absorbed in back-bombardment is given by

$$P_b = \int N u_n W dS,$$

where N is the number of electrons per cubic centimeter at a point near the cathode, W is the energy of an electron, u_n is the velocity of the

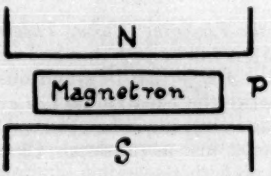

FIG. 2.

electrons normal to the surface and where the integration is extended all over the cathode. Now

$$Neu_n = i_n;$$

thus

$$P_b = \frac{1}{e} \int i_n W dS.$$

Now since W depends only upon $\mathbf{u}$, it is the same for both systems. Hence, since $dS_2 = dS_1/n^2$, and $i_{n2} = n^2 i_{n1}$,

$$(P_b)_2 = \frac{1}{e} \int i_{n2} W_2 dS_2 = \frac{n^2}{n^2} \int i_{n1} W_1 dS_1 = (P_b)_1.$$

Hence the power absorbed in back-bombardment is the same in the two systems. A similar result holds for anode power absorption.

Comment Regarding the Foregoing. In spite of the fact that the input power, the power radiated, the power lost in Ohm's law heating,

the power lost in back-bombardment, and the power lost at the anode are the same for the two systems above studied, we have to observe that the means of getting rid of the power lost in Ohm's law heating, in back-bombardment, and at the anode present a more serious problem in the case of the small magnetron than in that of the large one.

Inferences Regarding the Case Where the Electrical Conductivities are the Same in the Two Systems. In the case of the smaller system of the above problems the conductivity is larger than that for the larger system at corresponding points. If it is now made the same, all other *assigned* conditions being maintained, it is obvious that all currents will be reduced and the radiation will be reduced. If we now raise V so as to bring the power radiated from the antenna back to what it was before, we shall increase all the currents in the conductors and so the Ohm's law heat dissipated in them. The Ohm's law dissipation will therefore be no longer equal to the power radiated but will be greater. We thus conclude that for magnetron assemblies of the same material, in so far as Ohm's law losses are important at all, they are more important in relation to the energy radiated for small magnetrons than for large ones.

APPENDIX.

Generalization of the Foregoing Scaling Theorem. Reverting to the remark in footnote (5), it will be seen that had we replaced Eq. 5 by the more general form $\mathbf{i} = \sigma(\mathbf{E} + [\omega\mathbf{H}]/c)$, and observing that $\mathbf{i} = \omega\rho$ in the wire, we could write the equation as $\mathbf{i} = \sigma(\mathbf{E} + [\mathbf{iH}]/\rho c)$, and in the light of (8), (9), and (10), it will be observed that this more general equation scales properly, just as (5) does. Of course, the scaling of ρ in the wire is bound up with the scaling of σ and of the dimensions of the conductor.

We may proceed to even greater generality along the following lines. We may replace (1) to (4) and (5) by the relativistically invariant macroscopic equations [7]

$$\frac{1}{c}\left(\mathbf{i} + \rho\mathbf{w} + \frac{\partial \mathbf{D}}{\partial t}\right) = \text{curl } \mathbf{H}, \tag{1.1}$$

$$\rho = \text{div } \mathbf{D}, \tag{2.1}$$

$$-\frac{1}{c}\frac{\partial \mathbf{B}}{\partial t} = \text{curl } \mathbf{E}, \tag{3.1}$$

$$0 = \text{div } \mathbf{B}, \tag{4.1}$$

$$\mathbf{i} = \frac{\sigma}{(1 - \mathbf{w}^2/c^2)^{\frac{1}{2}}}\left\{\left(\mathbf{E} + \frac{[\mathbf{wB}]}{c} - \frac{\mathbf{w}(\mathbf{Ew})}{c^2}\right)\right\}, \tag{5.1}$$

[7] See, for example, E. CUNNINGHAM, "The Principle of Relativity," Cambridge University Press (1914), p. 121.

together with the relativistically invariant relations

$$\mathbf{B} - \frac{[\mathbf{wE}]}{c} = \mu\left(\mathbf{H} - \frac{[\mathbf{wD}]}{c}\right),$$

$$\mathbf{D} + \frac{[\mathbf{wH}]}{c} = k\left(\mathbf{E} + \frac{[\mathbf{wB}]}{c}\right),$$

where $\mathbf{w}$ is the velocity of the medium, μ and k are constants, or at any rate quantities invariant under the transformation (7) and the restricted relativity transformation.

We also replace (6) by

$$\frac{d}{dt}(m\mathbf{u}) = e\left(\mathbf{E} + \frac{[\mathbf{uB}]}{c}\right), \tag{6.1}$$

where $\mathbf{u}$ is the velocity of the electron.

It then becomes immediately obvious along the lines of the main paper that (14) holds and the equations (1.1) to (6.1) assume the same form in $\mathbf{E}_2, \mathbf{H}_2, \mathbf{D}_2, \mathbf{B}_2, \mathbf{u}_2, \rho_2, \mathbf{i}_2$, as in $\mathbf{E}_1, \mathbf{H}_1, \mathbf{D}_1, \mathbf{B}_1, \mathbf{u}_1, \rho_1, \mathbf{i}_1$, provided that

$$\begin{array}{llll}
\mathbf{E}_2 = \mathbf{E}_1/\epsilon; & \mathbf{H}_2 = \mathbf{H}_1/\epsilon; & & \\
\mathbf{D}_2 = \mathbf{D}_1/\epsilon; & \mathbf{B}_2 = \mathbf{B}_1/\epsilon; & & \\
\rho_2 = \rho_1/\epsilon^2; & \mathbf{i}_2 = \mathbf{i}_1/\epsilon^2; & & \\
\mathbf{w}_2 = \mathbf{w}_1; & \mathbf{u}_2 = \mathbf{u}_1; & \sigma_2 = \sigma_1/\epsilon; & \\
V_2 = V_1; & \mathbf{H}_{m2} = \mathbf{H}_{m1}/\epsilon. &
\end{array}$$

It immediately follows that the results cited under "Power Comparisons" also hold. In this connection, it is perhaps desirable to treat the power absorbed in Ohm's law heating rather differently, as follows: The power absorbed in an element of volume dv is $(\mathbf{Ei})dv$. This includes power absorbed in Ohm's law heating in the element and power ultimately radiated. In view of the scaling relations, this power is the same in the scaled and unscaled systems. Now the Poynting flux from the element dv is c div $[\mathbf{EH}]dv$. In view of the scaling relations, this is the same in the scaled as in the unscaled system. Hence the difference between this quantity and $(\mathbf{Ei})dv$ cited above, which difference represents the energy dissipated as heat within dv, is the same in the scaled as in the unscaled system.

Valuable Oil From Weed Seed.—The possibility of making a valuable oil from the seed of pennycress, a European weed common in middle western and western States, has been suggested.

This weed, also called fan-weed, French-weed, dish mustard, treacle-wort, and bastard cress, favors grasslands, gardens, and waste places, and is a serious nuisance in grain fields. It is a major constituent of grain screenings in some areas. Its seeds yield about a third of their weight in oil; the residual oil-free meal has a protein content higher than that of undecorticated cottonseed meal obtained by mechanical expression which contains about 28 per cent protein.

The potential value of pennycress oil naturally lies in its close resemblance to oils of rape and mustard, which are valued ingredients of certain lubricants, and are employed in machinery operating under heavy loads at high temperatures such as marine and Diesel engines. Rape oil is also used in producing factice, a rubber substitute. Domestic supplies of such oils are insufficient, and the U. S. imports as much as 15,000 tons of rapeseed oil annually. Under irrigation, as high as 1,500 lb. of seed per acre have been obtained, and without irrigation, up to 500 lb. per acre.

Both rape and mustard oils are used in some food products, and it is probable that with proper refinement, pennycress oil is edible. The oil is semi-drying and would be excellent as a machinery lubricant and for bearing surfaces subject to the flushing action of water. The meal has a flavor of combined garlic and mustard. Thus this research suggests that a common nuisance may become a practical raw material for the production of a valuable vegetable oil, a feed material, and perhaps a condiment. Moreover, it is possible that investigation may reveal other weed seeds that also yield useful oils.

R. H. O.

Two and a Half Acres Per Stomach.—Productive land is "the master key to peace among peoples," says Dr. H. H. Bennett of the U. S. Department of Agriculture in a recent address in which he emphasized that misuse of land does not stop at any nation's boundaries, and that conservation is a world-wide task.

Developing this theme, he "took a look" at the situation in the world and in the United States. The survey was based on nutritional studies that show "we need at least 2½ acres per capita of good productive land to furnish each person with a minimum nutritious diet."

In the world, he finds, there are only about 4 billion acres of immediately arable land for a world population of more than 2 billion people, which is increasing at a rate of about 20 million persons a year. On the 2½ acre per capita basis there is already a world shortage, he finds.

In the United States the situation is somewhat better. The U. S. today has about 460 million acres of high grade cropland for a population of 144 million—about 3 acres per capita. But population is continuing to increase—by about 2.2 millions in 1946. The margin above the 2½ acres is getting narrower both as a result of increasing numbers and because of destruction of good land by misuse, particularly by erosion.

Many parts of the world are already beyond the borderline of this safe ratio of land to population. For the United States, says Bennett, "The conclusion is plain: Time and land are running out, and we dare not delay for a single unnecessary reason in safeguarding the productive land which we have left."

R. H. O.

METHOD OF SOLVING DIFFERENTIAL EQUATIONS WITH CONSTANT COEFFICIENTS.

BY

W. V. LYON.[1]

The following method of solving ordinary differential equations with constant coefficients employs only well-known classical principles and consequently should be of interest to those who have not taken time to become familiar with one of the operational methods of solving these equations.

There are three distinct parts to the classical solution:

1. Finding the particular integral. This is adequately treated in any good text on differential equations.
2. Finding the algebraic roots of the characteristic equation. This is a necessary part of any method of solution and is not considered here.
3. Finding the coefficients in the complementary function.

It is the purpose of this note to show how a general expression can be developed for these coefficients from which their numerical values are readily computed.

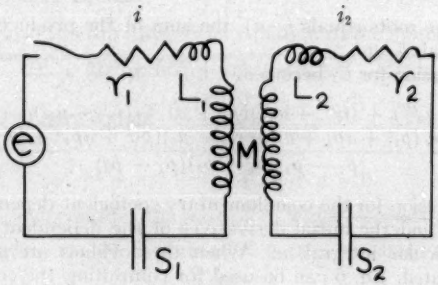

FIG. 1.

Consider the electrical circuit of Fig. 1 on which an emf. e is impressed at time $t = 0$. The differential equation which applies to this circuit is of the fourth order and the general solution for the current i is

$$i = u + C_1\epsilon^{p_1 t} + C_2\epsilon^{p_2 t} + C_3\epsilon^{p_3 t} + C_4\epsilon^{p_4 t}, \qquad (1)$$

where u is the particular integral and the roots $p_1, \cdots p_4$ of the charac-

[1] Department of Electrical Engineering, Massachusetts Institute of Technology, Cambridge, Mass.

teristic equation are all different. At $t = 0$

$$C_1 + C_2 + C_3 + C_4 = i_0 - u_0, \tag{2}$$

where the zero subscript indicates the value is at $t = 0$. Differentiate Eq. 1 and obtain at $t = 0$

$$p_1C_1 + p_2C_2 + p_3C_3 + p_4C_4 = i_0' - u_0', \tag{3}$$

where the prime indicates the derivative.

Differentiate a second and third time and obtain at $t = 0$

$$p_1^2C_1 + p_2^2C_2 + p_3^2C_3 + p_4^2C_4 = i_0'' - u_0'', \tag{4}$$

$$p_1^3C_1 + p_2^3C_2 + p_3^3C_3 + p_4^3C_4 = i_0''' - u_0'''. \tag{5}$$

Eliminate C_4 from these equations in the following way:

Multiply Eq. 2 by p_4 and subtract from Eq. 3
Multiply Eq. 3 by p_4 and subtract from Eq. 4
Multiply Eq. 4 by p_4 and subtract from Eq. 5

Proceed in a similar manner and eliminate C_3 and then C_2. In the final equation for C_1 introduce the relations that exist among the roots of the characteristic equation and its coefficients. If the characteristic equation is

$$p^4 + ap^3 + bp^2 + cp + d = 0,$$

the sum of the roots equals $(-a)$, the sum of the products taken two at a time equals b, etc.

The expression for C_1 becomes

$$C_1 = \frac{\begin{array}{l}(i_0''' - u_0''') + (i_0'' - u_0'')(p_1 + a) + (i_0' - u_0') \\ \times (p_1^2 + ap_1 + b) + (i_0 - u_0)(p_1^3 + ap_1^2 + bp_1 + c)\end{array}}{(p_1 - p_2)(p_1 - p_3)(p_1 - p_4)}. \tag{6}$$

This expression for the complementary coefficient depends upon the initial values and the initial derivatives of the dependent variable, i, and the particular integral, u. When these values are given or are readily computed, Eq. 6 can be used for computing the coefficients of the complementary function. However, the numerator of Eq. 6 can be converted into other forms which are more convenient to use in most practical problems.

The fourth order equation of which Eq. 1 is the solution is derived from two or more simultaneous equations. For example, the Kirchhoff equations which apply to the relaxed circuit of Fig. 1 are

$$(r_1 + L_1D + S_1D^{-1})i + MDi_2 = e, \tag{7}$$

$$MDi + (r_2 + L_2D + S_2D^{-1})i_2 = 0, \tag{8}$$

where $D = \frac{d}{dt}$ and $D^{-1}i = \int_0^t i\,dt$. In general if a capacitor has an initial potential v_0, the subsequent value of the potential is $v_0 + SD^{-1}i$. Integrate both sides of the Kirchhoff equations, noting that, in general, $D^{-1}Di = \int_0^t \frac{di}{dt}\,dt = i - i_0$.

Since the circuit is relaxed the integrated equations are

$$(r_1D^{-1} + L_1 + S_1D^{-2})i + Mi_2 = D^{-1}e, \tag{9}$$

$$Mi + (r_2D^{-1} + L_2 + S_2D^{-2})i_2 = 0. \tag{10}$$

The current i_2 can be eliminated from these equations by treating the integrating operator D^{-1} as an algebraic quantity. Thus the integrated equation for i is

$$\begin{vmatrix} (r_1D^{-1} + L_1 + S_1D^{-2}), & M \\ M, & (r_2D^{-1} + L_2 + S_2D^{-2}) \end{vmatrix} i = \begin{vmatrix} D^{-1}e, & M \\ 0, & (r_2D^{-1} + L_2 + S_2D^{-2}) \end{vmatrix}$$

Expand both determinants and divide by the constant term in the coefficient of i, which in this case is $(L_1L_2 - M^2)$. The integrated equation can be written in the form

$$(1 + aD^{-1} + bD^{-2} + cD^{-3} + dD^{-4})i = f(D^{-1})e, \tag{11}$$

where $f(D^{-1})$ here equals $\frac{(r_2D^{-1} + L_2 + S_2D^{-2})}{L_1L_2 - M^2}D^{-1}$. The fourth derivative of Eq. 11 is the differential equation of the system

$$(D^4 + aD^3 + bD^2 + cD + d)i = f''''(D^{-1})e, \tag{12}$$

where $f''''(D^{-1})$ here equals $\frac{(r_2D^2 + L_2D^3 + S_2D)}{L_1L_2 - M^2}$. The characteristic equation is

$$p^4 + ap^3 + bp^2 + cp + d = 0. \tag{13}$$

In Eq. 6 first consider the part of C_1 which depends upon i and its derivatives at $t = 0$. Note that at $t = 0$, $D^{-1}i = (D^{-1}i)_0 = \int_0^0 i\,dt = 0$. Also as an abbreviation let $f(D^{-1})e = \phi$. At $t = 0$, Eq. 11 reduces to

$$(i)_0 = (\phi)_0. \tag{14}$$

Differentiate Eq. 11 and obtain at $t = 0$

$$(Di)_0 + a(i)_0 = (\phi')_0. \tag{15}$$

Differentiate a second and third time and obtain

$$(D^2i)_0 + a(Di)_0 + b(i)_0 = (\phi'')_0, \tag{16}$$

$$(D^3i)_0 + a(D^2i)_0 + b(Di)_0 + c(i)_0 = (\phi''')_0. \tag{17}$$

Multiply Eq. 14 by p^3, Eq. 15 by p^2, Eq. 16 by p and add their sum to Eq. 17. It is then seen that the part of Eq. 6 which depends upon i and its derivatives becomes

$$(\phi''')_0 + p_1(\phi'')_0 + p_1^2(\phi')_0 + p_1^3(\phi)_0.$$

Next consider the part of Eq. 6 which depends upon the particular integral u and its derivatives.

Subtract the characteristic Eq. 13 from the differential Eq. 12 and obtain

$$\{(D^4 - p^4) + a(D^3 - p^3) + b(D^2 - p^2) + c(D - p)\}u = \phi''''. \quad (18)$$

$(D - p)$ is a factor of the left-hand side of Eq. 18 and hence the equation can be written:

$$(D - p)\left\{\begin{matrix} D^3 + pD^2 + p^2D + p^3 \\ + a(D^2 + pD + p^2) \\ + b(D + p) \\ + c \end{matrix}\right\}u = \phi''''$$

or

$$\{u''' + (p + a)u'' + (p^2 + ap + b)u' + (p^3 + ap^2 + bp + c)u\} = \frac{1}{D - p}\phi''''. \quad (19)$$

Consequently the part of Eq. 6 which depends upon the particular integral and its derivatives at $t = 0$ is:

$$-\left[\frac{1}{D - p_1}\phi''''\right]_0.$$

Therefore Eq. 6 can be written

$$C_1 = \frac{(\phi''')_0 + p_1(\phi'')_0 + p_1^2(\phi')_0 + p_1^3(\phi)_0 - \left[\frac{1}{D - p_1}\phi''''\right]_0}{(p_1 - p_2)(p_1 - p_3)(p_1 - p_4)}. \quad (20)$$

In Eq. 20, ϕ is obtained from the integrated forms of the differential equations and in general will depend in part upon the initial values of the kinetic and potential energies. If the circuit is relaxed, as is assumed in Fig. 1, ϕ depends only upon the circuit constants and the applied emf. and consequently the fourth order integrated equation has the form

$$(1 + aD^{-1} + bD^{-2} + cD^{-3} + dD^{-4})i = (G_0 + G_1D^{-1} + G_2D^{-2} + G_3D^{-3} + G_4D^{-4})e. \quad (21)$$

That is,

$$\phi = (G_0 + G_1D^{-1} + G_2D^{-2} + G_3D^{-3} + G_4D^{-4})e. \quad (22)$$

At $t = 0$

$$\phi_0 = G_0(e)_0. \quad (23)$$

Differentiate Eq. 22 and obtain at $t = 0$

$$(\phi')_0 = G_0(De)_0 + G_1(e)_0. \tag{24}$$

Differentiate a second and third time and obtain at $t = 0$

$$(\phi'')_0 = G_0(D^2e)_0 + G_1(De)_0 + G_2(e)_0, \tag{25}$$

$$(\phi''')_0 = G_0(D^3e)_0 + G_1(D^2e)_0 + G_2(De)_0 + G_3(e)_0. \tag{26}$$

Differentiate a fourth time and obtain

$$\phi'''' = G_0D^4e + G_1D^3e + G_2D^2e + G_3De + G_4e. \tag{27}$$

The value of $\frac{1}{D-p}\phi''''$ can be obtained by operating on the individual terms in Eq. 27.

Fifth term,

$$G_4\frac{1}{D-p}e = G_4\epsilon^{pt}\int \epsilon^{-pt}e\,dt. \tag{28}$$

Fourth term,

$$G_3\frac{1}{D-p}De = G_3\epsilon^{pt}\int \epsilon^{-pt}De\,dt.$$

Integrate by parts.

$$G_3\frac{1}{D-p}De = G_3\left(e + p\frac{1}{D-p}e\right). \tag{29}$$

Third term,

$$G_2\frac{1}{D-p}D^2e = G_2\left(De + pe + p^2\frac{1}{D-p}e\right). \tag{30}$$

Second term,

$$G_1\frac{1}{D-p}D^3e = G_1\left(D^2e + pDe + p^2e + p^3\frac{1}{D-p}e\right). \tag{31}$$

First term,

$$G_0\frac{1}{D-p}D^4e = G_0\left(D^3e + pD^2e + p^2De + p^3e + p^4\frac{1}{D-p}e\right). \tag{32}$$

If Eqs. 23, 24, 25, 26 and $\left[\frac{1}{D-p}\phi''''\right]_0$ are substituted in the numerator of Eq. 20

$$C_1 = \frac{(G_0p_1^4 + G_1p_1^3 + G_2p_1^2 + G_3p_1 + G_4)\left[-\frac{1}{D-p_1}e\right]_0}{(p_1-p_2)(p_1-p_3)(p_1-p_4)}. \tag{33}$$

If Eq. 21 is differentiated four times the result is the differential equation of the system. The right-hand side of this differential equa-

tion is

$$(G_0D^4 + G_1D^3 + G_2D^2 + G_3D + G_4)e. \tag{34}$$

Therefore the coefficient of $\left[-\frac{1}{D - p_1} e \right]_0$ in Eq. 33 is found by replacing the differential operator D in the right-hand side of the differential equation by p_1.

In the following summary the values of the particular integral and $\left[-\frac{1}{D - p} e \right]_0$ are given for a few common values of the applied emf.

SUMMARY.

An emf. e is applied to a relaxed system the differential equation for which is

$$F(D)i = f(D)e.$$

The characteristic equation is

$$F(p) = 0,$$

and the roots, all different, are $p_1, \cdots p_n$.

The first term in the complementary function is

$$C_1\epsilon^{p_1t} = \frac{f(p_1)\left(-\frac{1}{D - p_1} e \right)_0}{(p_1 - p_2) \cdots (p_1 - p_n)} \epsilon^{p_1t}.$$

V.24
1948

e	$\left[-\frac{1}{D-p} e \right]_0$	Particular integral
1	$\frac{1}{p}$	$\frac{f(0)}{F(0)}$
$\epsilon^{\alpha t}$	$\frac{1}{p - \alpha}$	$\frac{f(\alpha)}{F(\alpha)} \epsilon^{\alpha t}$
$\epsilon^{j\omega t}$	$\frac{1}{p - j\omega}$	$\frac{f(j\omega)}{F(j\omega)} \epsilon^{j\omega t}$
$\cos \omega t$	$\frac{p}{p^2 + \omega^2}$	$R_e\left(\frac{f(j\omega)}{F(j\omega)} \epsilon^{j\omega t} \right)$
$\sin \omega t$	$\frac{\omega}{p^2 + \omega^2}$	$R_e\left(-j \frac{f(j\omega)}{F(j\omega)} \epsilon^{j\omega t} \right)$
$t\epsilon^{\alpha t}$	$\frac{1}{(p - \alpha)^2}$	$\left(\frac{f(\alpha)}{F(\alpha)} \right) t\epsilon^{\alpha t} + \left(\frac{\partial}{\partial \alpha} \frac{f(\alpha)}{F(\alpha)} \right) \epsilon^{\alpha t}.$

NOTES FROM THE NATIONAL BUREAU OF STANDARDS.*

ELECTRON OPTICAL SCHLIEREN EFFECT.

Electron-microscope experiments conducted by Dr. L. L. Marton of the National Bureau of Standards have developed, in the electron optical analogy to the Schlieren effect, a valuable tool for the quantitative study of electrostatic or magnetic fields that are not susceptible to any other type of investigation. By means of the new technique, a dark-field image of magnetic or electric fields occurring between an electron source and a magnetic lens is formed beyond the focal plane of the lens. In this way it has been possible to obtain a visual representation of fringe fields from the small domains of spontaneous magnetization in ferromagnetic materials. The characteristics of such a pattern may then be used to compute the field distribution in the region under study. Extension of the principle provides a powerful means of broadening present knowledge concerning space-charge fields, fields produced by contact potentials, wave-guide problems, and the microstructure of metals.

The Schlieren method as applied to light rays involves the formation of an image of a light source on a convenient stop which intercepts all direct rays. If in the space between the source and lens there is a variation of the index of refraction, an image of that inhomogeneity will then be produced by means of the same lens in a conjugate plane beyond the stop. Thus a dark-field image of the variation in optical density of the refractive medium is obtained.

This method was adapted to electron-optical investigations at the Bureau in connection with the problem of measuring the magnetization of ferromagnetic wire used in the reproduction of sound and for recording data in electronic computing machinery. A magnetized wire was placed approximately 3 cm. from a magnetic lens having a free bore of about 16 mm. and was irradiated with an electron beam accelerated by a difference of potential of 40 kv. After a magnified image of the wire was properly focused on a fluorescent screen, the direct rays were intercepted by a center stop about 1 mm. in diameter. When the stop was placed partially across the visual field, a partly bright-field, partly dark-field image of the wire was obtained, in which the Schlieren image of the magnetic fields extending on both sides of the wire was readily recognizable. Thus, in addition to electron emission and scattering, a new category of "objects"—namely, field intensity patterns—was made available for study by means of electron optical systems.

* Communicated by the Director.

For a representation of ferromagnetic domains, experiments were carried out with thin laminar steel provided with a fine feather edge. After the samples were magnetized to saturation parallel to the edge, they were placed in an electron microscope, and the objective lens was slightly misaligned in order to bring in one edge of the objective aperture parallel to the observed edge. In this way the direct rays were intercepted by the objective aperture, and only the electrons scattered or deflected at the edge of the specimen reached the final image plane to form a dark-field image.[1] The image consisted of a bright line interrupted at irregular intervals averaging a few tenths of a micron. Wherever the line was interrupted, a faint pattern was visible at right angles to the edge. This pattern was assumed due to the fringe field of the ferromagnetic domains or of grain boundaries. Such a pattern is produced only if the average thickness of the specimen edge in the direction of the electron beam is no greater than one domain. This observation was repeated with the objective aperture at an angle to the observed edge of the sample. Part of the image was thus dark-field, and part was a bright-field image of the magnetized edge. By overexposing the bright-field portion, a fringe pattern at right angles to the edge corresponding to that of the dark-field image was observed in the bright-field image.

Perhaps the greatest value of the electron-optical Schlieren method lines in its utility for exploring complex electric and magnetic fields of extremely small dimensions or in which a probe of size greater than the electron would disturb the field under study. In the past, calculations of the field intensity at a point have been limited to those special cases in which the geometry of the field exhibits a high degree of symmetry. However, once images of the field have been obtained by the Schlieren method, the actual intensity in the neighborhood of a sample of any shape can be computed to a good approximation from the intensity distribution of the pattern or from the apparent displacement of a deflected image. The mathematical basis for these calculations has been worked out by S. H. Lachenbruch of the National Bureau of Standards.

For example, in a study of the field intensity about a magnetized wire the field may be assumed to be approximately that of an ideal magnetic dipole. If this assumption is made, an expected Schlieren intensity distribution based upon the theoretical trajectories of electrons approaching the wire in the midplane of a dipole can be calculated. Such a distribution may then be compared with the actual intensity variation of the Schlieren image in a line perpendicular to the image of the wire and bisecting the dipole pattern. In this way a better approximation to the field intensity in the midplane is obtained.

[1] The micrographs were made with the cooperation of Max Swerdlow of the Bureau's Electron Microscopy Laboratory.

The use of wave guides as conductors and circuit elements in ultra-high frequency radar and communication—and more recently in some experiments in nuclear physics—often leads to arrangements whose geometry is too complicated for expression in any known system of mathematical coordinates. The electronics engineer, having in many cases only an intuitive picture of the field distribution in such parts of the guide as elbows, must rely on empirical methods in designing wave-guide techniques and equipment. Experiments being undertaken at the Bureau by D. L. Reverdin are expected to provide a method utilizing the electron-optical Schlieren effect that may permit the calculation of field intensities in regions of a guide that are not at present susceptible to analytical treatment.

Ferromagnetism offers unique possibilities for investigation of the structure and elastic properties of metals, and it has been suggested that the electron-optical Schlieren effect may prove useful in metallurgical problems of this kind. Since the direction of magnetization in a single domain of a metallic specimen—and thus the magnetic properties of the specimen as a whole—are determined by the regularity and orientation of the atomic arrangement and the interaction between electrons of neighboring atoms, any factor tending to disturb these conditions must seriously affect the ferromagnetic properties. Magnetic data subject to reliable interpretation should thus provide valuable information on metallic purity, grain orientation, and strains caused by precipitation, grain boundaries, and unequal heating or cooling. Experiments now being planned at the National Bureau of Standards include a study of the behavior of the fringe field patterns as a function of temperature up to the Curie point (at which temperature ferromagnetic substances become paramagnetic) and repetition of these measurements on a single crystal material having very large domains. An extension to ferroelectric materials is also contemplated for the purpose of checking the domain theory of such materials.

CONTROL OF FADING LAMPS WITH LIGHT-SENSITIVE PAPER.

A practicable, inexpensive, and yet reliable means of controlling the performance of fading lamps has been developed in the Bureau's Textile Section as a solution to problems arising from the lack of reproducibility among such lamps. This is accomplished by the use of a special light-sensitive paper, which, when placed in the lamp with commercial materials being tested, will fade to an endpoint that can be visually matched with a standard. A very simple method of control independent of the unavoidable variation of radiant energy output of fading lamps is thus provided.

The use of arc lamps to test the light-stability of commercial products has become accepted procedure in many branches of industrial produc-

tion and research. It is estimated that between one and two thousand irradiation units are in practically constant operation. The results are often used to assess the relative, and even absolute, light-stability of materials used in very large-scale applications. It is therefore important that such arc lamps operate reliably.

With increasing use of irradiating units, however, it has become apparent that these arcs do not function reproducibly from unit to unit or in a given unit from day to day. As a result of recent surveys it has been determined that the variations in performance of the same make of lamp are often quite large. Among textile fading lamps, which can be considered typical, some of the weakest lamps required from two to three times as long to produce the same fading as the strongest lamps. Over one-third of the lamps included in the group were found to deviate by more than 15 per cent from a mean value.

There are a variety of explanations for such behavior but the most generally applicable one is variation of line voltage. The radiant energy output in the 300 to 400 millimicron range, which is perhaps for most applications the most effective region of the glass enclosed arc, is decreased 11 per cent by a 4 per cent drop in line voltage. Voltage variations at most substations in the District of Columbia are about 4 per cent, which are probably smaller than in most communities because of the limited amount of heavy manufacturing in the District. To this must be added the variable voltage drop in the mains, transformers, and individual plant wiring which may be as high as 11 per cent. It is thus apparent that voltage difficulties can account for very large differences in lamp performance. Although the irradiating units are provided with transformer or rheostat taps for matching line voltages, the latter are difficult to measure without a recording voltmeter, and even then are subject to change after measurement. The taps, furthermore, may not adequately match the mean line voltage.

V.2
194

It is obvious that solving line voltage problems as a means of securing uniform arc lamp behavior would be difficult. An attempt has therefore been made to develop a simple, reliable method of gaging the performance of arc lamps by the use of a light-sensitive paper.

These papers are permanent in the dark, and can be produced in large uniform batches. In use, a piece of the paper is placed in the lamp along with the materials to be irradiated, and exposure is continued until the test paper matches a standard exposure of, for example, 20 "Standard Fading Hours," regardless of the actual time elapsed.

The "standard fading hour" now under trial was recommended by the committees on colorfastness to light of textiles of the American Association of Textile Chemists and Colorists, and of the American Society for Testing Materials. It is considered to be in agreement with the "Fade-Ometer hour" used by the dyestuff and textile industries for a number of years for rating colorfastness to light of dyed textiles.

The newer "Fade-Ometers" are somewhat faster in their fading action than those on which the concept of the "Fade-Ometer hour" was developed.

The standard exposures are produced from the same batch of paper by exposing it to the Bureau's standard fading lamp. This lamp has been developed as a means of obtaining accurately measured, definite dosages of radiant energy under reproducible conditions. The light-quantities are measured with "photon counters," light-integrating meters adapted for high-intensity sources. The standard exposures thus produced are permanent in the dark and change negligibly during a year's normal use. They are mounted in strip form in a protecting booklet along with plus and minus 10 per cent steps, to allow the user to estimate the degree of overexposure or to anticipate the end of the period.

The use of light-sensitive paper should make it possible to set up more rigid specifications of light-stability for all materials where this property is important. The work of the Bureau is still in the experimental stage. Neither the paper thus far developed nor the lamp used in standardization is considered to be the final form of this method for lamp control. In fact, there have been requests from diverse industries for papers useful for controlling exposures over much shorter and longer periods of time, and for use in lamps with water spray. The experience gained from this work has pointed the way toward more sensitive papers of wider scope. Papers useful over exposure periods lasting a few hours to a week are now under development and the radiometric technique is being improved.

ZEEMAN EFFECT OF NEUTRAL NITROGEN AND OXYGEN.

Excited atoms of the chemical elements emit radiations of various frequencies depending on the initial and final energy states between which the radiative process occurs. The total number of radiations that an atom is capable of emitting is its spectrum, each individual radiation being called a spectrum line. When the radiative process occurs in a magnetic field the energy states of the atom become complex so that previously single lines now are separated into an array of closely spaced lines of different intensities, symmetrically grouped about the undisturbed position of the line. This array, or magnetic pattern, known as the Zeeman effect, uniquely identifies the energy levels between which the radiative transition occurs. It furnishes for each energy level a numerical quantity called its g-value or splitting factor.

When the Zeeman patterns of such metals as molybdenum, tantalum, and manganese, are photographed in the red and infrared regions of the spectrum, there usually appear also on the spectrograms the patterns of atmospheric nitrogen and oxygen. The relative positions

and estimated intensities in the magnetic patterns of these lines have now been determined for the first time from precise measurements of spectrograms by Dr. C. C. Kiess of the National Bureau of Standards and Dr. George Shortley of the Ohio State University.

Because the multiplet levels of these elements are very close to each other, the effect of the magnetic field is to displace the component levels from their positions of symmetry about the undisturbed position by amounts depending on numerical quantities, or quantum numbers, associated with the levels. As a consequence of this influence, known as the Paschen-Back interaction, the magnetic patterns of the lines are distorted out of their patterns of symmetry. In the case of nitrogen the distortions are slight; but in the case of oxygen they are so pronounced that the pattern bears no resemblance either to that of a weak field or to the triplet that results from complete Paschen-Back interaction.

The interpretation of the measurements of Kiess and Shortley has afforded an interesting application of the quantum theory to the elucidation of the Paschen-Back effect. The *g*-values derived for the nitrogen and oxygen energy levels are the first to be announced for neutral atoms of atomic number less than 10, or neon, and are found to conform with those required theoretically for the lighter chemical elements.

THE FRANKLIN INSTITUTE.

LIBRARY NOTES.

The Committee on Library desires to add to the collections any technical works that members would wish to contribute. Contributions will be gratefully acknowledged and placed in the library. Duplicates received will be transferred to other libraries as gifts of the donor.

Photostat Service. Photostat prints of any material in the collections can be supplied on request. Orders received in the morning are filled the same day. The average cost for a print 9 × 14 inches is thirty-five cents.

The Library and reading room are open on Mondays, Tuesdays, Wednesdays, and Fridays from 9 A.M. until 5 P.M., Thursdays from 2 P.M. until 10 P.M. and Saturdays from 9 A.M. until 12 noon.

RECENT ADDITIONS.

AERONAUTICS.

GRAY, GEORGE W. Frontiers of Flight. 1948.
THEODORSEN, THEODORE. Theory of Propellers. 1948.

ARCHITECTURE AND BUILDING.

MOON, PARRY H. AND SPENCER, DOMINA E. Lighting Design. 1948.
SHOEMAKER, RICHARD W. Radiant Heating. 1948.

ASTRONOMY.

THOMPSON, ALLYN J. Making Your Own Telescope. 1947.

BACTERIOLOGY.

HAMMER, BERNARD WERNICK. Dairy Bacteriology. Third Edition. 1948.
SALLE, A. J. Fundamental Principles of Bacteriology. 1948.

BIBLIOGRAPHY.

UNITED STATES. NATIONAL ADVISORY COMMITTEE ON AERONAUTICS. Index of N.A.C.A. Technical Publications. 1948.

BIOGRAPHIES.

ARCHIBALD, RAYMOND CLARE. Mathematical Table Makers. 1948.

CHEMISTRY AND CHEMICAL TECHNOLOGY.

BAILEY, ALTON EDWARD. Cottonseed and Cottonseed Products. 1948.
BERGMANN, ERNST DAVID. The Chemistry of Acetylene and Related Compounds. 1948.
BOGUE, ROBERT HERMAN. Chemistry of Portland Cement. 1947.
CLARK, W. MANSFIELD. Topics in Physical Chemistry. 1948.
DE MENT, JACK AND DAKE, H. C. Handbook of Uranium Minerals. 1947.
DYSON, GEORGE MALCOLM. A New Notation and Enumeration System for Organic Compounds. 1947.
GARDNER, WILLIAM. Chemical Synonyms and Trade Names. Fifth Edition. 1948.
HICKINBOTTOM, W. J. Reactions of Organic Compounds. Second Edition. 1948.
HILDITCH, T. P. The Chemical Constitution of Natural Fats. Second Edition. 1947.
HOUWINK, R. Technology of Synthetic Polymers. 1947.
LONG, J. S. AND ANDERSON, H. V. Chemical Calculations. Fifth Edition. 1948.

Newer Methods of Preparative Organic Chemistry. 1948.
RALSTON, A. W. Fatty Acids and Their Derivatives. 1948.
SHEELY, M. L. Production of Synthetic Fatty Acids. No Date.
SNELL, F. D. AND SNELL, C. T. Colorimetric Methods of Analysis. 1948.
THEILHEIMER, W. Synthetic Methods of Organic Chemistry. Volume 1. 1948.
TYLER, CHAPLIN. Chemical Engineering Economics. Third Edition. 1948.
WILLIAMS, HERBERT E. Cyanogen Compounds. Second Edition. 1948.

DICTIONARIES.

ZIMMERMAN, O. T. AND LAVINE, IRVIN. Scientific and Technical Abbreviations, Signs and Symbols. 1948.

EDUCATION.

AMERICAN COUNCIL ON EDUCATION. American Universities and Colleges. 1948.

ELECTRICITY AND ELECTRICAL ENGINEERING.

DAS, M. M. Electricity. 1948.
FORSYTHE, WILLIAM E. AND ADAMS, ELLIOT Q. Fluorescent and Other Gaseous Discharge Lamps. 1948.
GLASOE, G. N. AND LEBACQZ, JEAN V. Pulse Generators. 1948.
KIMBARK, EDWARD WILSON. Power System Stability. Volume 1. 1948.
UNITED STATES. WAR DEPARTMENT. Electrical Communication Systems Engineering. 1945.
VEINOTT, CYRIL A. Fractional Horsepower Electric Motors. Second Edition. 1948.

ELECTRONICS.

GABOR, DIONYS. The Electron Microscope. 1948.
GREENWOOD, IVAN A., JR.; HOLDAM, J. VANCE, JR.; AND MACRAE, DUNCAN, JR. Electronic Instruments. 1948.
KIVER, MILTON S. Television Simplified. Second Edition. 1948.
LOVELL, BERNARD. Electronics and Their Application in Industry and Research. 1947.
WEINBACH, MENDELL P. Electric Power Distribution. 1948.
ZELUFF, VIN AND MARKUS, JOHN. What Electronics Does. 1948.

ENGINEERING.

BATLEY, R. L. AND BARBER, E. GORDON. Boiler Plant Technology. Second Edition. 1947.
CISSEL, JAMES H. Stress Analysis and Design of Elementary Structures. Second Edition. 1948.
DUDLEY, L. Light Metals in Structural Engineering. 1946.
ITERSON, F. K. T. VAN. Plasticity in Engineering. 1947.
TERZAGHI, KARL AND PECK, RALPH B. Soil Mechanics in Engineering Practice. 1948.

FOOD.

GORTNER, WILLIS A.; ERDMAN, F. S.; AND MASTERMAN, N. K. Principles of Food Freezing. 1948.

INDUSTRIAL MANAGEMENT.

CUSHMAN, FRANK AND CUSHMAN, ROBERT W. Improving Supervision. 1947.

LANGUAGES.

PERRY, JAMES W. Chemical Russian, Self Taught. 1948.

MANUFACTURE.

BARRON, HARRY. Modern Rubber Chemistry. 1948.
CADY, EDWIN LAIRD. Precision Investment Castings. 1948.
DE CARLE, DONALD. Practical Watch Repairing. 1946.
GRANT, JULIUS. Wood Pulp and Allied Products. 1947.

V.24
1948

RAWLINGS, A. L. The Science of Clocks and Watches. 1948.
SCOVILLE, WARREN C. Revolution in Glassmaking. 1948.

MARINE ENGINEERING.

KING, RENO C., JR. Practical Marine Engineering. 1948.

MATHEMATICS.

FINNEY, D. J. Probit Analysis. 1947.
FORT, TOMLINSON. Finite Differences and Difference Equations in the Real Domain. 1948.
KATTSOFF, LOUIS O. A Philosophy of Mathematics. 1948.
USPENSKY, J. V. AND HEASLET, M. A. Elementary Number Theory. 1939.

MECHANICAL ENGINEERING.

HUNTER, MARCUS C. INMAN. Rotary Valve Engines. 1946.
MERRITT, HENRY E. Gear Trains. 1947.
PARKINSON, A. C. AND DAWNEY, W. H. Gears, Gear Production and Measurement. 1948.
STEPANOFF, A. J. Centrifugal and Axial Flow Pumps. 1948.
VINCENT, E. T. Supercharging the Internal Combustion Engine. 1948.
WOODCOCK, FREDERIC L. Design of Metal Cutting Tools. 1948.

METALLURGY.

AMERICAN SOCIETY FOR TESTING MATERIALS. Symposium on Powder Metallurgy. 1943.
BROWN, HIRAM. Aluminum and Its Applications. 1948.
BULLENS, DENNISON K. Steel and Its Heat Treatment. Volume 2. 1948.
ELLIS, OWEN W. Copper and Copper Alloys. 1948.
HARRINGTON, R. H. The Modern Metallurgy of Alloys. 1948.
HEAT-TREATER. Fundamental Principles and Applications of Induction Heating. 1947.
PALMER, FRANK R. AND LUERSSEN, GEORGE V. Tool Steel Simplified. 1948.
WHITE, A. E. AND SIEBERT, C. A. Literature Survey on Low Temperature Properties of Metals. 1947.
WOLDMAN, NORMAN E. Metal Process Engineering. 1948.

PATENTS.

MEINHARDT, PETER. Inventions, Patents and Monopoly. 1946.
TOULMIN, HARRY AUBREY. Patent Law for Executive and Engineer. Second Edition. 1948.

PETROLEUM.

WEIL, BENJAMIN HENRY AND LANE, J. C. Synthetic Petroleum from the Synthine Process. 1948.

PHARMACY AND PUBLIC HEALTH.

BAMFORD, FRANK. Poisons. 1948.

PHOTOGRAPHY.

BOND, FRED. Kodachrome and Ektachrome from all Angles. Third Edition. 1947.
CUSTIS, ELEANOR PARKE. Composition and Pictures. 1947.
JAMES, T. H. AND HIGGINS, G. C. Fundamentals of Photographic Theory. 1948.
SMITH, W. J.; TURNER, E. L.; AND HALLAM, C. D. Photoengraving in Relief. Second Edition. 1947.

PHYSICS.

BATES, LESLIE FLEETWOOD. Modern Magnetism. Second Edition. 1948.
FAIRES, VIRGIL MORING. Elementary Thermodynamics. 1948.
GEYER, E. W. AND BRUGER, E. A. Tables of Properties of Gases. 1948.
JÁNOSSY, L. Cosmic Rays. 1948.
KING, HORACE W.; WISLER, C. O.; AND WOODBURN, J. G. Hydraulics. Fifth Edition. 1948.
LUHR, OVERTON. Physics Tells Why. 1943.

MAURAIN, CHARLES. La Foudre. 1948.
MORSE, PHILIP MCCORD. Vibration and Sound. Second Edition. 1948.
SUITS, C. G. AND OTHERS. Applied Physics. 1948.
TOLANSKY, S. Introduction to Atomic Physics. 1948.
VENABLE, WILLIAM MAYO. The Interpretation of Spectra. 1948.

PHYSIOLOGY.

FRANKLIN INSTITUTE. BIOCHEMICAL RESEARCH FOUNDATION. Neutron Effects on Animals. 1947.
LEA, D. E. Actions of Radiation on Living Cells. 1947.

PLASTICS.

HICKS, JOSEPH S. AND FRANCIS, R. J. Low Pressure Laminating of Plastics. 1947.
MARK, H. AND PROSKAUER, E. S. The Science of Plastics. Volume 1. 1948.

RADIO.

BOYCE, WILLIAM F. AND ROCHE, JOSEPH J. Radio Data Book. 1948.
GRAMMER, G. AND GOODMAN, B. The A.R.R.L. Antenna Book. 1948.
MENZEL, DONALD H. Elementary Manual of Radio Propagation. 1948.
RIDER, JOHN FRANCIS AND USLAN, SEYMOUR D. FM Transmission and Reception. 1948.
SPANGENBERG, KARL R. Vacuum Tubes. 1948.
VAN VOORHIS, S. N. Microwave Receivers. 1948.

RAILROADS.

ALEXANDER, EDWIN P. The Pennsylvania Railroad; a Pictorial History. 1947.
KIEFER, P. W. A Practical Evaluation of Railroad Motive Power. 1947.

SANITARY ENGINEERING.

HOPKINS, EDWARD S. Water Purification Control. Third Edition. 1948.

SCIENCE.

DAVIS, HARRY M. Energy Unlimited; the Electron and Atom in Everyday Life. 1947.
GIEDION, SIEGFRIED. Mechanization Takes Command. 1948.
STEWART, IRWIN. Organizing Scientific Research for War. 1948.

TEXTILES.

AMERICAN VISCOSE CORP. TEXTILE RESEARCH DEPT. Rayon Technology. 1948.
BERGEN, WERNER VON AND MAUERSBERGER, H. R. American Wool Handbook. Second Edition. 1948.
LINTON, GEORGE E. AND PIZZUTO, JOSEPH J. Applied Textiles. 1948.
OLNEY, LOUIS ATWELL. Textile Chemistry and Dyeing. Tenth Edition. 1947.

WOOD-WORKING.

HANSEN, HOWARD J., Editor. Timber Engineers' Handbook. 1948.

PUBLICATIONS RECEIVED.

Microwave Transmission Circuits, edited by George L. Ragan, 725 pages, 16 × 23 cm., tables, drawings and illustrations. New York, McGraw-Hill Book Co., 1948. Price, $7.00.

Mechanics of Machinery, by C. W. Hamm and E. J. Crane. Third edition, 538 pages. 16 × 23 cm., tables and drawings. New York, McGraw-Hill Book Co., 1948. Price, $5.00.

Popular Gemology, by Richard M. Pearl. 316 pages, 14 × 21 cm., illustrations and drawings. New York, John Wiley & Sons, Inc.; London, Chapman & Hall, Ltd.; 1948. Price, $4.00.

Principles of Servomechanisms, by Gordon S. Brown and Donald P. Campbell. 400 pages, 15 × 24 cm., tables and drawings. New York, John Wiley & Sons, Inc.; London, Chapman & Hall, Ltd.; 1948. Price, $5.00.

M.I.T. in World War II, by John Burchard. 354 pages, 15 × 23 cm., illustrations. New York, John Wiley & Sons, Inc.; London, Chapman & Hall, Ltd.; 1948. Price, $3.50.

Rotary Valve Engines, by Marcus C. Inman Hunter. 216 pages, 14 × 21 cm., illustrations, tables and drawings. New York, John Wiley & Sons, Inc., no date. Price, $5.00.

The Chemical Constitution of Natural Fats, by T. P. Holditch. Second edition, 554 pages, 15 × 25 cm., tables and drawings. New York, John Wiley & Sons, Inc., 1947. Price, $9.00.

Steam, Air, and Gas Power, by William H. Severns and Howard E. Degler. Fourth edition, 509 pages, 15 × 23 cm., tables, drawings and illustrations. New York, John Wiley & Sons, Inc.; London, Chapman & Hall, Ltd.; 1948. Price, $4.75.

The Chemistry of the Polysaccharides by Robert J. McIlroy. 118 pages, 14 × 22 cm. New York, Longmans, Green & Co.; London, Edward Arnold & Co., 1948. Price, $2.50.

History of Factory and Mine Hygiene, by Ludwig Teleky. 342 pages, 14 × 22 cm., tables. New York, Columbia University Press, 1948. Price, $4.50.

Mineral Resources of the United States, by the Staffs of the Bureau of Mines and Geological Survey. 212 pages, 21 × 28 cm., maps, charts and tables. Washington, D.C., Public Affairs Press, 1948. Price, $5.00.

The Theory of Mathematical Machines, by Francis J. Murray. Revised edition, 139 pages, 21 × 28 cm., drawings. New York, King's Crown Press, 1947 and 1948. Price, $3.00 (Paper).

Television How it Works, by John F. Rider. 203 pages, 21 × 28 cm., drawings and illustrations. New York, John F. Rider, 1948. Price, $2.70 (Paper).

BOOK REVIEWS.

SUPERCHARGING THE INTERNAL COMBUSTION ENGINE, by E. T. Vincent. 315 pages, illustrations, plates, 16 × 23 cm. New York, McGraw-Hill Book Co., Inc., 1948. Price, $5.00.

The earliest experiments with supercharging were conducted almost fifty years ago. The increase in power output was then incidental, as supercharging was applied with the idea of controlling the maximum temperature of the cycle.

Practical application did not occur until about ten years later (1910), when the German companies of Junkers and Sulzer utilized the principle in conjunction with diesel engines.

By the end of the First World War experimentation was in an advanced stage, and supercharging was quickly applied to the aircraft engine.

The most rapid development took place between 1920 and 1930, when considerable advances were made in developing materials which would stand up under the high exhaust-gas temperatures.

Professor Vincent's book brings together the accumulated knowledge in this specialized field. In the first chapters the thermodynamics and the engine cycle are discussed, before the types of compressors and their integral parts are introduced. Chapters estimating the operating conditions and describing the testing of superchargers, turbosuperchargers, and axial-flow compressors follow. A consideration of supercharging the oil engine concludes the book.

Persons in the internal-combustion-engine field who are not directly connected with the theory or development of superchargers will find the material contained in this book to be a valuable and comprehensive reference.

H. N. MICHAEL.

AIRCRAFT ENGINES, by Rollen H. Drake. 348 pages, illustrations, 16 × 24 cm. New York, The Macmillan Co., 1948. Price, $5.90.

This book is written principally for the layman, the teacher, and the airplane mechanic. It deals with the fundamentals of structure and operation of aircraft engines. The value of

this book is enhanced by the fact that it contains enough information to enable the student to qualify for a Civil Aeronautics Administration's aircraft engine mechanic certificate.

The book is outstanding in its simplicity of presentation. To secure this desirable trait, the author has avoided the use of unnecessary graphs, formulas, tables, etc., which so often discourage the non-technically trained, yet interested and capable student.

In its twenty-two chapters the book covers most of the fundamentals pertinent to aircraft power units. The principles of internal combustion, the metals and alloys used, and the types of engines, are taken up first. After this general treatment, the component parts are dealt with: the cylinders, piston assemblies, crankshafts, crankcases, valves, etc. The accessory systems are treated next and include the ignition, fueling, supercharging, lubricating, and cooling systems. There are also chapters on propeller fundamentals, engine instruments, and on the later developments in jet propulsion.

The book is very adequately illustrated with drawings and photographs.

It may be recommended as outstandingly practical and easy to understand.

H. N. MICHAEL.

JOURNAL OF THE SOCIETY OF MOTION PICTURE ENGINEERS. INDEX, JANUARY, 1936 to DECEMBER, 1945. 156 pages, 15 × 23 cm. New York, Society of Motion Picture Engineers, 1948. Price, $2.00.

This is the third general index to be issued by the Society of Motion Picture Engineers since the appearance of its initial publication in 1916. Two indexes are included in this volume, one to authors and one to subjects. The subject index is arranged alphabetically by rather broad headings, with subdivisions under the larger groupings. "Sound recording" with eight and a half pages of references and "sound reproduction" with nearly five pages might well have also been subdivided. Numerous cross references are provided, both from headings not used and to other headings bearing on related topics. Under the subject headings the entries are arranged with the most recent first.

As files of a periodical accumulate, general indexes become an invaluable aid in making their contents readily accessible. The Society of Motion Picture Engineers merits commendation for its efforts in making such indexes available for its Journal.

G. E. PETTENGILL.

LORAN, LONG RANGE NAVIGATION, edited by J. A. Pierce, A. A. McKenzie, R. H. Woodward. 476 pages, illustrations, 15 × 23 cm. New York, McGraw-Hill Book Co., Inc., 1948. Price, $6.00.

One of the important uses of radio introduced during the last war is indicated in the derivation of its coined name "Loran," from *long range navigation*. Developed to meet the needs of the Navy in convoy operations and to provide all-weather navigation for aircraft by day and night, it promises to have great usefulness in peacetime activities as well. Figures revealing its development are impressive. At the end of the war there were 70 Loran transmitting stations providing night-time service over 60 million square miles or three tenths of the earth's surface; 75,000 receiver-indicators had been manufactured, and 2¼ million charts prepared and shipped.

Although dependent upon the transmission and reception of pulsed radio signals like radar, Loran differs in that it employs lower radio frequencies and does not involve reflection from a target. "The primary fact upon which Loran is based is that the transmission time taken by a radio pulse to travel over a distance measures the distance." As actually operated Loran depends upon the absolute delay between the emission of pulses alternately from two stations and the time difference between their reception by the navigator.

In its treatment of the subject this volume commences with a brief comparison of Loran with other methods of navigation by means of radio aids. A historical chapter gives details of its development from the first proposal in October, 1940, through the various experimental stages to its practical operation. The different stations set up in the various theaters of war are discussed as well as the history of charting and training.

V.24
194

The principles of Loran are thoroughly treated with considerable attention being paid to the geometry of Loran, indicating the service area of the pair, triplets, chains and quadrilaterals. Different types have been developed, namely, standard Loran, sky-wave synchronized Loran, and low frequency Loran. Procedures for its use in navigation are indicated and a chapter on future trends considers possible developments and uses.

Part II is devoted to Loran equipment with chapters on timers, switching equipment, transmitters, antenna systems, and receiver-indicators. This material is quite detailed on the special applications and includes many diagrams, both schematic and block. An appendix gives the Loran program in the Hydrographic Office, a list of Loran ground stations and other data. The bibliography is comprehensive and provides a helpful indication of where material may be secured, especially necessary because of the nature of much of the material cited.

This volume well serves its purpose of recording the development of Loran and until significant changes occur, will undoubtedly remain the standard work on the subject.

G. E. PETTENGILL.

PRACTICAL MARINE ENGINEERING, by Reno C. King, Jr. 470 pages, illustrations, diagrams. 14 × 20 cm. New York, Prentice-Hall, Inc., 1948. Price, $6.00.

Designed for the operator of a marine steam power plant, this volume is thoroughly practical in nature. The author has based it on many lectures which he has given to applicants for Merchant Marine Engineering-Officer licenses. In addition to considering the various aspects of propulsion machinery, boilers, steam engines and steam turbines, the book also includes material on other subjects with which the marine engineer must be familiar—electricity, refrigeration, pumps and unfired pressure vessels, respiratory apparatus and fire-fighting equipment. Adequate attention has been paid to both routine and emergency operation and maintenance.

The illustrations and many diagrams as well as the questions, which are typical of those given in the license tests, make the book well adapted for self study.

G. E. PETTENGILL.

HOUSEHOLD ELECTRIC REFRIGERATION, by John F. Wostrel and John G. Praetz. Second ed. 458 pages, illustrations, 16 × 23 cm. New York, McGraw-Hill Book Co., Inc., 1948. Price, $4.50.

From the time of the first printing of this book in 1938, there were few developments in household refrigeration. Thus, the new, second edition follows the first rather closely, with the exception of amplifications on mechanical details and service instructions for refrigerators that were introduced to the market after 1938.

The book, written in non-technical language, is particularly well suited for those servicing household refrigerators. The various steps are taken up very thoroughly. The basic physical laws governing refrigeration are explained before the systems are described. For all practical purposes there are only two principles employed in the refrigerators of today—compression and absorption. These are explained before the variations of the different commercial products are taken up.

The emphasis of the book is on servicing and a major part of it is devoted to the control devices, to installation, testing and servicing.

Chapters on food preservation and insulation materials should also prove helpful to those engaged in the production and distribution branches of the field.

H. N. MICHAEL.

CENTRIFUGAL AND AXIAL FLOW PUMPS, by A. J. Stepanoff. 428 pages, illustrations, diagrams, 15 × 24 cm. New York, John Wiley & Sons, Inc., 1948. Price, $7.50.

During recent years the rapid advancement in the design and application of centrifugal pumps has caused radical adjustments to be made in the former limitations of pressure, capacity, temperature, speed of operation, etc. . The problems arising out of such changes are numerous and may be grouped under several headings: mechanical, hydraulic, operating, and economic.

Dr. Stepanoff's book deals with the necessary theoretical and experimental studies which make the advance in pump design possible. These include cavitation, operation outside the normal head capacity and speed range, axial and radial thrust, effect of stuffing boxes on the critical speed of pump shaft, control of head capacity and brake-horsepower curves, and the pumping of viscous liquids.

Of particular interest is Dr. Stepanoff's theoretical treatment of the pump impeller. Based on a single pattern of flow, identical reasoning, and similar procedure of impeller layout for centrifugal, mixed flow, and axial flow pumps, it results in a simple diagram which combines the design elements and performance characteristics of all centrifugal pumps, thus creating a "Mollier diagram" for all centrifugal and axial flow pumps.

The book is well supplied with charts, diagrams, and illustrations.

H. N. MICHAEL.

NICOLAUS COPERNICUS. DE REVOLUTIONIBUS. PREFACE AND BOOK I, translated by J. F. Dobson, assisted by S. Brodetsky. 32 pages, plates, diagrams, 17 × 25 cm. London, Royal Astronomical Society, 1947. Price, 3s 6d.

JOHN COUCH ADAMS AND THE DISCOVERY OF NEPTUNE, by W. M. Smart. 56 pages, portraits, 17 × 25 cm. London, Royal Astronomical Society, 1947. Price, 5s.

These two pamphlets appeared originally as *Occasional Notes* 10 and 11, respectively, of the Royal Astronomical Society. The first comprises a translation into English of parts of Copernicus' *De Revolutionibus*, which is one of the foundation works of astronomical literature, with its outlining of the theory that the earth moves around the sun. The translation is readable and is accompanied by extensive notes.

The other paper is two-fold in scope—in it Dr. Smart recounts the major facts about the life of John Couch Adams and he surveys the controversy which arose over the discovery of Neptune. Adams and Le Verrier had both become interested in the possibility of a trans-Uranium planet and both men, nearly simultaneously, deduced from mathematical calculations the existence and position of such a planet. Its subsequent telescopic discovery on September 23, 1846, in Berlin, gave rise to controversy as to the relative claims of the two men for the honor of initial discovery. This balanced appraisal of the various aspects of the matter will prove valuable in placing their work in proper perspective.

Both pamphlets should appeal to those concerned with the history of astronomy.

G. E. PETTENGILL.

LA FOUDRE, by Charles Maurain. 215 pages, illustrations, 11 × 16½ cm. Paris, Librairie Armand Colin, 1948. Price, 120 fr. (paper).

Lightning, which has been the subject of investigation ever since the middle of the eighteenth century has become an object of even greater study in the twentieth century. The various manifestations of atmospheric electricity have assumed an increasing importance with the growth in the use of electricity and the development of aerial travel.

Mr. Maurain discusses the general electrical properties of the atmosphere and then proceeds to consider the structure and properties of the lightning flash, the thunder cloud, and the theories relative to the production of electricity in the thunder cloud. Considerable attention is also paid to the question of atmospherics. The final chapter offers some comments on lightning arresters.

A bibliography and an index of names are included. This book is a useful summary of the present knowledge of lightning.

G. E. PETTENGILL.

ENCYCLOPEDIA OF CHEMICAL REACTIONS, by C. A. Jacobson. Volume II, 917 pages, 15 × 24 cm. New York, Reinhold Publishing Corp., 1948. Price, $12.00.

The first volume of this work was reviewed in the JOURNAL for August, 1946. This second volume includes some 3331 reactions for the elements cadmium, calcium, carbon, cerium,

cesium, chlorine and chromium. It has the same general arrangement as the previous volume, first as to the formulas of the reactants and next as to those of the reagents.

The list of "Journals used by abstractors" has been revised and some changes made in the abbreviations employed. Unfortunately *Chem. Anal.* now stands for two publications, *Chemische Analyse* and *Chemist Analyst.* One is also rather surprised at the form of *Bio Chem. J.* and *Bio Chem. Z.*

The amount of volunteer labor that has gone into the production of this set merits the thanks of chemists everywhere who will profit by the accessibility of the compiled data.

G. E. PETTENGILL.

DAIRY BACTERIOLOGY, by Bernard W. Hammer. Third edition, 593 pages, illustrations, 15 × 23 cm. New York, John Wiley & Sons, Inc., 1948. Price, $6.00.

Originally written as a text-book for a beginning dairy bacteriology course, this book, through its comprehensive coverage, has also become an important reference to the technical personnel of the dairy industry. It presumes a knowledge of general bacteriology. In the third edition of this work, minor rearrangements of material included in the earlier editions were made and new important developments have been added. The increased production of milk powder during the war, for instance, has presented many problems, the solution of which provided much useful material.

There is an entirely new chapter on dairy-plant water supply, in which particular attention is paid to the spoilage that a deficient water supply may cause in milk products.

Only special dairy laboratory methods are discussed. The standardized procedures are to be sought in the latest edition of "Standard Methods for the Examination of Dairy Products."

H. N. MICHAEL.

THE GENIUS OF INDUSTRIAL RESEARCH, by D. H. Killeffer. 263 pages, diagrams, 15 × 23 cm. New York, Reinhold Publishing Corp., 1948. Price, $4.50.

Industrial research is playing an ever greater role in the world today. Consequently, knowledge of its techniques and methods is of vital importance. In the present volume the author has stated some of the principles which he feels are generally applicable. He has leaned heavily on the case method and a large part of the text consists of extracts from the writings of others describing research which they have done. The examples have been chosen from the field of industrial chemistry, although the principles will be germane to most industrial research.

After a consideration of the difference between pure and applied research, the author points out the necessity of ability to state the problem in such terms that its solution becomes practical. Then the two basic methods of research are discussed—the Baconian or Edisonian method of trying everything, and the Aristotelian method of formulating a theory and then searching for facts to bolster it. Examples of both types are cited from the work of Thomas Midgley, Jr. The "discovery of the effectiveness of tetraethyl lead in inhibiting fuel knock in internal combustion engines" represents the Edisonian method, while the Aristotelian method method is demonstrated in Midgley's research leading to the fluorinated hydrocarbons as safe refrigerants.

The necessity of thinking out the problem is reviewed and then the author turns his attention to different types of research. These are *process research* which involves developing a new process for the manufacture of a known compound or product; *product research* which contemplates the development of new chemical products to meet existing needs—for example, rayon, cellophane, Freon; and *equipment research* which investigates the changing of a design to adapt it for performing a new function.

The progressive development of an idea through various stages is traced using the synthesis of rubber as an example. Other topics considered are the value of imagination and ingenuity, the importance and operation of a pilot plant, the writing of reports, and the evaluation of research.

The treatment of the subject is logical and the presentation stimulating. The quoting of the actual words of the researchers adds greatly to the interest of the illustrative material. Students will surely profit from a reading of the volume and the experienced chemist, plant supervisor or development engineer will undoubtedly find suggestions of value.

G. E. PETTENGILL.

GROWTH OF PLANTS. TWENTY YEARS' RESEARCH AT THE BOYCE THOMPSON INSTITUTE, by William Crocker. 459 pages, illustrations, 16 × 23 cm. New York, Reinhold Publishing Corp., 1948. Price, $10.00.

This book reports on the major and minor projects that have been conducted by the staff of the Boyce Thompson Institute since its foundation in 1924. Some of these projects are still being continued. The twelve major projects are described in the first eleven chapters, and the concluding twelfth chapter is devoted to the miscellaneous minor problems of plant research.

Among the early problems approached by the Institute were the "yellows" and virus diseases of plants and the "duck food problem" which deals with winter feeding grounds of migratory wild fowl in the tide-water regions of Virginia and North Carolina. These undertakings are described in the first chapter.

Chapters II and III deal with the life span of seeds and dormancy in seeds, respectively.

The next two chapters are devoted to the study of the physiological effects of ethylene and other unsaturated carbon-containing gases and of lethal gases upon plant growth.

In Chapter VI, Dr. P. W. Zimmerman attacks the problem of plant hormones, a problem still under investigation at the Institute.

Researches leading to the discovery of chemicals that force buds out of their normal state of dormancy are described in Chapter VII, entitled "Dormancy in Buds."

Problems relating to the formation and structure of plant cell membranes have been approached through microscopic, chemical and X-ray diffraction analyses of cell membranes. Mrs. Wansen K. Farr reports these studies in Chapter VIII.

Next the growth of plants under controlled environmental conditions is described. The controlled conditions included the following: light of various intensities, quality and daily duration; artificial light with various day lengths, with controlled temperatures and humidities, and with increased concentrations of CO_2; combinations of sunlight and artificial light; growth under a full solar spectrum and under various portions of the solar spectrum. The plants produced under these conditions were studied as to rate and nature of growth, dry and wet weight increase, chemical composition, and pigment development. Content, size, form, and anatomy of the several organs, as well as vegetative or reproductive development were also considered.

The last two major research projects are described by Drs. Hartzell and McCallan. They deal with insecticides and fungicides, respectively.

Chapter XII presents fourteen shorter projects, most of which have been finished or discontinued. The subject matter here is diverse, dealing with such phenomena as "Diurnal and Autumn Changes in Leaves of Deciduous Plants," or "Effect of Nitrogenous and Carbohydrate Reserves on Growth of Seedlings," *et al.*

Dr. Crocker's book provides a convenient critical summary of articles which appeared in the past in the various pertinent publications, as well as those that have not been hitherto published. It should prove of considerable value to further research as well as to the fields of application.

H. N. MICHAEL.

V.2
194

NOTES FROM THE BIOCHEMICAL RESEARCH FOUNDATION.

Radiation Survey Meter.—T. ENNS. A simple portable instrument with a wide range of sensitivity has been constructed. The apparatus consists of an aluminum ionization chamber, and an electrometer circuit using the Victoreen VX 41 electrometer tube.

The electrometer circuit is shown in Fig. 1. It is based on the circuits described by Penick [1] and is balanced so that small changes (approximately 5 per cent) in the potential of the power battery produce no appreciable change in the reading of the output meter. All power for the electrometer circuit is supplied by a 7½-v. Burgess 5540 "C"

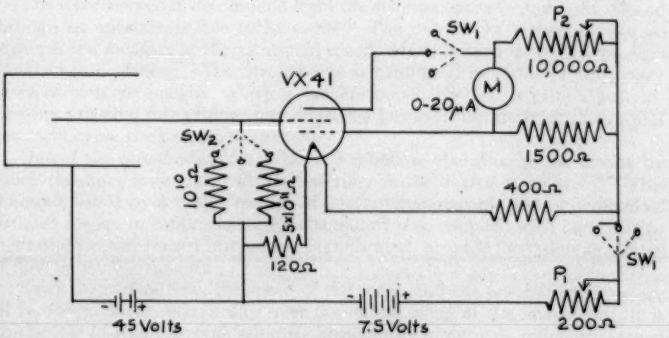

FIG. 1. Electrometer circuit.

battery. Throughout the useful life of the battery (170 hr.) the potentiometer P_1 can be adjusted to completely compensate for the drop in battery potential. This adjustment is made so that the filament emission as measured by the space charge grid current remains unchanged. The space charge grid current is measured by disconnecting the plate and setting the plate resistor P_2 at maximum value. The space charge grid current is chosen at 193 microamperes, or a meter reading of 20 microamperes.

The grid resistor switch SW_2 is a standard low capacity switch with silver contacts. The bakelite insulator has been replaced by a lucite insulator. It has three positions, two of them connect the grid to the resistors and the third gives a free grid for the rate of drift measurements.

[1] D. B. PENICK, *Rev. Sci. Instruments*, 6: 115 (1935).

The circuit is housed in two standard metal cases each 4 by 4 by 2 in. combined to form a 4 by 4 by 4-in. case. The ion chamber is a 2-in.-diameter-by-2½-in.-long aluminum coil shield projecting from this case and insulated by a bakelite base.

Approximate sensitivities of the instrument to gamma radiation are:

with 10^{10} grid resistor—one microampere = 0.720 *r* per hour
with 5×10^{11} grid resistor—one microampere = 0.0144 *r* per hour
with rate of drift setting—one microampere per second = 0.108 *r* per hour.

Maximum range of the instrument is 14.4 *r* per hour. Minimum practical range is one microampere per minute or 0.0018 *r* per hour.

CURRENT TOPICS.

The Stroboflow, An Oscilloscope for Hydraulics.—The Stroboflow, for reproducing desired rates of flow in liquids, comprises a precision-made turbine, mounted on stainless steel pivots in Graphitar bearings between transparent panes, and allowed to rotate, practically floating in synchronism with the liquid.

The rotational speed of the turbine is used as a measure of the quantity of liquid flowing. Since there is a straight-line relationship between the speed of the rotor and the quantity of the liquid, and since the Stroboflow provides a very precise means of determining rotor speed, these two factors are combined in this instrument and constitute a highly accurate method of flow-rate indication.

The rotor's speed is determined from the stroboscopic effect of light viewed through an aperture in the turbine disc. The number of virtual images so obtained is a measure of the rotational speed, which in turn is directly proportional to rate of flow. The Stroboscope is calibrated in terms of stationary patterns of these images. Once a predetermined pattern is established, indicating a desired rate of flow, any deviation however minute from this rate of flow, will cause the pattern to precess.

One of the outstanding features of Stroboflow operation is the means by which the range is extended without sacrifice in the degree of accuracy. This is accomplished by a simple change of jets, interchangeable in any Stroboflow without change in calibration. Five standard jets, supplied with each instrument and for which each instrument is calibrated, provide forty different rates of flow in one instrument.

Since the rate of flow, the speed of the rotor, and the jet characteristic are all in direct, linear relationship over the entire range of the instrument, it is practicable to adapt several, separate Stroboflows to indicate different rates of flow while exhibiting identical patterns. This simplifies monitoring of flow rates in processes requiring coordinated multiple flows.

R. H. O.

Rocket Motor Test Station.—A test station which will static-test rocket propulsion motors up to 50,000-lb. thrust, equivalent to 500,000 hp., has been constructed near Schenectady.

This test station, the first of its kind, has been in operation for over a year, contributing invaluable data for basic rocket-motor design and fuel development.

The test station has three heavily-constructed steel-re-inforced concrete rocket-motor static-test pits. Each pit is set into the forward slope of a small hill, and earth is mounded around its sides.

Three covered stairways lead down into the interior of the test pit, which is divided into four rooms; control room, motor room, and two reactant rooms. Three-foot steel-re-inforced concrete walls separate the motor room from the rest of the structure, while all other walls and the roof are 2 ft. in thickness. Heavy steel doors seal off each room when tests are in progress.

The control room, lying parallel to the motor room, contains all the valves and controls used in regulating "runs" of rocket motors under test in the pit. Roughly, two thirds of the wall space is filled with observation ports and panels containing valves, switches, and gages. The rest of the area contains banks of photoelectric recorders which calibrate and record data continuously during the tests.

Fire is an ever-present danger in rocket-motor development and extensive precautions have been taken throughout the entire test station.

No smoking is permitted in or near the test pits. Power driven ventilation fans clear any fumes from the reactant rooms. Automatic alarm systems are located in the interior and outside of each test pit.

Within the pits a high-pressure water system, at 140-psi., can operate either automatically or manually by means of controls located in the control room. In the motor room, three different flooding systems can be used. In each of the reactant rooms, high-pressure nozzles are directed down upon the reactant tanks. Carbon dioxide extinguishers are located throughout the sites.

Sirens, starting five minutes before and continuing through each "run," as well as flashing red lights above the pits, warn personnel in the test area. Guards are also placed a safe distance from the pit under test to prevent persons entering the area. Sirens continue to sound some time after the "run" to allow a safety period after shutdown.

R. H. O.

New Type Manometer.—Unprecedented simplicity and high precision in making either absolute or differential measurements of pressure and vacuum are now obtainable through a new type manometer which reduces the arduous task of cleaning and filling a closed end manometer to the same relatively simple process of cleaning and filling an open end U-tube type. Only a single reading is required to obtain a precise measurement automatically corrected for ambient temperature and reduced to a height of mercury at 0° C.

The principle of operation of this new absolute and differential manometer is as follows: The closed end is effected by means of a U-tube which traps mercury to form the vacuum seal and an oblique bore stopcock above the trap to hold up the mercury seal. For differential readings the stopcock is kept open and connected to the lower source of pressure. The ratio of the diameters of the manometer tube and reservoir is adjusted exactly to counteract the increase in mercury height due to its lower density at room temperature than at 0° C.

Thus, a single reading of the mercury level in the manometer tube gives the true corrected pressure in mm. of Hg at 0° C. The coefficient of expansion of the vinylite scale is of such value that a precision of 0.1 mm. is maintained for room temperature variation between 20° and 30° C. A vernier is provided to simplify reading of the scale to a precision of 0.1 mm.

The glass part and scale of this new instrument are mounted on a functionally designed aluminum stand having a rigid three point support. The vinylite scales also have high dimensional stability and are designed to preserve the markings with a laminated cover of transparent vinylite over a milk white base upon which the markings are clearly printed in black. This new type manometer, Range: 0–200 mm., vernier reading to 0.1 mm., is made of pyrex brand glass, and is supplied mounted on aluminum stand, but without mercury.

Liquid Rheostats.—The liquid rheostat is particularly suited for control of larger motors, especially where other types of control cannot be used because of rating limitations.

Speed control systems using liquid rheostats are noteworthy for their stepless speed control, minimum maintenance and maximum dependability. Most applications in recent years have been on motors from 1,000 to 30,000 hp. in size.

Basically, the liquid rheostat consists of metal electrodes, half of which are movable, submerged in a tank of electrolyte that is usually a solution of sodium carbonate in water. The stationary electrodes are insulated from the steel in the tank by an insulating cell. Current flows between the electrodes and resistance is approximately proportional to the distance between them. Resistance properties of the electrolyte depend upon the concentration of sodium carbonate and the temperature of the solution.

There are three types of rheostat control systems: (1) The manual control system, where the electrodes are positioned by manual control through the pilot motor rheostat; (2) The speed regulating control system, offering a more refined scheme of speed adjustment, with the pilot motor being energized by an amplidyne; and (3) The kind of control that can be applied to maintain constant input to the motor or to prevent the load on the motor from exceeding a selected value.

The liquid rheostat, as a system element in conjunction with the proper control, can be applied in other ways to regulate temperature, flow, level, and pressure.

R. H. O.

Heat Conducting Glass Keeps Ice from Windshield.—Heat-conducting glass, put to use for de-icing windshields in one of the severest winters on record in the last quarter century, stands ready to give the American traveler new safety and additional comfort in cold weather.

Glass normally is used as an insulator, but it becomes a conductor of electricity by coating it with an invisible film.

The research staff of Libbey-Owens-Ford Glass Co., which holds patent rights on the new windshield, declares that the winter-long tests bear out successful results of earlier laboratory experiments with this novel glass, and satisfy every qualification for its commercial manufacture.

"Ice doesn't have a chance; it just can't form on the warm surface of the glass," according to R. A. Gaiser, one of the researchers who installed a windshield on his automobile and tested it in repeated freezing rains and sleet storms as well as in sub zero weather.

Higher voltage than is normally found on the average family automobile is required for efficient operation of the de-icer. The most feasible method of supplying current, Mr. Gaiser believes, is to replace the conventional generator with an a-c. generator. The alternating current then can be transformed to voltages sufficiently high to perform the necessary de-icing operation. Many police and fire cars and ambulances have a-c. equipment for radio transmitting purposes. No additional equipment would be needed in those cars.

Carbonyl Iron Powders.—Because of the widespread interest that has been aroused in Carbonyl Iron Powders as a result of an invention of a new mag-

netic clutch, in which these powders are used, by Jacob Rabinow, of the National Bureau of Standards, the following brief history and description of the powders has been prepared.

Iron Carbonyl Powders are manufactured exclusively by General Aniline & Film Corporation in a plant constructed expressly for the purpose at Grasselli, New Jersey, shortly after the outbreak of World War II. The manufacture of these powders expanded rapidly to meet the heavy war time demand for use as an important agent in various electrical devices, particularly in the field of communication, including radar, short wave transmitters, carrier telephony and in frequency modulation devices. One major application is in the form of cores in high frequency magnetic fields.

It is estimated that over 90 per cent of all automobile radio sets constructed since January 1947 are built with cores made from Carbonyl Iron Powders. They have been accepted by radio engineers as the "heart of inductance (push button) tuning." These cores have made push button tuning in auto radio sets possible.

Carbonyl Iron Powders are manufactured under rigid production control. They are made by the reaction of carbon monoxide gas with iron-containing ores to form liquid Iron Penta Carbonyl. This liquid is then heated to a temperature where it decomposes into powdered iron and the carbon monoxide gas is liberated. The results of this method are unique: Iron Penta Carbonyl is obtained which is chemically pure, and the iron powder particles formed by its decomposition are all minute spheres.

While the process of manufacture appears simple, the closest attention to detail is necessary to insure a product whose characteristics never vary. To illustrate: the powders are never exposed to air, but only to inert gases; ammonia is added to the packing containers to check any possible action of moisture and carbon dioxide during storage and shipment.

The new type of electromagnetic clutch, developed by Jacob Rabinow at the National Bureau of Standards, has the automobile, aviation, marine and farm implement people—in fact just about everyone in the motive power transmission field—enormously interested.

Rabinow's development, based on his discovery that frictional forces between solid surfaces and certain types of fluid media can be controlled by application of magnetic fields, is being studied by engineers, and Rabinow's visitors at his laboratory in Washington include representatives of the major automobile companies and clutch manufacturers.

The clutch is characterized by ease of control, high efficiency, smooth operation, long life and simplicity of construction.

Two clutch discs, one on the drive shaft and one on the shaft to be driven, are contained in a housing, with the discs immersed in oil in which millions of particles of iron powder are held in suspension. When this mixture of oil and iron is acted on by a magnetic field, the iron particles are mutually attracted and become "bound" together in the field. The magnetic field is, of course, produced by an electric current so that it is simple to control the binding force. The amount of power required is very small and the control is smooth from the minimum—characterized by a viscous 'drag'—to the maximum immediate rigidity following magnetic saturation of the iron.

Having no axially moving parts, the clutch is easy to build and the models show no sign of wear after long tests.